

“...And I ask, as the lungs are so close at hand, and in continual motion, and the vessel that supplies them is of such dimensions, what is the use or meaning of this pulse of the right ventricle? And why was nature reduced to the necessity of adding another ventricle for the sole purpose of nourishing the lungs?”

-William Harvey “Exercitatio Anatomica de Motu Cordis et Sanguinis in Animalibus”, 1628

University of Alberta

Experimental Therapies for the Hypertrophied Right Ventricle

by

Jayan Nagendran

A thesis submitted to the Faculty of Graduate Studies and Research
in partial fulfillment of the requirements for the degree of

Doctor of Philosophy

in

Experimental Medicine

Department of Medicine

©Jayan Nagendran

Fall 2009

Edmonton, Alberta

Permission is hereby granted to the University of Alberta Libraries to reproduce single copies of this thesis and to lend or sell such copies for private, scholarly or scientific research purposes only. Where the thesis is converted to, or otherwise made available in digital form, the University of Alberta will advise potential users of the thesis of these terms.

The author reserves all other publication and other rights in association with the copyright in the thesis and, except as herein before provided, neither the thesis nor any substantial portion thereof may be printed or otherwise reproduced in any material form whatsoever without the author's prior written permission.

Examining Committee

Supervisor: Evangelos D. Michelakis, Department of Medicine

Co-Supervisor: Jason R. Dyck, Department of Pharmacology

Committee member: David B. Ross, Department of Surgery

Committee member: Ian Adatia, Department of Pediatrics

Committee member: Todd Anderson, Department of Medicine, University of Calgary

Table of Contents:

Abstract: pg 5

Chapter 1- Introduction: pg 6-42.

Chapter 2- Materials and Methods: pg 43-53.

Chapter 3- Phosphodiesterase type 5 (PDE5) is highly expressed in the hypertrophied human right ventricle and acute inhibition of PDE5 improves contractility: pg 54-99.

Chapter 4- A dynamic and chamber-specific mitochondrial remodeling in right ventricular hypertrophy can be therapeutically targeted: pg 100-135.

Chapter 5- Endothelin receptor antagonists decrease contractility in the hypertrophied right ventricle: Direct clinical implications for patients with PAH: pg 136-176.

Chapter 6- Discussion: 177-197.

Abstract:

The right ventricle (RV) of the heart is clearly an extremely important component of cardiovascular function and physiology. The RV is affected in many cardiovascular disease processes, including pulmonary arterial hypertension (PAH), congenital heart disease, and left ventricular failure. In PAH, the performance of the RV is the strongest predictor of morbidity and mortality. Several advances in PAH therapies have occurred over the past decade, including the use of phosphodiesterase-5 (PDE5) inhibitors, endothelin receptor antagonists (ETRAs), and experimental metabolic modulators (Dichloroacetate-DCA). Most therapies for PAH are focused on decreasing RV afterload by vasodilation of the pulmonary vasculature, though there is a surprising lack of focus on direct effects of therapies on the RV. In PAH, the RV compensates to the increase in afterload by hypertrophy, this hypertrophic defense mechanism eventual falls short and the RV progresses to failure and patient death.

The specific aims of our investigations are to assess the effects of PAH therapies on RV in normal and hypertrophied states, as seen in PAH. We utilize human RV samples attained from cardiac surgical procedures to perform in-vitro analysis of protein and mRNA expression of the targets of PAH therapies. We also use a rat model of PAH and subsequent RV hypertrophy to verify human data and to also perform applied physiology experiments to isolate ex-vivo effects of PAH therapies on the RV. In the case of metabolic modulation by altering mitochondrial membrane potential ($\Delta\psi_m$) with DCA, human samples were acutely analyzed for $\Delta\psi_m$, which was then translated into correlations with the animal PAH model. In the case of PDE5 inhibitors, we found that target, PDE5, was highly expressed in patients and rats with RV hypertrophy (RVH), a novel finding as PDE5 was thought not to exist in the myocardium based on previous human and animal studies on normal RVs. This increased expression of PDE5 in RVH led to PDE5 inhibition causing a significant increase in contractility, while having no effect in the

normal RV. A novel and unexpected finding, though it correlated with previously unexplained human data. The experiments with ETRAs showed human and rat expression of ET Receptor-A and Endothelin-1 (ET-1) was significantly increased in RVH. Since ET-1 is a positive inotrope in normal and hypertrophied myocardium, it was verified that ETRAs led to a decrease in contractility in both normal and to a greater magnitude in RVH ex-vivo hearts. The results of PDE5 inhibitors and ETRAs provide the grounds for a much more comprehensive assessment of RV function in PAH clinical trials, as the RVH myocardium is directly effected beyond mere reduction in afterload by decreased PVR. In the studies using metabolic modulation by DCA, we observed that in human and rat RVH there was a significant hyperpolarization of the $\Delta\psi_m$ compared to the normal RV. We were able to return $\Delta\psi_m$ toward baseline levels by treatment with DCA in-vitro, and ex-vivo contractility experiments revealed that DCA caused improved contractility in RVH, which was associated with a decrease in lactate production. The mechanism for DCA improving contractility results from improved coupling of glycolysis to glucose oxidation by DCA promoting entry of pyruvate into the mitochondria to cause aerobic oxidative phosphorylation.

The experiments and data gathered in this thesis represent the insight into the importance of the RV in PAH therapies and how these therapies directly mediate the state of inotropy of the RV. A conclusion of greater importance is the better understanding of RV-specific changes in gene expression when the RV undergoes hypertrophy. By demonstrating the up-regulation of protein expression in RVH we are able to potentially tailor therapies to only improve performance of the diseased RV, while sparing the LV if it is otherwise normal. This is a true shift in paradigm as all current cardiac therapeutics effect both right and left ventricle.

Introduction:

Preface: Why study the RV?

The right ventricle has been overseen as the forgotten ventricle, thought merely to be a conducting vessel of deoxygenated venous blood to the lungs as first described by Sir William Harvey in 1616¹. Since this original description, there were other experimental data that supported the lack of importance of the right ventricle, including open-pericardium dog models from the 1950's that showed extensive cauterization of the free wall of the RV led to minimal decrease in cardiac output, without significant increase in central venous pressure². It was later recognized that in a close-chest animal model that RV infarction indeed lead to significant morbidity and mortality, based on the ventricular, pericardial, and ventilatory interactions that occur with the RV in-situ³. These animal experiments were further verified by human data showing the significant mortality associated with inferior myocardial infarctions involving the RV being a much worse predictor of death, shock, heart block, and ventricular arrhythmia⁴. As the relevance of RV pathology has increased by adverse clinical outcomes associated with RV disease, the interest to study RV function and failure has been put forth in 2006 by the National Heart, Lung, and Blood Institute Working Group⁵. The journal of the European Society of Cardiology dedicated a supplement journal to the importance of Right Ventricular Function in Pulmonary Hypertension in December 2007⁶, and the journal of the American Heart Association has published in 2008 a two part contemporary review in cardiovascular medicine on Right Ventricular Function in Cardiovascular Disease^{7,8}. This recent surge of literature on the right ventricle make it an opportune time to further investigate the molecular and metabolic changes that occur in RV disease and how these

ventricle-specific targets may lead to improved therapeutic strategies for treating the hypertrophied RV.

1.1.1 RV Embryology:

Cardiac development is the basis of normal structure and function of the right ventricle. Traditionally, it was believed that the entire contribution of cardiomyocytes that created the heart was derived from the anterior splanchnic mesoderm⁹. This tubular group of cardiomyocytes oriented in the craniocaudal axis with an anterior arterial pole and posterior venous pole then undergo dextroventricular looping, where the outflow tracts move further anterior and the venous poles move behind the outflow tracts¹⁰. The embryological development of the right ventricle as with the left ventricle was thought to be comprised from the primary heart field only¹¹. It was only recently recognized that there is a contribution from the pharyngeal mesoderm that migrates to form the arterial pole¹² and outflow tract of the heart¹³. This novel heart field called the secondary, or anterior, heart field was found to actually be the source of precursor cells that becomes the RV cardiomyocytes, such that the anterior heart field is where both arterial outflow tracts and RV myocardium originates¹⁴. This knowledge of the RV originating from different embryological sources than the LV is the framework for which a paradigm of RV specific medicine is born. It is not suffice to merely extrapolate data gathered from studies of the LV to the RV from the cellular level to ventricular function. The inherent differences between the RV and LV is the fundamental basis for the hypotheses and work of this thesis. Moreover, in-utero the RV and LV free-wall thickness is similar because

the pulmonary vascular resistance is high and there is a flat midline interventricular septum¹⁵. After birth and a decrease in pulmonary vascular resistance, along with closure of the ductus arteriosus and foramen ovale, there is an increase in RV compliance and regression of muscle mass and shifting of the interventricular septum toward the RV in a concave shape.

1.1.2 RV anatomy:

The structure of the RV is labeled based on its functional components. In normal anatomy, the RV is closest to the sternum and thus the most anterior chamber of the heart. The RV is defined by the annuli of the tricuspid and pulmonary valves. The RV has three components as described by Walt Lillehi from the University of Minnesota as: 1) the inlet, including the tricuspid valve and sub-valvular apparatus with valvular attachments of the chordae tendinae and subsequent attachments to the papillary muscles; 2) the apical myocardium, which is coarse and trabeculated; and 3) the infundibulum, which is the RV outflow tract and is smooth in nature¹⁶. The RV can be differentiated anatomically from the LV by several criteria. There is a septomarginal trabeculation that traverses inferiorly that attaches to the anterior papillary muscle, called the moderator band. The moderator band distinguishes the RV from the LV and it carries the right branch of the atrioventricular bundle of the conduction system. The moderator band is supplied from the first septal perforator off the left anterior descending artery and is usually spared in isolated right coronary artery infarctions¹⁷. Another distinguishing anatomical feature of the RV is that the atrioventricular valve is tricuspid, whereas it is

bicuspid on the LV. The overall shape of the RV is triangular in coronal-section and crescent shaped in cross-section, while the LV is elliptical in coronal-section and circular in cross-section⁸. The muscle layers that make the RV can be described as superficial and deep layers, with the superficial layer being directed circumferentially around the RV, and connecting with the fibers of the LV¹⁸. The deeper layers of muscle fibers are arranged more in the cranial to caudal orientation with contraction occurring from base toward apex. In contrast, the LV has a thick middle layer that is concentric around the ventricle that allows for the rotational torsion and vortex-like jet created from the LV. The RV free wall in adulthood is significantly thinner than the LV free wall at 3mm versus 9 mm, respectively¹⁹. The RV mass is also only 1/3 of the LV²⁰. Interestingly, the RV has a larger volume than the LV and has a greater end-diastolic volume than the LV by 12%, which in turn means that the RV ejection fraction is proportionately less than the LV. Since the RV is connected to the LV in series, the amount of blood pumped out of the RV (stroke volume) is similar to that of the LV. The RV also has three or more papillary muscles, while the LV only has two, and the RV papillary muscles can attach directly to the interventricular septum, unlike in the LV. The blood supply to the RV is also distinct. In a right-dominant system, which is the case when the right coronary artery supplies the posterior descending artery (80% of the time), the acute marginal branches supply the lateral free-wall of the RV, and the posterior descending artery supplies the posterior wall. The left anterior descending artery supplies the anterior wall and septal region of the RV²¹. The venous drainage of the RV is both into the coronary sinus and into the thebesian veins which comprise over 30% of the RV venous drainage. The thebesian veins drain directly into the RV and right atrium, while the structured cardiac

venous system drains into the coronary sinus.

1.1.3 RV Physiology

The normal physiology of the adult RV is determined by the three parameters that also define LV function, which are preload (filling conditions), inotropy (state of contractility), and afterload (resistance to forward flow). The preload to the ventricle is largely based on the volume status of the body, as the RV end-diastolic pressure is equal to the central venous pressure in the absence of ventricular and valvular dysfunction. This is why the majority of therapy targeted at improving RV function is based on fluid resuscitation to improve loading conditions of the RV. The Frank-Starling principle that was originally created to describe the improved stroke volume of contraction of the LV as it is volume loaded, also applies to the RV. As the RV is better filled, there is an increase in stroke volume ejected by the ventricle based on stretching load of the myofibrils. The sarcomere stretch to developed pressure relationship shows that the RV is more compliant than the LV²². The state of contractility is based on neurohormonal stimulation of the myocardium by both beta- and alpha-adrenergic tone. The contracting of the RV starts at the base of the RV at the inlet and extends to the apex, with the infundibulum contracting last¹⁸. As the RV contracts, there is an inward motion of the free-wall and shortening of the long axis where the inlet is displaced toward the apex as well as traction on the RV from LV contraction²³. Also, the larger surface of the RV compared to the LV allows for less inward wall motion to create similar stroke volumes as the LV.

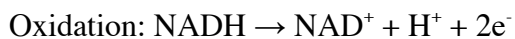
The afterload on the RV is a low pressure, highly compliant pulmonary vascular bed. Since the RV systolic pressures are only 1/6 of the LV systolic pressures, there is an early peak and a brisk fall in developed pressure compared to the longer and more rounded LV developed pressure²⁴. This also explains the shorter time required for RV isovolumic contraction, as the afterload is much less than that of the LV. The low impedance that the RV faces does not allow the RV to handle acute increases in afterload like the LV, where RV stroke volume declines rapidly with small increases in afterload²⁵. For simplicity, the pulmonary vascular resistance, (calculated from the difference in mean pulmonary arterial pressure from the left atrial pressure divided by the cardiac output) is the index of RV afterload. This is not completely accurate as there are static and dynamic pulmonary vascular factors influencing impedance to RV contraction, and tricuspid valvular regurgitation that can decrease the afterload faced by the RV²⁶. There can also be RV outflow tract obstructions that occur, predominantly in congenital heart disease that lead to RV hypertrophy without increased pulmonary vascular resistance.

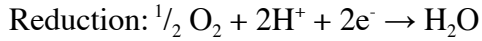
One of the intriguing relationships of the RV and LV is the concept of ventricular interdependence. Since the RV and LV share a common ventricular septum, conditions that alter loading of the RV can directly affect the LV through the dynamics of the septum, that lead to systemic consequences of RV filling. In the normal state of systole, the LV contraction including fractional shortening of the septum accounts for 1/3 of RV ejection volume²⁷. When there is excessive diastolic filling of the RV or increased pulmonary vascular resistance causing increased RV distension, there is a shifting of the interventricular septum toward the LV and decreases LV filling by increasing LV

diastolic pressures, and hence decreasing LV stroke volumes²⁷. Conversely, when the LV is volume overloaded or faces acute increasing in systemic vascular resistance, there is a decrease in RV filling from restriction by the interventricular septum²⁸.

1.1.4 RV Metabolism

There is a great paucity in the literature of the metabolic profiles between the normal right and left ventricle. As cardiomyocytes from both RV and LV are phenotypically similar, we must extrapolate the literature to describe the principles of myocardial metabolism in the normal RV, though the studies described look at data from the LV. In a normal resting state, >95% of ATP comes from oxidative phosphorylation through the mitochondrial electron transport chain, while the rest comes from glycolysis²⁹. Given the heart's extreme metabolic demands, and low ATP storage (5mmol/g wet weight), the heart must turnover the entire ATP pool every 10 seconds³⁰. Roughly 2/3 of ATP hydrolysis is utilized for sarcomere lengthening (diastole) of the ventricle, while the rest is used for the sarcoplasmic reticulum Ca²⁺-ATPase and ionic channels³¹. The oxidative phosphorylation at the level of the mitochondria occurs through the reducing agents NADH and FADH₂ as they are oxidized to release electrons and a hydrogen ion in three basic equations of phosphorylation, oxidation, and reduction:





The metabolic substrate used in resting state oxidative phosphorylation is derived from fatty acid β -oxidation, which comprises 60-80% of energy production, while the rest comes from glucose-oxidation coupled with glycolysis³². Glucose enters the cardiomyocyte through glucose transporters expressed on the surface of cardiomyocytes. Once glucose enters the cell, it is rapidly phosphorylated by hexokinase to create glucose-6-P, which is then trapped inside the cardiomyocyte. Glucose-6-P has several metabolic fates, and can be fully exploited for energy production by coupling glycolysis to glucose oxidation in the mitochondria in oxygen consuming aerobic respiration. Glucose-6-P can end its energy production after glycolysis, in anaerobic respiration when pyruvate gets converted to lactate, this form of respiration only produces 2 ATP per glucose molecule, whereas in aerobic respiration there is an additional 32 ATP molecules produced for a total of 36 ATP per glucose molecule. The critical step in the regulation of glucose oxidation is the conversion of pyruvate to acetyl-CoA by pyruvate dehydrogenase (PDH). Pyruvate dehydrogenase is inhibited by PDH kinase (PDK) and activated by PDH phosphatase. Another level of control on glucose oxidation occurs at the level of the Randle cycle. As per the Randle cycle, Acetyl-CoA produced through β -oxidation inhibits PDK activity. This relationship allows for a reciprocal relationship between glucose oxidation to β -oxidation. Glucose-6-P can also be stored as glycogen for rapid use when needed later. Finally, Glucose-6-P can be shunted down the pentose phosphate pathway where two molecules of NADP^+ are reduced to NADPH and glucose-6-P is

converted into ribulose-5-P. Rates of glucose and fatty acid oxidation are inversely related, and were originally defined by Philip Randle in 1963³³. As per the Randle's cycle, when fatty acid oxidation is reduced there is a reciprocal increase in glucose oxidation. This metabolic phenotype over portion of fatty acid to glucose oxidation shifts significantly in disease and will be addressed in subsequent paragraphs.

1.1.5 Differences between the RV and LV:

The physiology and pathobiology of the RV is quite different from the LV. While the LV can compensate well to acute or chronic increases in its afterload (i.e. systemic hypertension) the RV does not. A patient with systemic hypertension can live asymptomatic for many decades whereas a patient with pulmonary hypertension becomes quickly symptomatic because of RV failure and decreased cardiac output; and patients with PAH have only a few years of life expectancy. Acute increases in the RV afterload cannot be tolerated at all. For example, a significant rise in PVR because of thromboembolism can result in RV failure, decrease in cardiac output, hypotension and death in less than one hour; similar increases in PVR occurring during transplant or congenital heart disease surgery are quite difficult to manage and often lead to death. This has to do mainly with the lack of RV-specific therapies. The existing therapies for LV failure (whether targeting the LV, i.e. inotropes, or targeting its afterload, i.e. the systemic vasculature, i.e. systemic vasodilators), often cannot be applied to these conditions, where the systemic vessels are intact and the LV is functionally normal, but with decreased volume due to the expansion of the pressure overloaded RV and the flattening of the septum. For example, increasing the inotropy and chronotropy in such an

LV will result in further decreases in volumes and filling times, actually decreasing cardiac output; and a decrease in systemic pressure is catastrophic for a patient with pulmonary hypertension and RV failure. Another example of the differences of the 2 ventricles and their response to therapy comes from the very recent experience with synthetic Brain Natriuretic Peptide (BNP). BNP is expressed in the LV and its levels in the serum correlate with the degree of LV failure^{34, 35}. We, and others, have shown that BNP is also expressed in the RV and its levels in the serum correlate with the severity of RV failure and PAH. It is thought that the expression of BNP might be an inadequate compensatory response (BNP also has vasodilating and natriuretic properties, beneficial to the heart failure syndrome). This forms the rationale for its exogenous administration as a means of therapy. However, while exogenous BNP (nesiritide) significantly improves cardiac output, symptoms and performance in patients with LV failure (it is now an approved therapy for acute LV failure)³⁶ its administration in patients with pulmonary hypertension and RV failure has not beneficial effects and cardiac output does not increase^{37,38}.

The biochemistry and the metabolism of the 2 ventricles is different, not surprising if one considers that the 2 chambers are designed to function under quite different hemodynamic conditions (the normal pulmonary pressures are only 30-40% of the systemic pressures and the venous return in the RV is much more erratic (position, activity etc) compared to the venous return in the LV. The very thin and compliant RV is well suited for these conditions but unable to defend to rises in afterload. Even the embryology of the RV is different from that of the LV. The RV develops from a population of myocardial precursor cells in the pharyngeal mesoderm, the anterior heart

field, and is distinct from the linear heart tube from which the LV arises¹⁴. Therefore concepts or therapies developed for the LV cannot be extrapolated to the RV and more work is needed to study the differences of the 2 ventricles in order to develop the much-needed RV-specific therapies. The ideal RV-specific therapy needs to a) increase RV but not LV inotropy and b) decrease the RV afterload (decrease the PVR) without affecting the systemic vasculature.

Based on recent clinical observations and preliminary experiments in human tissues and animal models, we hypothesized that PDE5i are a potential RV-specific therapy. In addition to the well-recognized ability of the PDE5i to dilate the pulmonary vasculature without affecting the systemic vasculature, we now provide evidence and propose to study further the ability of these drugs to increase RV, but not LV inotropy, thus fitting the profile of the ideal RV-specific therapy.

1.1.6 RV remodeling and RV hypertrophy:

Following acute increases in the afterload, the RV initially dilates and via the Frank Starling mechanism this initially tends to preserve the cardiac output. In severe increases of the afterload the RV is unable to compensate, resulting in decrease in cardiac output, hypotension and death; a scenario that is not uncommon in acute pulmonary thromboembolism or in transplant surgery when a normal heart is placed in a patient with higher than normal PVR. In less severe, sub-acute or progressive increases in the afterload (as it happens for example with patients developing PAH) signaling leading to cardiac hypertrophy is activated and even within a matter of days the RV mass starts to increase and the free wall thickens in another attempt to preserve contractility and cardiac

output. The thickened and hypertrophied RV however, as we discussed above, is far less effective than LVH. The reason for this is obviously unknown since essentially nothing is known regarding the mechanisms underlying RVH. Usually concepts from the LV are extrapolated to the RV, since often both clinicians and basic scientists are not viewing the 2 ventricles as different entities.

The “pathologic” RVH (i.e. RVH in response to increased PVR due to a disease) is reminiscent of the “physiologic” RVH that characterizes the heart of the newborn. All mammals are born with a hypertrophied RV and normal LV. This is because the circulation in utero is unique; constricted PAs do not allow for the blood to flow through the lungs (which are not oxygenated) and shift the blood to the placenta (the “fetal lung”) through the ductus arteriosus. This increased PVR explains the RVH in utero. Upon birth, and within minutes, the PAs dilate and the ductus arteriosus constricts, initiating the transition to the adult circulation. This explains the fact that the RVH seen in the normal fetus regresses quickly after birth when the PVR drops dramatically as the lungs are ventilated, and within days to weeks the RV mass and thickness decreases to the adult size. Patients that are born with congenital heart disease (such as intra-cardiac shunts, etc), maintain higher PVR (the transition to the normal pulmonary circulation never occurs) and therefore the transition to the thinner adult RV never occurs. It is remarkable that this “persistent, fetal” RVH that accompanies them throughout their adult lives is much more competent than the pathologic RVH that we see in patients with PAH. Patients with Eisenmenger’s syndrome have a far better prognosis than patients with PAH despite similar rises in PVR³⁹. It is likely that the RV remodeling in pathologic RVH is not as optimal as the one in physiologic RVH. While this is fascinating, it is not the

subject of this proposal. The reason that this “Eisenmenger’s story” is important for us is that it clearly shows that it is possible that with the appropriate physiologic or molecular manipulation, the pathologic RVH heart may behave like the physiologic RVH; i.e. the suboptimal remodeling in RVH may be *dynamic*.

In LVH and in LV failure, the “fetal heart genetic and metabolic profile” is thought to be reactivated, and this might be, at least in part, true for RVH. However, this field is complicated by the fact that often scientists do not distinguish RV versus LV in the fetal heart, which, as we discussed are quite different. In fact, a few recent reports are describing different metabolic profiles in RVH versus LVH and this is supported by some preliminary data from our lab, describing significant differences in the mitochondrial function between the RV and the LV both in human and animal hypertrophied hearts. Similarly, as we show in our preliminary data, PDE5 is expressed in the fetal RV but not in the LV.

1.1.7 Dichloroacetate: a metabolic modulator of mitochondrial function

As described above, the Randle cycle contributes to an inversely proportional ratio of glucose to fatty acid oxidation. A well-described metabolic phenotype of cardiac hypertrophy is the increased glycolytic phenotype that exists. Where there is increased mitochondrial glycolysis and up-regulation of glucose transporters into the cell, yet there is a lack of glucose oxidation. This is observed by increased lactate production by hypertrophic myocardium, utilizing glucose through glycolysis for anaerobic respiration. As cardiac hypertrophy and transition into heart failure is associated with subendocardial ischemia and an overall lack of vascularization for the increased muscle mass. It follows

that the myocardium is in a relative state of ischemia. As such, the metabolic switch to anaerobic respiration through glycolysis and lactate production from pyruvate, rather than pyruvate entry into the mitochondria by action of PDH in glucose oxidation, becomes the predominant phenotype. A potential short-term solution to improve energy production in the failing heart is to increase glucose oxidation, as the relative ischemia of the heart can be improved by coronary vasodilation in the short-term to improve oxygen delivery. One such potential target is to remove tonic inhibition of PDH by PDKinase (PDK). Since PDK inhibits PDH and is up regulated in many glycolytic phenotypes, including PAH⁴⁰ and cancer⁴¹, therapeutically targeting PDK with an inhibitor may lead to an increase in glucose oxidation and improve cardiomyocyte energy production in the setting of cardiac hypertrophy. A simple therapeutic agent that has shown to be a potent inhibitor of PDK is Dichloroacetate (DCA)⁴². Indeed, in the two diseases above, PAH⁴³ and cancer⁴⁴, DCA did increase glycolysis to glucose oxidation coupling, as seen by the decrease in lactate production, which in turn led to a normalization of mitochondrial function and energy metabolism. In cancer, the normalization of mitochondrial function allowed for programmed cell death by apoptosis to occur as the increase in reactive oxygen species (ROS) production and opening of voltage-dependent anion channels (VDAC) allowed for cytochrome C to be released from the mitochondria as well as apoptosis inducible factor⁴⁴. The findings that many cancers may share a common distal pathway of aerobic glycolysis have brought insight into a new potential metabolic targeting of therapy in oncology⁴⁵. In PAH, the normalization of mitochondrial function led to apoptosis in pulmonary arterial smooth muscle cells, which in turn led to regression of the disease phenotype⁴³. In both PAH and cancer, oxygen supply is not insufficient, there is actual

aerobic glycolysis that occurs in cancer. In cardiac hypertrophy, the lack of oxygen supply from inadequate vascular supply indeed limits the amount of compensated hypertrophy possible⁴⁶. We hope to utilize observations from these other two diseases with DCA treatment to improve contractility in the hypertrophied RV, which may further improve function of the RV-PA unit that is diseased in PAH.

1.1.8 The RV-PA unit

The RV and PA system function as pump and capacitance for deoxygenated blood, respectively. There has been a compartmentalization of the two, with a large volume of study on the pulmonary vasculature in PAH⁴⁷, and a general neglect of RV specific therapies. This seems counterintuitive, as the best predictor of survival in patients with PAH is the status of RV function⁵. The lack of focus on the RV as at least an equal if not greater partner in patients with PAH may explain the clinical lack of efficacy of many approved therapies for PAH, which show in-vitro and in-vivo significant improvements in regression of PVR, yet fail to lead to significant improvements in functional status or mortality from disease.

1.1.9 Right heart angiography

The current gold standard of right heart function is invasive catheterization and angiography. The pressures measured directly, and flow calculated indirectly provides data that is correlated with patient prognosis in PAH, including right atrial pressures, cardiac output, and mean PA pressures⁴⁸. Though invasive, right heart catheterization is associated with an extremely low rate of procedural associated mortality of 0.055%⁴⁹. The value of right heart catheterization in PAH is that it allows for diagnosis of PAH,

identification of possible etiology of PAH, and aforementioned markers of prognosis. Unfortunately, there is variability in procedural techniques for acquiring data that are to be minimized by taking all measurements at end-expiration, which is the point in the respiration cycle of least negative intrathoracic pressure, or the point where intrathoracic pressure is most similar to atmospheric pressure⁵⁰. The distinction of point in the respiration cycle for data acquisition is more important in patients with significant variations in thoracic pressures during respiration, including those with COPD, obesity and restrictive lung disease. Cardiac output measured with right heart catheterization is based on thermodilution and is accurate most patients, except those with severe tricuspid regurgitation or cardiogenic shock⁵¹. Another important feature to right heart catheterization is the ability to assess treatment effect in PAH. When patients with PAH are challenged with a vasodilator acutely to determine the effect on PA pressures, a favorable vasodilator response to inhaled nitric oxide is determined by a >10mmHg to a value of <40mmHg without a drop in cardiac output⁵².

1.1.10 Right-sided pressure volume loops

Pressure-volume (PV) loops are well described in LV hemodynamics by the effects of preload (LV filling), afterload (aortic valve/systemic vascular impedance), and inotropy (state of contractility) on cardiac output and performance⁵³⁻⁶⁵. There is a lack of studies on PV loops in the RV, though there is evidence that reproducible results are possible in animal models⁶⁶. A reluctance to utilize PV loops in the RV results from a misconception that accurate measurements are not attainable, given the crescent-like shape of the normal RV, as it wraps around the conical shaped LV. This is true in the normal physiology of the RV, however in disease the morphology of the RV becomes more like the LV, as the

interventricular wall flattens and RV geometry is shifted more toward a conical shape. Use of PV loops by conductance catheters are not only possible, but critical to the interpretation of PAH therapies on the RV, as we will demonstrate the significant effect therapies including phosphodiesterase-5 inhibitors⁶⁷⁻⁶⁹ and endothelin receptor antagonists⁷⁰⁻⁷² have on the myocardium. The effects of approved and experimental therapies may be positive or negative, leading to a clinical disparity in expected and observed efficacy. One such example of an experimental PAH therapy, which is used in the treatment of chronic myelogenous leukemia, is the tyrosine kinase inhibitor imatinib mesylate (Gleevec). A therapy that may lead to increased apoptosis in PA smooth muscle cells in PAH, however there is also significant cardiotoxicity caused by imatinib⁷³.

1.1.11 Magnetic resonance imaging of the RV

A mode of imaging that may provide significant advances to the evaluation of the RV in a comprehensive manner is magnetic resonance imaging (MRI)⁷⁴. Since MRI is non-invasive, and is becoming increasingly available at many centers, it may become the “single stop” assessment tool for the RV. Many cardiac MRI studies utilize contrast-enhanced studies using small volumes of peripherally injected gadolinium, which is a lanthanide element and the atomic number is 64. Gadolinium is the contrast agent in MRI because of it is a paramagnetic element, which means that it only exhibits magnetic properties when exposed to a magnetic field. Whereas ferromagnets always exhibit magnetic properties and are considered to be the permanent magnets. Magnetic resonance imaging can provide RV specific structural data on RV volumes, RV myocardial mass, and pulmonary angiography. The imaging modality can also provide important physiological data on RV ejection fraction and pulmonary vascular perfusion. Of equal

importance, the modality is time efficient and can acquire these data with current software performing analyses to give these values in under one hour. MRI as an imaging technique has advanced significantly over the last decade, including ECG gating, and respiratory subtraction to allow for decreased image artifact, allowing for more accurate measures of the RV volume and mass in patients with PAH^{75, 76}. Accurate mass and volumes of the RV have also been reported on normal patients using standardized data acquisition protocols²⁰.

1.1.12 Phosphodiesterases (PDEs)

Phosphodiesterases are a diverse family of enzymes that hydrolyze cyclic nucleotides and by regulating the levels of cAMP and cGMP play a critical role in multiple cell signaling pathways. PDEs are in every cell in the body but there is substantial diversity in the expression of the PDEs in the 11 gene families (PDE1 to PDE11) that have been described so far. Each PDE has different affinity for cAMP or cGMP; this along with their diversity in tissue expression and the development of specific PDE inhibitors (PDEi) have allowed their evolving role as major therapeutic targets for a number of diverse diseases⁷⁷. PDEs in the heart: Currently, the PDEs thought to be expressed in the heart are PDE1, PDE2, PDE3, PDE4D, and PDE7⁷⁸. PDE1 is Ca⁺⁺/calmodulin stimulated, and has the ability to hydrolyze both cAMP and cGMP with similar efficiency, but despite its emerging role in the vasculature it appears to have a minor role in the heart⁷⁹. PDE2 is cGMP-activated that hydrolyses cAMP, and has an important role in blunting beta-adrenergic stimulation via the beta-3-receptor-NO-cGMP pathway, which acts as a negative feedback loop to the positive inotropic response to sympathetic stimulation⁸⁰. In that sense PDE2 might be involved in the mechanisms that we propose

to study here. We are aware of this possibility but although we plan to measure its levels in our models along with PDE5, we will not pursue this in detail, in order to stay focused in PDE5. This is because we have a number of specific PD5 inhibitors already clinically available and along with the fact that the expression pattern of PDE5 is narrower, we can build a more clinically relevant and translational research program. The most studied PDE in the heart is PDE3, which hydrolyses cAMP, and has been exploited clinically with inhibitors causing increased inotropy, such as milrinone and enoxamone^{35,81}. PDE4, another cAMP hydrolyser, was not thought to have a significant role in the heart until recently. Lehnart et al recently described the role of PDE4 in intracellular Ca⁺⁺ handling and showed that the cardiac ryanodine receptor, required for excitation-contraction coupling, exists in a complex with PDE4⁸². The role of PDE7 in the heart is lacking detail thus far⁸³.

PDE5, is thought be absent from in the myocardium and is supposed to be limited only to the heart vasculature (along with minor expression in visceral smooth muscle, the penile circulation, etc). Sildenafil was developed as a specific PDE5i for the treatment of erectile dysfunction. However, its first year of use was complicated by several cardiac-related deaths that alarmed the medical community. It was soon realized that these deaths were likely due to hypotension from the combination of sildenafil with nitrates (taken as patients having sex were developing angina). Nevertheless, research in the possible role of PDE5 in the heart was ignited and many reports showed lack of any meaningful PDE5 expression in the heart (other than the coronary vessels). Most of these studies were focusing on normal animal hearts and healthy volunteers or patients with angina. Expert panels and professional bodies like the ACC/AHA writing group published position

statements on the effects of sildenafil, clearly stating that it lacks primary effects on the myocardium: “ *Furthermore, PDE5 is not present in cardiac myocytes, and sildenafil has been shown to have no direct inotropic effects...., page 171*”⁸⁴. Even now, publications in leading journals, do not list PDE5 as one of the PDEs present in the myocardium ⁸⁵.

There is some evidence however that suggests that this might not be true. In 2002 we were the first to show that PDE5 is a specific pulmonary vasodilator in patients with PAH. Along with our next publication on this subject, we showed that this mediated by opening of the large conductance calcium-activated potassium channels (BKCA) in PASMC, leading to PASMC hyperpolarization, closure of the voltage-gated calcium channels, decrease in intracellular Ca⁺⁺ and vasodilatation. The PDE5-induced increase in cGMP activates PKG, which then phosphorylates BKCA channels, activating them. PKG has many other targets, all resulting in decreasing intracellular Ca⁺⁺ and promoting vasodilatation. This is in contrast to the cAMP-activated PKA, who’s net result is increase in Ca⁺⁺ and vasoconstriction. Nevertheless, our clinical work showed that oral sildenafil (75mg) was equally effective with maximal doses of inhaled NO (iNO, 80ppm) in decreasing PA pressure⁸⁶ Because of its route of administration, iNO has direct effects in the lung vessels and spares the heart. iNO did not increase the cardiac output but, to our surprise, sildenafil did. If the only way to increase cardiac output was to decrease the RV afterload, then iNO should have increased cardiac output as well. This suggested that sildenafil might have had primary inotropic effects in the RV. We did not comment on this possibility in our paper since the field was then dominated by the notion that PDE5 was absent from the heart. Few years later, Wilnkins et al compared bosentan (an endothelin receptor blocker) to sildenafil in chronically treated PAH patients. He showed

that while the 2 therapies decreased PA pressure similarly, only sildenafil decreased RV mass significantly, also raising the possibility of direct, anti-hypertrophic actions in the heart. A Johns Hopkins group (with which we now collaborate in this proposal) showed with a publication in Nature Medicine that PDE5 was upregulated in rodents with LVH due to transverse aortic constriction (TAC)⁶⁹. PDE5i therapy caused a regression in LVH, despite ongoing TAC. They showed that the activation in cGMP-PKG pathway reversed the upregulation of several genes in cardiomyocytes belonging to the “hypertrophy/fetal” heart gene program. The authors did not study RV and did not study effects on contractility acutely or chronically. This remains the only group that has published with this one publication that PDE5 is upregulated in the hypertrophied LV; yet nothing is available on PDE5 in the RV or in human tissues, important topics that we are addressing in our proposal and preliminary data. In a follow up publication from the same group⁸⁷, healthy patients were studied using load-independent ECHO parameters, in response to oral sildenafil. Once again the group showed lack of hemodynamic effects in the heart, other than an inhibition of the adrenergic stimulation (from dobutamine infusion) in the heart. They postulated that despite its very low expression, PDE5 might be strategically compartmentalized, allowing for its involvement in the cGMP-PKG-NOS3 pathways in the adrenergic stimulation of the myocardium. This study did not evaluate effects on the RV (which is extremely difficult to be studied with ECHO due to its complex geometry).

1.1.13 Compartmentalization of cAMP/cGMP, PDEs and PKA/PKG in the heart:

The signaling caused by cyclic nucleotides is very complicated, as there is a high degree of compartmentalization in the heart⁸⁸. This is an evolving concept with many unanswered questions. It appears that overall intracellular rises in cAMP and cGMP are

not enough or necessary to cause specific regulation of target proteins. The activity of the cyclic nucleotide associated protein kinases, protein kinase A (PKA) for cAMP and protein kinase G (PKG) for cGMP require anchoring to a target site to have spatial-temporal control of phosphorylation. PKA-anchoring proteins orchestrate the coordination of multiple cAMP/PKA dependent signaling mechanisms⁸⁹. In the case of cGMP/PKG, there has not been a specific anchoring protein identified thus far⁸⁸. PKG is phylogenetically similar to PKA⁹⁰, and is likely to have similar anchoring protein regulated activity. So far, PKG has been shown to directly associate with troponin T⁹¹, myosin⁹², and natriuretic peptide receptor⁹³.

Local inhibition of PDE-cyclic nucleotide-PKG complex for example, within these strategic complexes around anchoring proteins, might be more important than what one would predict following a “generalized” increase in the levels of the cyclic nucleotide. These complexes might also be altered in disease states like hypertrophy. Nevertheless, a finding that its critical to the development of our hypothetical model is that PKG activity is suppressed in hypertrophy⁹⁴. This explains the observations that the negative effects of NO (which causes increase in cGMP and PKG activation) are blunted in hypertrophy. It is also in keeping with the fact that cGMP is not a negative inotrope in knockout mice lacking PKG1, the isozyme found in the heart. If this is true in RVH, then the increase in cGMP caused by PDE5i might not lead to negative inotropy, because PKG (its effector) is inhibited/downregulated. Rather, the increase in cGMP might inhibit the cGMP-sensitive PDE3, causing an increase in cAMP-PKA and positive inotropy (see proposed mechanism in Figure 12).

1.1.14 PDE5 expression and NFAT: Essentially nothing is known about the regulation of expression of PDE5, particularly in disease states. Our preliminary work and our hypothesis suggest that PDE5 might be a part of the fetal group of genes activated in hypertrophy. A leading transcription factor that has been shown to “orchestrate” the multiple pathways and mechanisms involved in hypertrophy is the Nuclear Factor of Activated T-cells (NFAT)⁹⁵. 4 out of the 5 isoforms that have been described, are activated by calcineurin, which is activated by sustained increases in intracellular Ca⁺⁺, a very early event in hypertrophy. NFAT is found in the cytoplasm in a hyperphosphorylated form; it is de-phosphorylated by calcineurin at multiple conserved serine residues in the N-terminus, and a nuclear localization signal is revealed^{96, 97}. Then NFAT translocates to the nucleus and causes transcription of genes associated with cardiac hypertrophy, including BNP. Indeed, constitutive expression of NFAT causes cardiac hypertrophy without any up-stream stimulus, thus implying it’s implicit control of cardiac hypertrophy^{98, 99}. In the nucleus NFAT forms complexes with other important transcription factors like GATA4, AP1 or Mef, thus achieving a high degree of integration of multiple signaling pathways. NFAT activation promotes BNP transcription in cardiomyocytes¹⁰⁰ and it is possible that it also increases PDE5 expression. The promoter region of PDE5A has been described as a 139 base-pair region, which includes 78 base-pairs of the first exon of PDE5A¹⁰¹. When stimulated by cGMP and cAMP, the promoter region expands both up and down stream and has at least two putative NFAT binding sites, shown by GGAAA, the NFAT binding sequence. There are other putative binding sites for NFAT outside the described promoter region, as NFAT can bind upstream of the promoter region where polymerase II binds and can activate transcription

from more distant regions¹⁰². A decrease in the PKG activity that has been described in hypertrophy, is compatible with NFAT activation. This is because the decreased PKG activity will promote an increase in intracellular Ca⁺⁺, thus activating calcineurin and NFAT; The resulting increase in PDE5 expression will decrease cGMP, further increasing Ca⁺⁺ potentiating a feedback loop.

1.1.15 Endothelin in the Heart:

Endothelin-1 (ET-1) is a 21 amino acid peptide discovered in 1988¹⁰³. Endothelin-1 is predominantly secreted by vascular endothelium, which leads to paracrine potent vasoconstrictive effects in the surrounding vascular bed¹⁰⁴. In the processing of Endothelin-1, it is translated from mRNA to a large 205 amino acid peptide prepro-endothelin, which is then modified to become big-endothelin (a 38 amino acid peptide), which in turn is cleaved by Endothelin converting enzyme-1 to ET-1. Though the pulmonary vascular endothelium produces the majority of circulating endothelin-1, the G-protein coupled Endothelin Receptor A (ET_A-R) and B (ET_B-R) are found on pulmonary smooth muscle cells¹⁰⁵, while only ET_A-R is found in the heart myocardium¹⁰⁶. Since there is a significant expression of ET_A-R on the sarcolemma of cardiomyocytes, there is also a significant role for ET-1 stimulation in cardiomyocytes. Beyond the well-described role of ET-1 in the induction of cardiac hypertrophy¹⁰⁷⁻¹⁰⁹, ET-1 stimulation can cause increased inotropy acutely. There is an increase in cardiomyocyte contractility by ET-1, which is consistent in the literature, though the precise mechanism for increased contractility remains controversial. The downstream effector after ET-1 stimulation of ET_A-R is argued to be actions mediated by protein kinase C (PKC) after activation by diacylglycerol (DAG) by several groups¹¹⁰⁻¹¹³. Though there are conflicting results

showing that the increase in cardiomyocyte contractility is caused by downstream effects of phospholipase C (PLC) and not PKC^{114, 115}. At the level of intracellular calcium fluxes leading to contraction, there is further controversy based on the role of intracellular alkalosis. There is data supporting sensitization of the cardiomyocyte to calcium and increased contraction by ET-1 stimulation through activation of the Na⁺/H⁺ exchanger at the level of the sarcolemma causing an increase in pH¹¹¹. This is also disputed in the literature that ET-1 can cause increased contractility through PKC without altering pH¹¹⁶. Moreover, others implicate reverse mode of the Na⁺/Ca²⁺ exchanger through Na⁺/H⁺ exchanger dependent and independent pathways¹¹⁷.

1.1.16 Endothelin Receptor Antagonists:

Endothelin receptor antagonists is a family of drugs currently approved for the treatment of PAH in North America and Europe and vary in affinity for Endothelin Receptor A and B. Where Bosentan (Tracleer; Actelion Pharmaceuticals) is a mixed ET_A-R and ET_B-R antagonist which was the first ETRA approved in 2001 for the treatment of PAH with ET_A-R: ET_B-R affinity ratio of 40:1¹⁰⁴. A more recently developed pharmaceutical agent that was approved in Europe in 2006 was Sitaxsentan (Thelin; Encysive Pharmaceuticals) with an ET_A-R: ET_B-R affinity ratio of 6000:1. The varying affinity of ETRA to ET_A-R versus ET_B-R will likely have significance on clinical efficacy as both receptors are expressed in the pulmonary and coronary vasculature, though this has yet to be elucidated, and likely to be examined in ongoing and future clinical trials.

The ET_A-R binding of ET-1 leads to a significant vasoconstriction by G-protein coupled activation of phospholipase C, which leads to potentiating of vasoconstriction by 3

pathways. Firstly, there is a hydrolysis of phosphatidylinositol-4,5 biphosphate into inositol triphosphate and diacylglycerol, where inositol triphosphate leads to increased calcium release from the sarcoplasmic reticulum. Secondly, the metabolite of inositol triphosphate (inositol tetraphosphate) combined with increased intracellular calcium released by calcium stores causes voltage-gated L-type Ca^{++} channels to activate and opening further influx of calcium into the cell. Thirdly, diacylglycerol activates protein kinase C, which also has downstream effects of increased contraction¹¹⁸.

The genesis of ETRAs was originally targeted for the treatment of congestive heart failure (CHF). Pre-clinical studies demonstrated that patients with CHF had increased serum levels of endothelin and it was hypothesized that blocking this vasoconstrictive peptide may lead to coronary, systemic, and pulmonary vasodilation causing improvement in symptoms¹⁰⁴. The theoretical benefits of ETRAs in CHF did not correlate with the results of clinical trials in both the management of acute and chronic CHF¹¹⁹. In spite of the lack of efficacy observed in CHF trials, the predominance of endothelin production and ET_A -R in the pulmonary vasculature in both control and PAH provided optimism for investigators who considered the use of this orphan family of therapeutics for the treatment of PAH¹²⁰. In the landmark randomized controlled clinical trial in 2001 there was a mild, yet significant improvement in six-minute walk test in patients with PAH treated with Bosentan at a dose of 125mg¹²¹. This clinical trial led to the FDA approval of bosentan for the treatment of PAH.

The widespread use of ETRAs in the treatment of PAH has been very successful, yet the specific effects of ETRAs on the RV remain unknown. It is well described that PAH

leads to the compensatory pressure overload hypertrophy of the RV resulting in RVH and eventual RV failure. Interestingly, endothelin is a known cardiac inotrope, leading to increased contractility¹¹⁴, though the ET_A-R is only expressed in low concentrations in the RV compared to the normal LV, and thus ETRAs are unlikely to have significant decreases in normal RV contractility. However, in PAH and subsequent RVH, there is a significant increase in both endothelin-1 and ET_A-R expression¹²². This at least suggests that ETRAs may have a negative affect on RVH contractility in patients with PAH and RVH utilizing these agents. Indeed, the clinical efficacy of ETRAs is less than expected by the significant decrease in pulmonary vascular resistance without improvement in cardiac output¹²³. This would imply that a decrease in pulmonary vascular resistance that is not accompanied by an increase in cardiac output is secondary to a decrease in cardiac inotropy. It is based on this clinical outcome of only minor improvements in patient functionality on treatment with ETRAs that we hypothesize that ETRAs decrease contractility in patients with RVH.

In part, lessons learned from CHF trials may lead to the better understanding of the effects of ETRAs on the hypertrophied RV. This is very clinical relevant in the design and interpretation of clinical trials evaluating ETRAs as therapies for PAH.

References:

1. Harvey W. *Exercitiatio Anatomica de Motu Cordis et Sanguinis in Animalibus*; 1628.
2. Kagan A. Dynamic responses of the right ventricle following extensive damage by cauterization. *Circulation*. 1952;5(6):816-823.
3. Goldstein JA, Vlahakes GJ, Verrier ED, Schiller NB, Tyberg JV, Ports TA, Parmley WW, Chatterjee K. The role of right ventricular systolic dysfunction and elevated intrapericardial pressure in the genesis of low output in experimental right ventricular infarction. *Circulation*. 1982;65(3):513-522.
4. Mehta SR, Eikelboom JW, Natarajan MK, Diaz R, Yi C, Gibbons RJ, Yusuf S. Impact of right ventricular involvement on mortality and morbidity in patients with inferior myocardial infarction. *J Am Coll Cardiol*. 2001;37(1):37-43.
5. Voelkel NF, Quaife RA, Leinwand LA, Barst RJ, McGoon MD, Meldrum DR, Dupuis J, Long CS, Rubin LJ, Smart FW, Suzuki YJ, Gladwin M, Denholm EM, Gail DB. Right ventricular function and failure: report of a National Heart, Lung, and Blood Institute working group on cellular and molecular mechanisms of right heart failure. *Circulation*. 2006;114(17):1883-1891.
6. Sanchez MA, Torbicki A. Foreword: right ventricular function and pulmonary hypertension. *European Heart Journal Supplements*. 2007;9(Supplement H):H3-H4.
7. Haddad F, Doyle R, Murphy DJ, Hunt SA. Right ventricular function in cardiovascular disease, part II: pathophysiology, clinical importance, and management of right ventricular failure. *Circulation*. 2008;117(13):1717-1731.
8. Haddad F, Hunt SA, Rosenthal DN, Murphy DJ. Right ventricular function in cardiovascular disease, part I: Anatomy, physiology, aging, and functional assessment of the right ventricle. *Circulation*. 2008;117(11):1436-1448.
9. Yutzey KE, Kirby ML. Wherefore heart thou? Embryonic origins of cardiogenic mesoderm. *Dev Dyn*. 2002;223(3):307-320.
10. Harvey RP. Patterning the vertebrate heart. *Nat Rev Genet*. 2002;3(7):544-556.
11. Viragh S, Challice CE. Origin and differentiation of cardiac muscle cells in the mouse. *J Ultrastruct Res*. 1973;42(1):1-24.
12. Kelly RG, Brown NA, Buckingham ME. The arterial pole of the mouse heart forms from Fgf10-expressing cells in pharyngeal mesoderm. *Dev Cell*. 2001;1(3):435-440.
13. Mjaatvedt CH, Nakaoka T, Moreno-Rodriguez R, Norris RA, Kern MJ, Eisenberg CA, Turner D, Markwald RR. The outflow tract of the heart is recruited from a novel heart-forming field. *Dev Biol*. 2001;238(1):97-109.
14. Zaffran S, Kelly RG, Meilhac SM, Buckingham ME, Brown NA. Right ventricular myocardium derives from the anterior heart field. *Circ Res*. 2004;95(3):261-268.

15. Hopkins WE, Waggoner AD. Severe pulmonary hypertension without right ventricular failure: the unique hearts of patients with Eisenmenger syndrome. *Am J Cardiol.* 2002;89(1):34-38.
16. Goor DA, Lillehei CW. *Congenital malformations of the heart: Embryology, Anatomy, and Operative Considerations.* 1 ed. New York; 1975.
17. Haupt HM, Hutchins GM, Moore GW. Right ventricular infarction: role of the moderator band artery in determining infarct size. *Circulation.* 1983;67(6):1268-1272.
18. Dell'Italia LJ. The right ventricle: anatomy, physiology, and clinical importance. *Curr Probl Cardiol.* 1991;16(10):653-720.
19. Jiang L. *Principle and Practice of Echocardiography.* Baltimore; 1994.
20. Lorenz CH, Walker ES, Morgan VL, Klein SS, Graham TP, Jr. Normal human right and left ventricular mass, systolic function, and gender differences by cine magnetic resonance imaging. *J Cardiovasc Magn Reson.* 1999;1(1):7-21.
21. Brown FK, Brown WJ, Jr., Ellison RG, Hamilton WF. Electrocardiographic changes during development of right ventricular hypertrophy in the dog. *Am J Cardiol.* 1968;21(2):223-231.
22. Leyton RA, Sonnenblick EH. The sarcomere as the basis of Starling's law of the heart in the left and right ventricles. *Methods Achiev Exp Pathol.* 1971;5:22-59.
23. Jiang L, Vazquez de Prada JA, Handschumacher MD, Guererro JL, Vlahakes GJ, King ME, Weyman AE, Levine RA. Three-dimensional echocardiography: in vivo validation for right ventricular free wall mass as an index of hypertrophy. *J Am Coll Cardiol.* 1994;23(7):1715-1722.
24. Dell'Italia LJ, Walsh RA. Acute determinants of the hangout interval in the pulmonary circulation. *Am Heart J.* 1988;116(5 Pt 1):1289-1297.
25. Chin KM, Kim NH, Rubin LJ. The right ventricle in pulmonary hypertension. *Coron Artery Dis.* 2005;16(1):13-18.
26. Petitjean C, Rougon N, Cluzel P. Assessment of myocardial function: a review of quantification methods and results using tagged MRI. *J Cardiovasc Magn Reson.* 2005;7(2):501-516.
27. Santamore WP, Dell'Italia LJ. Ventricular interdependence: significant left ventricular contributions to right ventricular systolic function. *Prog Cardiovasc Dis.* 1998;40(4):289-308.
28. Taylor RR, Covell JW, Sonnenblick EH, Ross J, Jr. Dependence of ventricular distensibility on filling of the opposite ventricle. *Am J Physiol.* 1967;213(3):711-718.
29. Stanley WC, Recchia FA, Lopaschuk GD. Myocardial substrate metabolism in the normal and failing heart. *Physiol Rev.* 2005;85(3):1093-1129.
30. Ingwall JS. *ATP and the Heart;* 2002.
31. Suga H. Ventricular energetics. *Physiol Rev.* 1990;70(2):247-277.
32. Opie LH. Metabolism of the heart in health and disease. II. *Am Heart J.* 1969;77(1):100-122 contd.
33. Randle PJ, Garland PB, Hales CN, Newsholme EA. The glucose fatty-acid cycle. Its role in insulin sensitivity and the metabolic disturbances of diabetes mellitus. *Lancet.* 1963;1(7285):785-789.

34. Magga J, Vuolteenaho O, Tokola H, Marttila M, Ruskoaho H. B-type natriuretic peptide: a myocyte-specific marker for characterizing load-induced alterations in cardiac gene expression. *Ann Med*. 1998;30 Suppl 1:39-45.
35. Tang WH, Francis GS. The year in heart failure. *J Am Coll Cardiol*. 2005;46(11):2125-2133.
36. Colucci WS, Elkayam U, Horton DP, Abraham WT, Bourge RC, Johnson AD, Wagoner LE, Givertz MM, Liang CS, Neibaur M, Haught WH, LeJemtel TH. Intravenous nesiritide, a natriuretic peptide, in the treatment of decompensated congestive heart failure. Nesiritide Study Group. *N Engl J Med*. 2000;343(4):246-253.
37. Michaels AD, Chatterjee K, De Marco T. Effects of intravenous nesiritide on pulmonary vascular hemodynamics in pulmonary hypertension. *J Card Fail*. 2005;11(6):425-431.
38. Klinger JR, Thaker S, Houtchens J, Preston IR, Hill NS, Farber HW. Pulmonary hemodynamic responses to brain natriuretic peptide and sildenafil in patients with pulmonary arterial hypertension. *Chest*. 2006;129(2):417-425.
39. Saha A, Balakrishnan KG, Jaiswal PK, Venkitachalam CG, Tharakan J, Titus T, Kutty R. Prognosis for patients with Eisenmenger syndrome of various aetiology. *Int J Cardiol*. 1994;45(3):199-207.
40. Michelakis ED, McMurtry MS, Wu XC, Dyck JR, Moudgil R, Hopkins TA, Lopaschuk GD, Puttagunta L, Waite R, Archer SL. Dichloroacetate, a metabolic modulator, prevents and reverses chronic hypoxic pulmonary hypertension in rats: role of increased expression and activity of voltage-gated potassium channels. *Circulation*. 2002;105(2):244-250.
41. Gatenby RA, Gillies RJ. Why do cancers have high aerobic glycolysis? *Nat Rev Cancer*. 2004;4(11):891-899.
42. Stacpoole PW, Henderson GN, Yan Z, James MO. Clinical pharmacology and toxicology of dichloroacetate. *Environ Health Perspect*. 1998;106 Suppl 4:989-994.
43. McMurtry MS, Bonnet S, Wu X, Dyck JR, Haromy A, Hashimoto K, Michelakis ED. Dichloroacetate prevents and reverses pulmonary hypertension by inducing pulmonary artery smooth muscle cell apoptosis. *Circ Res*. 2004;95(8):830-840.
44. Bonnet S, Archer SL, Allalunis-Turner J, Haromy A, Beaulieu C, Thompson R, Lee CT, Lopaschuk GD, Puttagunta L, Bonnet S, Harry G, Hashimoto K, Porter CJ, Andrade MA, Thebaud B, Michelakis ED. A mitochondria-K⁺ channel axis is suppressed in cancer and its normalization promotes apoptosis and inhibits cancer growth. *Cancer Cell*. 2007;11(1):37-51.
45. Michelakis ED, Webster L, Mackey JR. Dichloroacetate (DCA) as a potential metabolic-targeting therapy for cancer. *Br J Cancer*. 2008;99(7):989-994.
46. Sano M, Minamino T, Toko H, Miyauchi H, Orimo M, Qin Y, Akazawa H, Tateno K, Kayama Y, Harada M, Shimizu I, Asahara T, Hamada H, Tomita S, Molkentin JD, Zou Y, Komuro I. p53-induced inhibition of Hif-1 causes cardiac dysfunction during pressure overload. *Nature*. 2007;446(7134):444-448.
47. Michelakis ED, Wilkins MR, Rabinovitch M. Emerging concepts and translational priorities in pulmonary arterial hypertension. *Circulation*. 2008;118(14):1486-1495.

48. D'Alonzo GE, Barst RJ, Ayres SM, Bergofsky EH, Brundage BH, Detre KM, Fishman AP, Goldring RM, Groves BM, Kernis JT, et al. Survival in patients with primary pulmonary hypertension. Results from a national prospective registry. *Ann Intern Med.* 1991;115(5):343-349.
49. Hoepfer MM, Lee SH, Voswinckel R, Palazzini M, Jais X, Marinelli A, Barst RJ, Ghofrani HA, Jing ZC, Opitz C, Seyfarth HJ, Halank M, McLaughlin V, Oudiz RJ, Ewert R, Wilkens H, Kluge S, Bremer HC, Baroke E, Rubin LJ. Complications of right heart catheterization procedures in patients with pulmonary hypertension in experienced centers. *J Am Coll Cardiol.* 2006;48(12):2546-2552.
50. Barst RJ, McGoon M, Torbicki A, Sitbon O, Krowka MJ, Olschewski H, Gaine S. Diagnosis and differential assessment of pulmonary arterial hypertension. *J Am Coll Cardiol.* 2004;43(12 Suppl S):40S-47S.
51. Hemnes AR, Champion HC. Right heart function and haemodynamics in pulmonary hypertension. *Int J Clin Pract Suppl.* 2008(160):11-19.
52. Badesch DB, Abman SH, Simonneau G, Rubin LJ, McLaughlin VV. Medical therapy for pulmonary arterial hypertension: updated ACCP evidence-based clinical practice guidelines. *Chest.* 2007;131(6):1917-1928.
53. O'Rourke MF. Vascular impedance in studies of arterial and cardiac function. *Physiol Rev.* 1982;62(2):570-623.
54. O'Rourke MF, Yaginuma T, Avolio AP. Physiological and pathophysiological implications of ventricular/vascular coupling. *Ann Biomed Eng.* 1984;12(2):119-134.
55. Chen CH, Nakayama M, Nevo E, Fetis B, Maughan WL, Kass DA. Coupled systolic-ventricular and vascular stiffening with age: implications for pressure regulation and cardiac reserve in the elderly. *J Am Coll Cardiol.* 1998;32(5):1221-1227.
56. Cho PW, Levin HR, Curtis WE, Tsitlik JE, DiNatale JM, Kass DA, Gardner TJ, Kunel RW, Acker MA. Pressure-volume analysis of changes in cardiac function in chronic cardiomyoplasty. *Ann Thorac Surg.* 1993;56(1):38-45.
57. Kass DA. Clinical evaluation of left heart function by conductance catheter technique. *Eur Heart J.* 1992;13 Suppl E:57-64.
58. Kass DA. Age-related changes in ventricular-arterial coupling: pathophysiologic implications. *Heart Fail Rev.* 2002;7(1):51-62.
59. Kass DA, Midei M, Graves W, Brinker JA, Maughan WL. Use of a conductance (volume) catheter and transient inferior vena caval occlusion for rapid determination of pressure-volume relationships in man. *Cathet Cardiovasc Diagn.* 1988;15(3):192-202.
60. Kelly RP, Ting CT, Yang TM, Liu CP, Maughan WL, Chang MS, Kass DA. Effective arterial elastance as index of arterial vascular load in humans. *Circulation.* 1992;86(2):513-521.
61. Lee WS, Nakayama M, Huang WP, Chiou KR, Wu CC, Nevo E, Fetis B, Kass DA, Ding PY, Chen CH. Assessment of left ventricular end-systolic elastance from aortic pressure-left ventricular volume relations. *Heart Vessels.* 2002;16(3):99-104.

62. Liu CP, Ting CT, Yang TM, Chen JW, Chang MS, Maughan WL, Lawrence W, Kass DA. Reduced left ventricular compliance in human mitral stenosis. Role of reversible internal constraint. *Circulation*. 1992;85(4):1447-1456.
63. Nussbacher A, Gerstenblith G, O'Connor FC, Becker LC, Kass DA, Schulman SP, Fleg JL, Lakatta EG. Hemodynamic effects of unloading the old heart. *Am J Physiol*. 1999;277(5 Pt 2):H1863-1871.
64. Pak PH, Kass DA. Assessment of ventricular function in dilated cardiomyopathies. *Curr Opin Cardiol*. 1995;10(3):339-344.
65. O'Rourke MF, Safar ME. Relationship between aortic stiffening and microvascular disease in brain and kidney: cause and logic of therapy. *Hypertension*. 2005;46(1):200-204.
66. Hessel MH, Steendijk P, den Adel B, Schutte CI, van der Laarse A. Characterization of right ventricular function after monocrotaline-induced pulmonary hypertension in the intact rat. *Am J Physiol Heart Circ Physiol*. 2006;291(5):H2424-2430.
67. Takimoto E, Belardi D, Tocchetti CG, Vahebi S, Cormaci G, Ketner EA, Moens AL, Champion HC, Kass DA. Compartmentalization of cardiac beta-adrenergic inotropy modulation by phosphodiesterase type 5. *Circulation*. 2007;115(16):2159-2167.
68. Takimoto E, Champion HC, Belardi D, Moslehi J, Mongillo M, Mergia E, Montrose DC, Isoda T, Aufiero K, Zaccolo M, Dostmann WR, Smith CJ, Kass DA. cGMP catabolism by phosphodiesterase 5A regulates cardiac adrenergic stimulation by NOS3-dependent mechanism. *Circ Res*. 2005;96(1):100-109.
69. Takimoto E, Champion HC, Li M, Belardi D, Ren S, Rodriguez ER, Bedja D, Gabrielson KL, Wang Y, Kass DA. Chronic inhibition of cyclic GMP phosphodiesterase 5A prevents and reverses cardiac hypertrophy. *Nat Med*. 2005;11(2):214-222.
70. Motte S, McEntee K, Naeije R. Endothelin receptor antagonists. *Pharmacol Ther*. 2006;110(3):386-414.
71. Allanore Y, Meune C, Vignaux O, Weber S, Legmann P, Kahan A. Bosentan increases myocardial perfusion and function in systemic sclerosis: a magnetic resonance imaging and Tissue-Doppler echography study. *J Rheumatol*. 2006;33(12):2464-2469.
72. Packer M, McMurray J, Massie BM, Caspi A, Charlon V, Cohen-Solal A, Kiowski W, Kostuk W, Krum H, Levine B, Rizzon P, Soler J, Swedberg K, Anderson S, Demets DL. Clinical effects of endothelin receptor antagonism with bosentan in patients with severe chronic heart failure: results of a pilot study. *J Card Fail*. 2005;11(1):12-20.
73. Kerkela R, Grazette L, Yacobi R, Iliescu C, Patten R, Beahm C, Walters B, Shevtsov S, Pesant S, Clubb FJ, Rosenzweig A, Salomon RN, Van Etten RA, Alroy J, Durand JB, Force T. Cardiotoxicity of the cancer therapeutic agent imatinib mesylate. *Nat Med*. 2006;12(8):908-916.
74. Nagendran J, Michelakis E. MRI: one-stop shop for the comprehensive assessment of pulmonary arterial hypertension? *Chest*. 2007;132(1):2-5.

75. Boxt LM, Katz J, Kolb T, Czegledy FP, Barst RJ. Direct quantitation of right and left ventricular volumes with nuclear magnetic resonance imaging in patients with primary pulmonary hypertension. *J Am Coll Cardiol.* 1992;19(7):1508-1515.
76. Katz J, Whang J, Boxt LM, Barst RJ. Estimation of right ventricular mass in normal subjects and in patients with primary pulmonary hypertension by nuclear magnetic resonance imaging. *J Am Coll Cardiol.* 1993;21(6):1475-1481.
77. Lugnier C. Cyclic nucleotide phosphodiesterase (PDE) superfamily: a new target for the development of specific therapeutic agents. *Pharmacol Ther.* 2006;109(3):366-398.
78. Essayan DM. Cyclic nucleotide phosphodiesterases. *J Allergy Clin Immunol.* 2001;108(5):671-680.
79. Matsumoto T, Kobayashi T, Kamata K. Phosphodiesterases in the vascular system. *J Smooth Muscle Res.* 2003;39(4):67-86.
80. Mongillo M, Tocchetti CG, Terrin A, Lissandron V, Cheung YF, Dostmann WR, Pozzan T, Kass DA, Paolucci N, Houslay MD, Zaccolo M. Compartmentalized phosphodiesterase-2 activity blunts beta-adrenergic cardiac inotropy via an NO/cGMP-dependent pathway. *Circ Res.* 2006;98(2):226-234.
81. Degerman E, Belfrage P, Manganiello VC. Structure, localization, and regulation of cGMP-inhibited phosphodiesterase (PDE3). *J Biol Chem.* 1997;272(11):6823-6826.
82. Lehnart SE, Wehrens XH, Reiken S, Warriar S, Belevych AE, Harvey RD, Richter W, Jin SL, Conti M, Marks AR. Phosphodiesterase 4D deficiency in the ryanodine-receptor complex promotes heart failure and arrhythmias. *Cell.* 2005;123(1):25-35.
83. Hetman JM, Soderling SH, Glavas NA, Beavo JA. Cloning and characterization of PDE7B, a cAMP-specific phosphodiesterase. *Proc Natl Acad Sci U S A.* 2000;97(1):472-476.
84. Cheitlin MD, Hutter AM, Jr., Brindis RG, Ganz P, Kaul S, Russell RO, Jr., Zusman RM. ACC/AHA expert consensus document. Use of sildenafil (Viagra) in patients with cardiovascular disease. American College of Cardiology/American Heart Association. *J Am Coll Cardiol.* 1999;33(1):273-282.
85. Rochais F, Abi-Gerges A, Horner K, Lefebvre F, Cooper DM, Conti M, Fischmeister R, Vandecasteele G. A specific pattern of phosphodiesterases controls the cAMP signals generated by different Gs-coupled receptors in adult rat ventricular myocytes. *Circ Res.* 2006;98(8):1081-1088.
86. Michelakis E, Tymchak W, Lien D, Webster L, Hashimoto K, Archer S. Oral sildenafil is an effective and specific pulmonary vasodilator in patients with pulmonary arterial hypertension: comparison with inhaled nitric oxide. *Circulation.* 2002;105(20):2398-2403.
87. Borlaug BA, Melenovsky V, Marhin T, Fitzgerald P, Kass DA. Sildenafil inhibits beta-adrenergic-stimulated cardiac contractility in humans. *Circulation.* 2005;112(17):2642-2649.
88. Dodge-Kafka KL, Langeberg L, Scott JD. Compartmentation of cyclic nucleotide signaling in the heart: the role of A-kinase anchoring proteins. *Circ Res.* 2006;98(8):993-1001.

89. Dodge-Kafka KL, Soughayer J, Pare GC, Carlisle Michel JJ, Langeberg LK, Kapiloff MS, Scott JD. The protein kinase A anchoring protein mAKAP coordinates two integrated cAMP effector pathways. *Nature*. 2005;437(7058):574-578.
90. Takio K, Wade RD, Smith SB, Krebs EG, Walsh KA, Titani K. Guanosine cyclic 3',5'-phosphate dependent protein kinase, a chimeric protein homologous with two separate protein families. *Biochemistry*. 1984;23(18):4207-4218.
91. Yuasa K, Michibata H, Omori K, Yanaka N. A novel interaction of cGMP-dependent protein kinase I with troponin T. *J Biol Chem*. 1999;274(52):37429-37434.
92. Vo NK, Gettemy JM, Coghlan VM. Identification of cGMP-dependent protein kinase anchoring proteins (GKAPs). *Biochem Biophys Res Commun*. 1998;246(3):831-835.
93. Airhart N, Yang YF, Roberts CT, Jr., Silberbach M. Atrial natriuretic peptide induces natriuretic peptide receptor-cGMP-dependent protein kinase interaction. *J Biol Chem*. 2003;278(40):38693-38698.
94. Su J, Zhang Q, Moalem J, Tse J, Scholz PM, Weiss HR. Functional effects of C-type natriuretic peptide and nitric oxide are attenuated in hypertrophic myocytes from pressure-overloaded mouse hearts. *Am J Physiol Heart Circ Physiol*. 2005;288(3):H1367-1373.
95. Hogan PG, Chen L, Nardone J, Rao A. Transcriptional regulation by calcium, calcineurin, and NFAT. *Genes Dev*. 2003;17(18):2205-2232.
96. Clipstone NA, Crabtree GR. Identification of calcineurin as a key signalling enzyme in T-lymphocyte activation. *Nature*. 1992;357(6380):695-697.
97. Okamura H, Aramburu J, Garcia-Rodriguez C, Viola JP, Raghavan A, Tahiliani M, Zhang X, Qin J, Hogan PG, Rao A. Concerted dephosphorylation of the transcription factor NFAT1 induces a conformational switch that regulates transcriptional activity. *Mol Cell*. 2000;6(3):539-550.
98. Molkentin JD, Lu JR, Antos CL, Markham B, Richardson J, Robbins J, Grant SR, Olson EN. A calcineurin-dependent transcriptional pathway for cardiac hypertrophy. *Cell*. 1998;93(2):215-228.
99. Leinwand LA. Calcineurin inhibition and cardiac hypertrophy: a matter of balance. *Proc Natl Acad Sci U S A*. 2001;98(6):2947-2949.
100. Tokudome T, Horio T, Kishimoto I, Soeki T, Mori K, Kawano Y, Kohno M, Garbers DL, Nakao K, Kangawa K. Calcineurin-nuclear factor of activated T cells pathway-dependent cardiac remodeling in mice deficient in guanylyl cyclase A, a receptor for atrial and brain natriuretic peptides. *Circulation*. 2005;111(23):3095-3104.
101. Lin CS, Chow S, Lau A, Tu R, Lue TF. Identification and regulation of human PDE5A gene promoter. *Biochem Biophys Res Commun*. 2001;280(3):684-692.
102. Goodrich JA, Kugel JF. Non-coding-RNA regulators of RNA polymerase II transcription. *Nat Rev Mol Cell Biol*. 2006.
103. Yanagisawa M, Kurihara H, Kimura S, Tomobe Y, Kobayashi M, Mitsui Y, Yazaki Y, Goto K, Masaki T. A novel potent vasoconstrictor peptide produced by vascular endothelial cells. *Nature*. 1988;332(6163):411-415.

104. Dupuis J, Hoepfer MM. Endothelin receptor antagonists in pulmonary arterial hypertension. *Eur Respir J*. 2008;31(2):407-415.
105. Masuda Y, Miyazaki H, Kondoh M, Watanabe H, Yanagisawa M, Masaki T, Murakami K. Two different forms of endothelin receptors in rat lung. *FEBS Lett*. 1989;257(2):208-210.
106. Modesti PA, Vanni S, Paniccia R, Bandinelli B, Bertolozzi I, Polidori G, Sani G, Neri Serneri GG. Characterization of endothelin-1 receptor subtypes in isolated human cardiomyocytes. *J Cardiovasc Pharmacol*. 1999;34(3):333-339.
107. Sugden PH. An overview of endothelin signaling in the cardiac myocyte. *J Mol Cell Cardiol*. 2003;35(8):871-886.
108. Ito H, Hiroe M, Hirata Y, Fujisaki H, Adachi S, Akimoto H, Ohta Y, Marumo F. Endothelin ETA receptor antagonist blocks cardiac hypertrophy provoked by hemodynamic overload. *Circulation*. 1994;89(5):2198-2203.
109. Shubeita HE, McDonough PM, Harris AN, Knowlton KU, Glembotski CC, Brown JH, Chien KR. Endothelin induction of inositol phospholipid hydrolysis, sarcomere assembly, and cardiac gene expression in ventricular myocytes. A paracrine mechanism for myocardial cell hypertrophy. *J Biol Chem*. 1990;265(33):20555-20562.
110. Suzuki T, Hoshi H, Mitsui Y. Endothelin stimulates hypertrophy and contractility of neonatal rat cardiac myocytes in a serum-free medium. *FEBS Lett*. 1990;268(1):149-151.
111. Kramer BK, Smith TW, Kelly RA. Endothelin and increased contractility in adult rat ventricular myocytes. Role of intracellular alkalosis induced by activation of the protein kinase C-dependent Na(+)-H+ exchanger. *Circ Res*. 1991;68(1):269-279.
112. Endoh M, Fujita S, Yang HT, Talukder MA, Maruya J, Norota I. Endothelin: receptor subtypes, signal transduction, regulation of Ca²⁺ transients and contractility in rabbit ventricular myocardium. *Life Sci*. 1998;62(17-18):1485-1489.
113. Goldberg AT, Bond BR, Mukherjee R, New RB, Zellner JL, Crawford FA, Jr., Spinale FG. Endothelin receptor pathway in human left ventricular myocytes: relation to contractility. *Ann Thorac Surg*. 2000;69(3):711-715; discussion 716.
114. Kelso EJ, McDermott BJ, Silke B, Spiers JP. Endothelin(A) receptor subtype mediates endothelin-induced contractility in left ventricular cardiomyocytes isolated from rabbit myocardium. *J Pharmacol Exp Ther*. 2000;294(3):1047-1052.
115. Spiers JP, Kelso EJ, Allen JD, Silke B, McDermott BJ. Inotropic response to endothelin-1, isoprenaline and calcium in cardiomyocytes isolated from endotoxin treated rats: effects of ethyl-isothiourea and dexamethasone. *Br J Pharmacol*. 2000;130(6):1275-1282.
116. Kang M, Walker JW. Endothelin-1 and PKC induce positive inotropy without affecting pHi in ventricular myocytes. *Exp Biol Med (Maywood)*. 2006;231(6):865-870.
117. Aiello EA, Villa-Abrille MC, Dulce RA, Cingolani HE, Perez NG. Endothelin-1 stimulates the Na⁺/Ca²⁺ exchanger reverse mode through intracellular Na⁺

- (Na⁺i)-dependent and Na⁺i-independent pathways. *Hypertension*. 2005;45(2):288-293.
118. Ortega Mateo A, de Artinano AA. Highlights on endothelins: a review. *Pharmacol Res*. 1997;36(5):339-351.
 119. McMurray JJ, Teerlink JR, Cotter G, Bourge RC, Cleland JG, Jondeau G, Krum H, Metra M, O'Connor CM, Parker JD, Torre-Amione G, van Veldhuisen DJ, Lewsey J, Frey A, Rainisio M, Kobrin I. Effects of tezosentan on symptoms and clinical outcomes in patients with acute heart failure: the VERITAS randomized controlled trials. *Jama*. 2007;298(17):2009-2019.
 120. Williamson DJ, Wallman LL, Jones R, Keogh AM, Scroope F, Penny R, Weber C, Macdonald PS. Hemodynamic effects of Bosentan, an endothelin receptor antagonist, in patients with pulmonary hypertension. *Circulation*. 2000;102(4):411-418.
 121. Channick RN, Simonneau G, Sitbon O, Robbins IM, Frost A, Tapson VF, Badesch DB, Roux S, Rainisio M, Bodin F, Rubin LJ. Effects of the dual endothelin-receptor antagonist bosentan in patients with pulmonary hypertension: a randomised placebo-controlled study. *Lancet*. 2001;358(9288):1119-1123.
 122. Ueno M, Miyauchi T, Sakai S, Kobayashi T, Goto K, Yamaguchi I. Effects of physiological or pathological pressure load in vivo on myocardial expression of ET-1 and receptors. *Am J Physiol*. 1999;277(5 Pt 2):R1321-1330.
 123. Naeije R, Huez S. Expert opinion on available options treating pulmonary arterial hypertension. *Expert Opin Pharmacother*. 2007;8(14):2247-2265.

Chapter 2:

Materials and Methods:

Human Heart Tissue Samples: Human samples were acquired from patients undergoing surgery for congenital heart disease or transplantation at the University of Alberta Hospital. Excised ventricular tissue samples (free wall) were immediately placed on ice and stained with TMRM and Hoechst (a nuclear stain) for 30 minutes and visualized under confocal microscopy. The presence of hypertrophy was documented by the use of echocardiography for every patient and confirmed macroscopically by the surgeon.

Animal model of RVH: We studied RVH using a model of experimental PAH by injecting monocrotaline, an alkaloid from *crotalaria spectabilis*, a well rat PAH established model. Monocrotaline is selectively toxic to the pulmonary arterial endothelium and causes significant RV hypertrophy in 3-4 weeks post-intraperitoneal injection. We have repeatedly confirmed this using both invasive (right heart catheterization) and noninvasive (ECHO) methods. Here, we also confirmed the presence of PAH and RVH by ECHO using pulmonary artery acceleration time (PAAT) (a parameter that correlates with mean PA pressure and used clinically; the shorter the PAAT the higher the PA pressure) and RV free wall thickness in a short axis parasternal view. We further quantified RVH macroscopically at autopsy, using the dry weight ratio of the RV/LV+Septum.

Isolation of adult rat cardiomyocytes: Hearts were taken from male adult Sprague Dawley rats (250-300 grams) and the aortas were cannulated and hung on to a perfusion

system. Krebs buffer (NaCl-118mM, KCl-4.7mM, KH₂PO₄-1.2mM, MgSO₄7H₂O-1.2mM, CaCl₂2H₂O-2.5mM, NaHCO₃-25mM, glucose-5mM) at pH 7.4 (corrected to temperature=37.5⁰C) was retrogradely perfused through the coronary arteries for 5 minutes. Perfusate solution was then switched to a 2% w/v collagenase (Worthington Biochemical, Lakewood, NJ) supplemented Krebs buffer for 20 minutes. The hearts were then removed from the system, and the two ventricular free walls were surgically separated for myocyte isolation. Following another five-minute digestion with 2% w/v collagenase, the samples were triturated with a glass pipette filtered through a nylon mesh and the filtrate was centrifuged to yield cardiomyocytes.

Isolation and culture of neonatal rat cardiomyocytes: Hearts from 2 day old rats were excised and atria were removed. Free walls of LV and RV were isolated and kept separately in phosphate buffered saline. Ventricular tissue was minced in ice cold PBS then digested in an enzymatic cocktail containing 2%w/v collagenase, 0.5% w/v deoxyribonuclease (Worthington Biochemical, Lakewood, NJ), and 2%w/v trypsin (Worthington Biochemical, Lakewood, NJ) for 20 minutes at 37°C. After digestion, administering DMEM/F12 media (Sigma, Oakville, ON, Canada) supplemented with 20% fetal bovine serum (Sigma) stopped enzymatic reaction. The mixture was then centrifuged at 800rpm for 1min at 4°C to remove fibroblasts, red blood cells, and debris in the supernatant. The pellet was re-digested 2 to 3 times for another 20 minutes and centrifuged at 800rpm to separate cardiomyocytes into the supernatant. The collected supernatant was finally pooled and centrifuged twice for 7 minutes at 1700rpm to yield a pellet of cardiomyocytes. Due to the quick attachment of fibroblasts to the plates compared to the rate of attachment of cardiomyocytes, we separate any existing

fibroblasts in the mixture by removing the cardiomyocyte rich supernatant from the fibroblasts attached to the plates (differential plating) for 2 hours at 37°C. Our group has previously validated the efficacy and specificity of this procedure. The isolated neonatal rat cardiomyocytes were plated and maintained for 2.5 days in DMEM/F12 media supplemented with 5% fetal bovine serum, 10% horse serum (Invitrogen Canada Inc., Burlington, ON, Canada), and 50mg/L gentamicin (Invitrogen). Media also contained 10nM cytosine arabinoside (Sigma) to prevent fibroblast proliferation. Cultured cells were treated for 48 hours with 10mM phenylephrine to induce cardiomyocyte hypertrophy as previously described. Phenylephrine-treated cells were also treated with either 5mM dichloroacetate (DCA) or 4mM 11Arg-VIVIT (a competing peptide that selectively inhibits NFAT by blocking its binding to calcineurin) (EMD-Biosciences Canada); the high arginine content of the peptide significantly enhances its permeability into the cell.

Pharmacological agents: Phosphodiesterase-5 inhibitors used were MY-5445 (0.1-10 mM; Alexis), sildenafil (150 mg/kg PO; Pfizer), and sildenafil (0.1-10 mM; gift from Dr. G. Butrous, Pfizer). Phosphodiesterase-3 inhibitor used was milrinone (1-100 mM; Sigma), and b-agonist used was isoproterenol (0.01-1 mM; Sigma). Protein kinase-G inhibitors were KT-5823 (0.1-10 mM; Calbiochem), and Rp-8-CPT-cGMPS (1-100 mM; Calbiochem). Protein kinase-A inhibitor used was H-89 (0.1-10 mM; LC laboratories).

Immunoblots: Were performed on right ventricular tissue from humans and/or rats for PDE5 (1:500; MW=99.5 kDa; FabGennix), PDE3 (1:500; MW=80 kDa; FabGennix),

PKG-1 (1:1000; MW= 75 kDa; Abcam), VASP-P_{Ser239} (1:300; Calbiochem), and GAPDH (1:500; Santa Cruz) as previously described Homogenates of RVs were suspended in a buffer containing 10 mM Tris, pH 7.5, 1 mM phenylmethylsulfonyl fluoride, 1 mM EDTA, 0.1% Triton X-100, and 0.05 M dithiothreitol. Samples were then sonicated, and the proteins were isolated. Equal amounts of PV and PA protein (25 μ g) were loaded and run on a 7.5% discontinuous SDS-polyacrylamide gel and then transferred to a nitrocellulose membrane.

Staining of Cells and Tissue: TMRM was made up to a concentration of 20nM in plating media along with 0.5 μ M of Hoechst nuclear stain. Each 35mm X 10mm plate of cells received 2mL of the staining solution for a period of 30 minutes at 37°C. For ventricular rat tissue, the exposure was 40 minutes. The staining media was then removed, and each plate was rinsed once in media, and then left at 37°C in another 2mL of plating media. Staining of plates was staggered as to give each plate from each ventricle the same amount of exposure to TMRM, and same amount of time before imaging.

Immunohistochemistry and confocal microscopy: Were performed on paraffin sections after heat mediated antigen retrieval with citrate/citric acid buffer pH 6. Image enhancer IT (Invitrogen Canada Inc., Burlington, ON, Canada) was used for blocking, followed by Super Block Buffer #37535 + 0.05% Tween20 (Pierce, Rockford Il. U.S.A). Primary antibodies used included: goat anti-human myosin heavy chain (dilution 1:50, Biotechnology Inc., Santa Cruz, CA); mouse anti-human PDE5 (dilution 1:50-100-200, Leinco Technologies Inc. St. Louis, MO); rabbit anti-alpha smooth muscle actin (dilution 1:100, Lab Vision Corporation Fremont, CA); rabbit anti-BNP (dilution 1:500, Abcam,

Cambridge, MA); goat anti-human Endothelin-1 #sc-21625 (dilution 1:100), Santa Cruz Biotechnology Inc., Santa Cruz, CA); rabbit anti-rat Endothelin Receptor-A #AB3260-50uL (dilution 1:50);(Chemicon International). Secondary antibodies included: donkey anti goat tritc 1:100 for MHC (Molecular Probes, Invitrogen); goat anti-rabbit fitc 1:100 for ERA (Molecular Probes, Invitrogen); donkey anti goat fitc 1:100 for ET1 (Molecular Probes, Invitrogen); goat anti rabbit tritc 1:100 for ERA (Molecular Probes, Invitrogen). Antibodies were applied for 1 hr at 37°C. Secondary antibody-only staining confirmed lack of nonspecific staining for all antibodies used. All slides were also stained with a nuclear stain, DAPI (Invitrogen) 1 μ M for 10 minutes at room temperature, and imaged on Zeiss 510 confocal microscope (FITC: 488nm excitation, 500-550nm emission; TRITC: 543nm excitation, 565-615nm emission; DAPI: 740 nm two photon excitation, 390-465nm emission for DAPI).

Were performed on paraffin sections after heat mediated antigen retrieval with citrate/citric acid buffer pH 6. Blocking was done with Image enhancer IT (Invitrogen Canada Inc., Burlington, ON, Canada) followed by Super Block Buffer #37535 + 0.05% Tween20 (Pierce , Rockford Il. U.S.A). Primary antibodies used included: goat anti-human Myosin Heavy Chain (Y-20) #sc-12117 (dilution 1:50), Santa Cruz Biotechnology Inc.,Santa Cruz,CA); goat anti-human Endothelin-1 #sc-21625 (dilution 1:100), Santa Cruz Biotechnology Inc., Santa Cruz, CA); rabbit anti-rat Endothelin Receptor-A #AB3260-50uL (dilution 1:50);(Chemicon International). Secondary antibodies included: donkey anti goat tritc 1:100 for MHC (Molecular Probes, Invitrogen); goat anti-rabbit fitc 1:100 for ERA (Molecular Probes, Invitrogen); donkey anti goat fitc 1:100 for ET1 (Molecular Probes, Invitrogen); goat anti rabbit tritc 1:100

for ERA (Molecular Probes, Invitrogen). Antibodies were applied for 1 hr at 37 C. Lack of nonspecific staining for the antibodies used was confirmed by application of secondary antibody only. All slides were also stained with a nuclear stain, DAPI #D21490 (Invitrogen) 1 μ M for 10 minutes at room temperature. Slides were imaged on a Zeiss LSM 510 confocal microscope (FITC: 488nm excitation, 505-530 nm emission; TRITC: 543nm excitation, 565-615nm emission; DAPI: 740 nm two photon excitation, 390-465nm emission).

Laser-captured microdissection: 5 μ m-thick-slides of human RV tissue were prepared and studied using the PixCell II system (Arcturus) as previously described

Laser Capture Microdissection¹. LCM utilizes a microscope platform combined with a low energy infrared laser to melt a plastic capture film onto the flash frozen human and rat RV. The PixCell II LCM System (Arcturus Engineering, Mountain View, CA) is used to selectively remove myocardium versus coronary arteries. The machine settings were as follows: slice thickness 5 μ m, power 65mW, duration 1.5ms. The cryostat was used and kept at -20°C and frozen RV tissue blocks that were embedded in OCT were sliced and mounted without a coverslip on a DNA-free microscope slide. The tissue was dehydrated using the HistoGene LCM Frozen Section Staining Kit and then the dissected section was placed on a thermoplastic membrane pre-mounted on optically transparent caps. After visual confirmation of the adequacy of the dissection by examining the tissue in the cap, the specimen was placed in RNA-later for subsequent

qRT-PCR.

Real-Time Polymerase Chain Reaction¹: Total RNA was extracted using RNeasy Mini Kit (Qiagen, Mississauga, Canada) and quantified with UV spectrophotometry. Quantitative real-time polymerase chain reaction (qRT-PCR) was used to quantify human and rat ventricular tissue PDE5, MHC, SMA, ET-1, and ET_R-A mRNA and expression. The TaqMan One-Step RT-PCR Master Mix reagent kit was used (Applied Biosystems, Foster City, CA). The reaction used 50ng RNA in 50pl using the relevant primer (500nM), and TaqMan probe (200nM). The assay was performed using an ABI PRISM 7700 Sequence Detector System (Applied Biosystems). Reverse transcription proceeded for 30 min at 48°C. AmpliTaq Gold activation occurred for 10 min at 95°C. Subsequently, 40 cycles of PCR were performed. Each cycle consisted of 15 seconds of denaturing (at 95°C) and 1 minute of annealing and extension (at 60°C) 2^{DDCt} is a ratio of the expression of PDE5 to 18s (ribosomal subunit).

2^{DDCt} calculation: 2^{DDCt} is a conversion factor allowing the amount of PDE5 mRNA to be expressed in terms of copy number relative to the *calibrator* (the sample with the least amount of PDE5 mRNA) and normalized to expression of a housekeeping gene, 18s.

Ct=threshold cycle for target amplification:

The DCt of PDE5 was computed for each sample using Equation 1. The largest DCt (indicating the smallest amount of PDE5) is defined as the *calibrator*.

Equation (1) $\text{DCt PDE5} = \text{Ct}_{\text{PDE5}} - \text{Ct}_{18\text{s}}$

Then the relative copy number DDCt is calculated for each sample using Equation 2

Equation (2) $\text{DDCt} = \text{calibrator} - \text{DCt PDE5}$.

In the case of the sample that is experimentally selected as the *calibrator* (the lowest expressing sample), Equation 2 yields a value of 0 (subtracting the value from itself). By expressing the DDCt as an exponent of 2, the copy number in the calibrator becomes $2^0=1$, allowing easy expression of the larger amounts of Kv mRNA in other specimens relative to this value.

The same equations were used in calculating relative mRNA expression of MHC, SMA, ET and ET_R-A.

The choice of RT-PCR over traditional PCR is done to allow for improved sensitivity of only a 2-fold increase versus a 10-fold increase, respectively. Also, using the exponential phase of PCR, as is done in RT-PCR, allows for more precise detection without the confounding of reagent consumption and PCR product degradation.

Cell Shortening studies: RV myocytes were obtained. Cell shortening was measured using a video edge detector system at a frame rate of 60Hz using Clampex 8.1 software for data acquisition. Myocytes were field-stimulated with 10ms square pulses at a constant current, 10-20% above threshold value. Myocytes were superfused with a high Na⁺ solution containing 140mM NaCl, 5mM KCl, 10mM HEPES buffer, 2mM CaCl₂, 1.4mM MgCl₂ and 10mM glucose for 2-3 min to establish baseline after which high Na⁺ solution with 100nM isoproterenol was superfused for 7-8 min. High Na⁺ solution with 100nM isoproterenol and 1μM sildenafil was then superfused for 9-11min. Percentage cell shortening is expressed as $(\Delta\text{length} / \text{diastolic length}) \times 100$

Isolated RV Langendorff perfusion: Rats were anesthetized with intra-peritoneal injection of 60 mg/kg pentobarbital. A midline sternotomy was performed and within 1 minute the heart was isolated and the aorta was cannulated and perfused with Krebs buffer at 12-13 cc/min. The hearts had a mean intrinsic rate of ~180-190bpm (hearts with a native rate <160 bpm were not used). A 0.03 cc latex balloon (Harvard Apparatus, Saint-Laurent, Quebec, Canada) filled with water and attached to a pressure transducer (Cobe, Richmond Hill, Ontario, Canada) was placed in the RV via the right atrium and pressure traces were sampled at a rate of 1000 Hz by PowerLab. Pressure readings were converted into first derivative traces to give dP/dt and analyzed with Chart 5.4 software (ADInstruments Inc, Colorado Springs, CO).

Cyclic GMP and cyclic AMP levels: RV free walls were isolated from rat hearts (with or without pre-treatment with sildenafil po). cAMP and cGMP levels were determined using cAMP and cGMP EIA kits (Biomedical Technologies Inc., Stoughton, Massachusetts, USA) and expressed as pmoles per weight of myocardium.

Phosphodiesterase (PDE) activity assays: Total cGMP-PDE activity and cAMP-PDE activity was assayed at 1mM substrate (fluorescein-labeled derivatives of cGMP and cAMP, respectively) using a fluorescence polarization assay (Molecular Devices, Sunnyvale, CA, USA) under linear conditions, with and without a PDE5 inhibitor (sildenafil 1 μ M) or a PDE3 inhibitor (milrinone 10 μ M).

Protein kinase G (PKG) activity: PKG-1 activity was assayed in RV free wall tissues using colorimetric analysis (CycLex, Ina, Nagano, Japan), where a peroxidase coupled anti-phospho-G-kinase substrate monoclonal antibody is used as a reporter molecule in a 96-well ELISA. Activity was also studied by measuring the phosphorylation of VASP, a myocardial PKG-1 target, using immunoblots; densitometry (over GAPDH expression).

RT-PCR. Total RNA was isolated from homogenized rat PAs and PVs with a QIAGEN RNeasy Mini Kit (Mississauga, ON). RNA (2 μ g) was reverse transcribed with QIAGEN Omniscript reverse transcriptase. Primers were designed based on cloned rat sequences from GenBank. cDNA (1 μ l) was incubated with 150 ng of sense and 150 ng of antisense primers and amplified in QIAGEN HotStarTaq Master Mix. The cycling parameters were 95°C for 15 min, X°C for 1 min, and 72°C for 1 min, where X is the annealing temperature for the first cycle and 94°C for 30 s, X°C for 30 s, and 72°C for 1 min for the second to last cycle. The amplified PCR products were run on ethidium bromide-stained 2% agarose gels.

Endothelin immunoassay for coronary effluent and blood samples (Cayman Chemicals, Ann Arbor, MI, USA): a double-antibody sandwich technique is used. The wells of the plates are coated with a monoclonal antibody specific for endothelin. An acetylcholinesterase:Fab' conjugate, which binds the opposite side of the endothelin molecule that the monoclonal antibody binds. The excess reagent is washed off and the sandwiched endothelin molecules are quantified by measuring the enzymatic activity of the acetylcholinesterase by adding Ellman's reagent to the wells. The product of the acetylcholinesterase-catalyzed reaction is yellow and absorbs at 412nm. The intensity of

yellow attained by spectrophotometry is compared to the standards to calculate concentration of endothelin.

Imaging and Analysis of Data: All imaging was performed using a Zeiss LSM 510 confocal microscope. To maintain physiological activity and viability of the tissue, imaging was done on a heated platform at 37°C. Densitometry analysis was done by the use of Zeiss Image Browser software. Fluorescence intensity of TMRM was performed by measuring circular regions of interest (0.126mm² in area). A region of interest was drawn into each field of view where the circle encompassed myocardial tissue only and not coronary vessels. For cardiomyocytes, the TMRM intensity was measured in each cell excluding the area containing the nucleus (as marked by Hoechst stain in blue) and divided by the cytoplasmic area.

Comparison between LV and RV cardiomyocytes (from either neonatal or adult model) was done using a t-test. Statistical analysis of ventricular tissue (from either adult rat or human) and neonatal cultured neonatal cardiomyocytes were completed via one-way ANOVA with post-hoc Bonferroni correction. Significance was defined at a p-value of less than 0.05.

References:

1. Michelakis ED, Rebeyka I, Wu X, Nsair A, Thebaud B, Hashimoto K, Dyck JR, Haromy A, Harry G, Barr A, Archer SL. O₂ sensing in the human ductus arteriosus: regulation of voltage-gated K⁺ channels in smooth muscle cells by a mitochondrial redox sensor. *Circ Res.* 2002; 91:478-486.

Chapter 3:

Phosphodiesterase type 5 (PDE5) is highly expressed in the hypertrophied human right ventricle and acute inhibition of PDE5 improves contractility

Abstract

Background: Sildenafil was recently approved for the treatment of Pulmonary Arterial Hypertension (PAH). The beneficial effects of phosphodiesterase type 5 (PDE5) inhibitors in PAH are thought to result from relatively selective vasodilatory and anti-proliferative effects on the pulmonary vasculature; and are thought to spare the myocardium, based on early data showing lack of significant PDE5 expression in the normal heart.

Methods and Results: We studied surgical specimens from 9 patients and show for the first time that, while PDE5 is not expressed in the myocardium of the normal human right ventricle (RV), mRNA and protein are markedly up-regulated in hypertrophied RV (RVH) myocardium. PDE5 is also up-regulated in rat RVH. PDE5 inhibition (with either MY-5445 or sildenafil) significantly increases contractility, measured in the perfused heart (modified Langendorff preparation) and isolated cardiomyocytes, in the hypertrophied, but not normal, RV. PDE5 inhibition leads to increase in both cGMP and cAMP in the RVH but not normal RV. Protein kinase-G (PKG) activity is suppressed in RVH, explaining why the PDE5 inhibitor-induced increase in cGMP does not lead to inhibition of contractility. Rather, this leads to inhibition of the cGMP-sensitive PDE3, explaining the increase in cAMP and contractility. This is further supported by our findings that in RVH protein kinase A inhibition completely inhibits PDE5-induced inotropy, while PKG inhibition does not.

Conclusions: The ability of PDE5 inhibitors to increase RV inotropy and decrease RV afterload, without significantly affecting systemic hemodynamics, makes them ideal for the treatment of diseases affecting the RV, including PAH.

Background

The failing right ventricle (RV) is a common clinical problem, complicating pulmonary arterial hypertension (PAH), pulmonary thromboembolism, heart/lung transplant surgery or surgery for congenital heart disease. To be clinically effective, an ideal candidate therapy should increase RV inotropy, dilate the pulmonary circulation (its afterload) and not affect the systemic vasculature or the left ventricle (LV). RV remodeling and contractility is surprisingly understudied and currently there are no RV-specific standard or experimental therapies^{1,2}. Phosphodiesterase type 5 (PDE5) inhibitors like sildenafil are relatively selective pulmonary vasodilators and were just approved for the treatment of PAH³. PDE5 is thought to be expressed in the coronary vessels but not in the human myocardium⁴. Within the first year of sildenafil's use for erectile dysfunction, a number of cardiac deaths were reported; it was soon realized that these were mostly related to the interaction of sildenafil with nitrates, often required for intercourse-induced angina, resulting in profound hypotension. However, these early deaths led to extensive efforts to study potentially direct effects of sildenafil on the heart. PDE5 inhibitors were clearly shown to lack any significant direct effects to the myocardium of normal human and animal hearts in vitro⁵⁻⁷, and in healthy volunteers⁸ or even patients with coronary artery disease in vivo⁹. This was supported by the finding that PDE5 is not expressed in the normal myocardium⁶. Expert panels and professional bodies like the ACC/AHA writing group published position statements on the effects of sildenafil, clearly stating that it lacks primary effects on the myocardium: “*Furthermore, PDE5 is not present in cardiac*

myocytes, and sildenafil has been shown to have no direct inotropic effects... , page 171”

4.

Therefore, when PDE5 inhibitors started being studied for the treatment of PAH, they were thought to only have effects on the pulmonary vasculature. Their acute and chronic effects were thought to solely result from their ability to increase cGMP levels preferentially in the pulmonary artery smooth muscle cells, thereby inducing relatively selective pulmonary vasodilatation in addition to anti-proliferative and pro-apoptotic effects on the vessel wall ¹⁰⁻¹⁴. In one of the first reports of the hemodynamic effects of sildenafil in patients with PAH, we showed that a single oral dose of sildenafil (75mg) and maximal dose of inhaled nitric oxide (80ppm) had similar effects on systemic and pulmonary hemodynamics, but only sildenafil improved cardiac output ¹⁰. This suggested a primary inotropic effect of sildenafil on the RV (which is hypertrophied and/or failing in most patients with PAH) since the effects on the systemic vasculature were not significant. However, although we could not rule out that some of the increase in the cardiac output could be due to the decrease in the left ventricular afterload, this finding was obscured by the then prevalent dogma that PDE5 was absent in the human heart. Also, Lepore et al, followed a similar protocol, but suggested that sildenafil did not affect myocardial function ¹³. We now hypothesized that PDE5 is up-regulated in the hypertrophied RV (RVH) and that this upregulation is physiologically significant.

Methods

The authors had full access to and take full responsibility for the integrity of the data. All

authors have read and agree to the manuscript as written. All experiments on human tissues and rats were obtained with permission from the University of Alberta committees on human ethics and animal policy and welfare respectively.

Animal model of RVH: We studied RVH using a well-validated PAH model created by injecting intraperitoneally *monocrotaline*, an alkaloid from *crotalaria spectabilis*, in adult Sprague Dawley rats^{15, 16}. Monocrotaline is selectively toxic to the pulmonary arterial endothelium and causes significant PAH within 3 weeks post injection. This is associated with significant RVH, a finding that we have validated with extensive hemodynamic and echocardiographic studies^{16, 17}. We sacrificed the rats between 3-4 weeks post injection, at a time that the rats, despite the RVH, do not have severe right heart failure based on the absence of signs like significant edema or ascites.

Immunohistochemistry, confocal microscopy, immunoblots laser-capture microdissection and qRT-PCR were performed as recently described^{16, 17}; for details see Methods (Chapter 2).

Isolated RV Langendorff perfusion: Rats were anesthetized with intra-peritoneal injection of 60 mg/kg pentobarbital. A midline sternotomy was performed and within 1 minute the heart was isolated and the aorta was cannulated and perfused with Krebs buffer at 12-13 cc/min. The hearts had a mean intrinsic rate of ~180-190bpm (hearts with a native rate <160 bpm were not used). A 0.03 cc latex balloon (Harvard Apparatus, Saint-Laurent, Quebec, Canada) filled with water and attached to a pressure transducer (Cobe, Richmond Hill, Ontario, Canada) was placed in the RV via the right atrium and pressure traces were sampled at a rate of 1000 Hz by PowerLab. Pressure readings were

converted into first derivative traces to give dP/dt and analyzed with Chart 5.4 software (ADInstruments Inc, Colorado Springs, CO).

Cyclic GMP and cyclic AMP levels: RV free walls were isolated from rat hearts (with or without pre-treatment with sildenafil po). cAMP and cGMP levels were determined using cAMP and cGMP EIA kits (Biomedical Technologies Inc., Stoughton, Massachusetts, USA) and expressed as pmoles per weight of myocardium.

Phosphodiesterase (PDE) activity assays: Total cGMP-PDE activity and cAMP-PDE activity was assayed at 1mM substrate (fluorescein-labeled derivatives of cGMP and cAMP, respectively) using a fluorescence polarization assay (Molecular Devices, Sunnyvale, CA, USA)¹⁸ under linear conditions, with and without a PDE5 inhibitor (sildenafil 1 μ M) or a PDE3 inhibitor (milrinone 10 μ M).

Protein kinase G (PKG) activity: PKG-1 activity was assayed in RV free wall tissues using colorimetric analysis (CycLex, Ina, Nagano, Japan), where a peroxidase coupled anti-phospho-G-kinase substrate monoclonal antibody is used as a reporter molecule in a 96-well ELISA format^{19, 20}. Activity was also studied by measuring the phosphorylation of VASP, a myocardial PKG-1 target, using immunoblots; densitometry (over GAPDH expression) was performed and presented as previously described^{16, 17}.

Cell Shortening studies in RV myocytes were obtained as described previously^{21, 22}; for details see supplement.

Statistics: Data were expressed as mean±SEM, and significant differences were evaluated using the Student *t* test for unpaired data or 1-way ANOVA followed by post-hoc Fisher's PLSD as appropriate (SPSS 11, Chicago, IL). $p < 0.05$ was considered significant

Results

We studied hearts (surgical resection or biopsy specimens) from 9 patients with either normal or hypertrophied RVs as well from a patient with LV hypertrophy (but normal RV) (Table 1). RV free wall samples were studied. The diagnosis of RVH was based on standard echocardiographic criteria²³. Confocal microscopy and multiple-staining technique was used to detect the expression of PDE5 and co-localize this enzyme with myosin heavy chain (MHC) in the myocardium or smooth muscle actin (SMA) in coronary vessels. In both the normal LV and RV, PDE5 was only expressed in the coronary artery media and not in the myocardium. In contrast, PDE5 was markedly up-regulated in the myocardium of all the hypertrophied ventricles studied (Figure 1 and Supplement Figure 1A). This protein upregulation was also confirmed in one normal and RVH sample (where we had adequate amount of tissue) with an immunoblot (Supplement Figure 1B).

Patient #2 had hypertrophied LV but normal RV and showed PDE5 expression only in the LV myocardium. Although we did not systematically study PDE5 expression in the LV, we show both the LV and RV tissue from this patient, because it suggests that the PDE5 up-regulation is restricted only to the pressure-overloaded chamber and is likely not induced by circulating factors. Further confirmation that our hearts had significant hypertrophy came from the fact that all, but not the normal hearts, showed a marked up-regulation of brain natriuretic peptide (BNP) in the myocardium ^{24, 25} (Supplement Figure 2).

To determine whether PDE5 mRNA was also up-regulated, we studied whole RV tissue using quantitative reverse transcriptase-polymerase chain reaction (qRT-PCR). PDE5 mRNA levels were significantly higher in RVH, compared to normal RV (Figure 2A). In contrast, PDE3 mRNA (a phosphodiesterase known to be highly expressed in the myocardium ²⁶) did not differ between normal RVs and RVH. In order to compartmentalize PDE5 mRNA in the RV (vascular versus myocardial), we used laser-captured microdissection (LCM) to selectively isolate myocardium (characterized by high MHC and low SMA expression) and coronary vessels (characterized by low MHC and high SMA expression) in human RVs. PDE5 mRNA is significantly up-regulated in the RVH myocardium, whereas it is found in minimal amounts in the normal RV myocardium. Conversely, PDE5 mRNA is found in the coronary arteries from both the normal and RVH hearts, in agreement with our immunohistochemistry (Figure 2B-C). These human data were reproduced in the rat RVs as well (Supplement Figure 3).

Is the PDE5 up-regulation physiologically significant? This is difficult to assess in vivo since PDE5 inhibition will also decrease pulmonary vascular resistance ¹⁰ and the

decreased RV afterload will in itself improve RV function. PDE5 inhibitors may also decrease venous tone, decreasing preload. In addition, the small decrease in systemic pressure that might occur with PDE5 inhibitors may increase sympathetic input to the RV, also indirectly improving function²⁷. To exclude these confounding factors we used a modification of a Langendorff isolated, perfused rat heart model; the RV's contractile function was studied whilst the pressure was recorded in the RV by a balloon, the pulmonary artery (afterload) was occluded and the preload (balloon volume) was kept constant (Figure 3A).

Within 3 weeks post-monocrotaline injection, the rats develop severe PAH and RVH, which we and others have previously characterized using invasive hemodynamic and echocardiographic measurements^{16,17} (Figure 3B). Immunohistochemistry confirmed that, as in the human RV, PDE5 was significantly expressed only in RVH and not in normal RV or LV (Figure 3C). We also used LCM and qRT-PCR (as we did in human RVs, Figure 2) on rat RVs and demonstrated that the expression of PDE5 mRNA was upregulated in the rat RVH myocardium, in a manner similar to that in human RVH (Supplement Figure 4).

The β -agonist isoproterenol caused similar increases in RV developed pressure in normal and hypertrophied RV. However, while MY-5445, a relatively specific PDE5 inhibitor^{28, 29}, did not affect the normal RV, it caused a significant, dose-dependent increase in the developed pressure and both maximum and minimum contractility (dP/dt) in the hypertrophied RV (Figure 4). The native heart rate in the perfused hearts was not different between the normal RVs (192 ± 18 beats per minute, bpm) and RVH (185 ± 14 bpm) and was not altered by the PDE5 inhibitor.

In order to mimic clinical conditions, we used sildenafil (50 mg po) and we fed normal versus RVH rats, 60 minutes before running the isolated hearts. Because of differences in the metabolism of sildenafil in rats, this dose gives serum levels similar to those seen in humans³⁰. RVs from normal sildenafil-treated rats showed no difference in baseline contractile pressure compared to the non-treated controls. In contrast, hypertrophied RVs from sildenafil-treated rats showed a significant increase in the baseline developed pressure (Supplement Figure 4) and dP/dt (not shown), compared to the hypertrophied RVs from untreated controls. MY-5445 had no additional effects on the RVs from the sildenafil-treated rats, whether normal or hypertrophied, suggesting that the sildenafil-treated rats had maximal PDE5 inhibition (Supplement Figure 4).

To confirm that PDE5 inhibitors have primary inotropic effects in individual RV cardiomyocytes, we performed cell-shortening experiments. As in the whole heart experiments, sildenafil (10⁻⁶M) increased contractility in the cardiomyocytes from the hypertrophied but not the normal RVs (Figure 5A).

Normally, PDE5 inhibition causes an increase in cGMP and activation of protein kinase G (PKG). This is associated with a decrease in intracellular Ca⁺⁺ and it would predict a decrease in contractility. However, PKG activity has been reported to be decreased in the hypertrophied LV myocardium³¹. This suggests that the PDE5 inhibition-induced increase in cGMP might not be able to activate the PKG pathway downstream in the hypertrophied RV; instead, it might preferentially inhibit the cGMP-sensitive PDE3²⁶, increasing cAMP, activating PKA, which leads to increase in intracellular Ca⁺⁺ and enhanced inotropy, a mechanism exploited clinically by the PDE3-

inhibitor milrinone ²⁶. We proceeded to examine this hypothesis, using several pharmacological tools, as presented schematically in Figure 5B.

Treatment with sildenafil causes both an increase in cGMP levels and interestingly an increase in cAMP only in RVH ; while there is no effect on cGMP or cAMP levels in the normal RVs, since the target enzyme, i.e. PDE5, is not expressed in the normal myocardium. Isoproterenol, as expected, caused an increase in cAMP levels in both control and hypertrophied RVs, without any significant effect on cGMP levels. Interestingly isoproterenol and sildenafil increased cAMP to a similar degree (Figure 6A).

We then measured total cGMP and cAMP phosphodiesterase activities and by using the relatively specific inhibitors sildenafil and milrinone we were able to measure the components of the total activity that were due to PDE5 and PDE3 respectively. At baseline, cGMP-PDE total activity was significantly increased in RVH compared to the normal RV. This increase in overall cGMP-PDE activity in RVH was almost all contributed by PDE5, since sildenafil caused a decrease in activity to a level similar to the normal RV (Figure 6B). As expected, milrinone had no effects in cGMP-PDE activity. In contrast, cAMP-PDE total activity was similar at baseline in RVH versus normal RV. Interestingly, and as hypothesized, sildenafil significantly inhibited cAMP-PDE5 activity in RVH, in a manner similar to milrinone (Figure 6B). As expected, milrinone decreased cAMP-PDE activity in the normal RV (where PDE3 is expressed) but sildenafil had no effects (since PDE5 is not significantly expressed).

We then directly measured PKG activity and showed a significant decrease in RVH compared to normal RV (Figure 6C). In addition, we showed that the levels of phosphorylated vasodilator-stimulated phosphoprotein (VASP, a PKG-1 substrate in the myocardium) were decreased in RVH compared to normal RVs, further confirming a suppression of PKG activity in RVH (supplement Figure 5). Despite causing a significant increase in cGMP in the RVH myocardium (Figure 6A), sildenafil only slightly and non-significantly increased PKG1 activity ($p < 0.08$) (Supplement Figure 5).

In rat whole-RV tissue the small amount of PDE5 protein expression seen in the normal RV is likely mostly due to its expression in the coronary vessels (Figures 1 and 2). In contrast, PDE3 expression is similar between RVH and normal RV. Both the PDE5 and PDE3 expression pattern is in agreement with their activities (Figure 6 B). On the other hand, the expression of PKG1 does not appear to be significantly decreased, suggesting a functional inhibition of its activity in RVH (Figure 6C). In agreement with our immunohistochemistry data in the rat RV (Figure 3), PDE5 expression measured by immunoblots is significantly increased in RVH (Figure 6D)

We then studied the functional significance of the model proposed in Figure 5B in RV contractility, by using pharmacologic dissection of the pathway distal to PDEs (Figure 7 and supplement Figure 5B). PKG inhibitors (Rp-8-CPT-cGMPS and KT 5823) slightly increased contractility in the normal RV (suggesting that PKG might have some tonic negative inotropic effect) but had no significant effects on RVH. They did not inhibit the inotropic effects of isoproterenol (which are mediated by cAMP/PKA) but also did not inhibit the inotropic effects of sildenafil and MY-5445. This was in agreement with our hypothesis, that the inotropic effects of PDE5 inhibitors are not mediated by

cGMP-PKG but, rather, by cAMP-PKA. Indeed, PKA blockade (H89) completely inhibited the effects of PDE5 inhibitors and isoproterenol in RVH. Interestingly, there was a decrease in contractility beyond baseline in RVH treated with both a PDE5 inhibitor and H89 (Figure 7). This suggests that perhaps some negative inotropic effect of PKG might be exposed if PKA is inhibited.

Discussion

We report for the first time that PDE5 is markedly up-regulated in human RVH. We also show that in the rat, PDE5 inhibition with sildenafil or MY-5445 increases contractility (developed pressure, dP/dt max and myocardial cell shortening) in the hypertrophied RV, but not in the normal RV which lacks PDE5 expression. PDE5 inhibition in the hypertrophied RV is associated with an increase in cGMP, which would normally activate PKG (leading to a decrease in intracellular Ca^{++}) but also inhibit the cGMP-sensitive PDE3. Because overall PKG activity is inhibited in the hypertrophied RV, the pathway is preferentially shifted towards inhibition of PDE3; leading to an increase in cAMP, activation of PKA, increase in intracellular calcium and increased contractility (Figure 5B). The PDE5 inhibitor-induced increase in both contractility and cAMP levels in RVH is significant and similar in magnitude to isoproterenol (Figure 4, 6A, 7C, supplement 5). Our findings have immediate clinical applications; PDE5 inhibition might be a new means of enhancing RV function, which has been shown repeatedly to be a critical predictor of functional status in many cardiovascular diseases¹.

².

Despite its important role, the RV has been understudied compared to the LV. Extrapolating findings from the LV to the RV is not appropriate since their physiology^{1,2} and embryology³² are quite different. Similarly, extrapolating findings from the normal to the hypertrophied ventricle is also inappropriate given the dramatic molecular and metabolic changes that take place in the hypertrophied or failing myocardium². Very recently Borlaug et al³³ hypothesized that despite its very low expression in the normal LV, PDE5 is strategically compartmentalized within the myocytes³⁴ and its inhibition might alter heart function. The authors used load-independent echocardiographic parameters and showed that a single dose of sildenafil in healthy volunteers blunted the systolic response of the LV to b-adrenergic stimulation, i.e. dobutamine infusion³³. Interestingly, they also showed a small but significant increase in the baseline, unstimulated contractility of the LV; they speculated that this might be the result of either reflex sympathetic activation, consequent to a slight systemic vasodilatation, or a direct effect on the LV³³, but they did not study the RV. Because the RV Langendorff model uses a constant afterload and preload and eliminates circulating factors and autonomic input, our data suggest that the increased contractility of the hypertrophied rat RV is due to direct effects of the PDE5 inhibitors on the myocardium (Figures 4,6,7). This is further supported by the direct effects of sildenafil on isolated cardiomyocytes (Figure 5A).

Our proposed mechanism of the inotropic effects of PDE5 inhibitors on the hypertrophied RV (Figure 5B) is supported by the pharmacologic dissection of the pathway distal to PDEs. For example, as our model predicted, the effects of sildenafil and MY5445 in RVH were inhibited by a PKA inhibitor and not by a PKG inhibitor (Figure

7, supplement Figure 5). Clearly the role of PKG-1 activity is crucial for this proposed mechanism; although protein expression of PKG1 is not altered in RVH (Figure 6D), its activity is clearly suppressed in RVH compared to normal RV, as shown by 2 different techniques (Figure 6C and supplement Figure 5). However, there is a trend ($p=0.08$) toward an increase in PKG-1 activity in the RVH myocardium when treated with sildenafil (Supplement Figure 5). This is not surprising given the presence of PKG-1 protein in the RVH myocardium (Figure 6D) and the large sildenafil-induced increase in cGMP levels in RV (Figure 6A). We propose that the relative balance of the cGMP-PKG versus cAMP-PKA axis will determine the acute response of the myocardium to sildenafil. This might vary among different heart chambers, perhaps species and even stages of myocardial disease. In RVH (at least in during relatively compensated RV dysfunction) the predominant axis in this response is cAMP-PKA.

Other mechanisms might also be involved in the beneficial acute effects of PDE5 inhibitors in the hypertrophied RV. For example, PDE5 inhibition might also improve coronary perfusion⁹ (PDE5 inhibitors were first developed as anti-anginal agents) and this might be important in the relatively ischemic hypertrophied RV², further improving function, particularly diastolic relaxation (dp/dt min, Figure 4B).

Takimoto et al showed recently that chronic PDE5 inhibition improved LV function in a mouse model with LVH due to transverse aortic constriction³⁰. LVH regressed and LV contractility improved in mice treated with PDE5 inhibitors, despite the persistence of aortic constriction. The authors showed that PDE5 inhibition inactivated a number of genes of the fetal/hypertrophy heart gene program, which is pathologically activated in LVH³⁰. If similar mechanisms take place in the RV, then PDE5 inhibitors

might also cause regression of RVH and improvement of RV function, in addition to their effects on decreasing the RV afterload. In a double-blind randomized trial, Wilkins et al showed that sildenafil (but not bosentan, an endothelin receptor antagonist also approved for the treatment of PAH) decreased RVH (studied by MRI) ³⁵, although the relative importance of decreasing afterload versus direct anti-hypertrophic effects on the RV is difficult to determine in vivo. Because of its effectiveness, excellent toxicity profile and relative low price compared to the other available therapies ³⁶, sildenafil use is rapidly increasing in PAH patients and its potential benefit in a number of cardiovascular disorders is also being investigated.

The increased mortality, mainly due to ventricular arrhythmias, in patients with LV failure treated with PDE3 inhibitors (compared to placebo) ³⁷ might at first appear concerning, since according to our model, PDE5 inhibition translates into PDE3 inhibition in the hypertrophied RV. PDE3 inhibitor studies were performed mostly on patients with diseased LVs from ischemic heart disease. However, the LVs of patients with PAH do not typically have significant coronary disease. Furthermore, since the LV in these patients is also not hypertrophied, PDE5 is not significantly expressed in the LV myocardium (Figure 3C); so PDE5 inhibition should not affect the LV myocardium (since the target of the drug is absent). In that sense, PDE5 inhibitors are truly RVH chamber-specific. PDE5 inhibitors have been used now for a number of years in PAH patients; in the SUPER trial where long term follow up of at least one year was documented, there no reports of increased mortality, ventricular arrhythmias or cardiac-related deaths ³.

Limitations: More work is needed to study the long-term effect of PDE5 inhibitors in both compensated but also decompensated RV disease. We studied human RVs mostly from patients with RVH and relatively compensated RV dysfunction, who did not have signs of overt RV failure (except from patient #9) and underwent elective surgery. Similarly, our rat RVs showed hypertrophy (not dilated or thin-walled) and the rats did not have signs of severe right heart failure. It is possible that the regulation of PDE5 expression and function and the effects of sildenafil might be different in the RVs of patients with advanced disease or are perhaps dilated and thin-walled; our results cannot necessarily be extrapolated in patients with late stages of RV failure.

Conclusions: Our findings on human hearts and a well-established animal model raise a number of intriguing possibilities that need to be considered by clinicians treating PAH patients with PDE5 inhibitors, or designing trials with this class of drugs. PDE5 inhibitors might have the very desirable combination of primary inotropic, anti-hypertrophic³⁰ and afterload-reducing effects on the RV, without significantly affecting systemic hemodynamics^{10, 38}, making them very attractive for the treatment of many diseases involving the RV.

Figure 1:

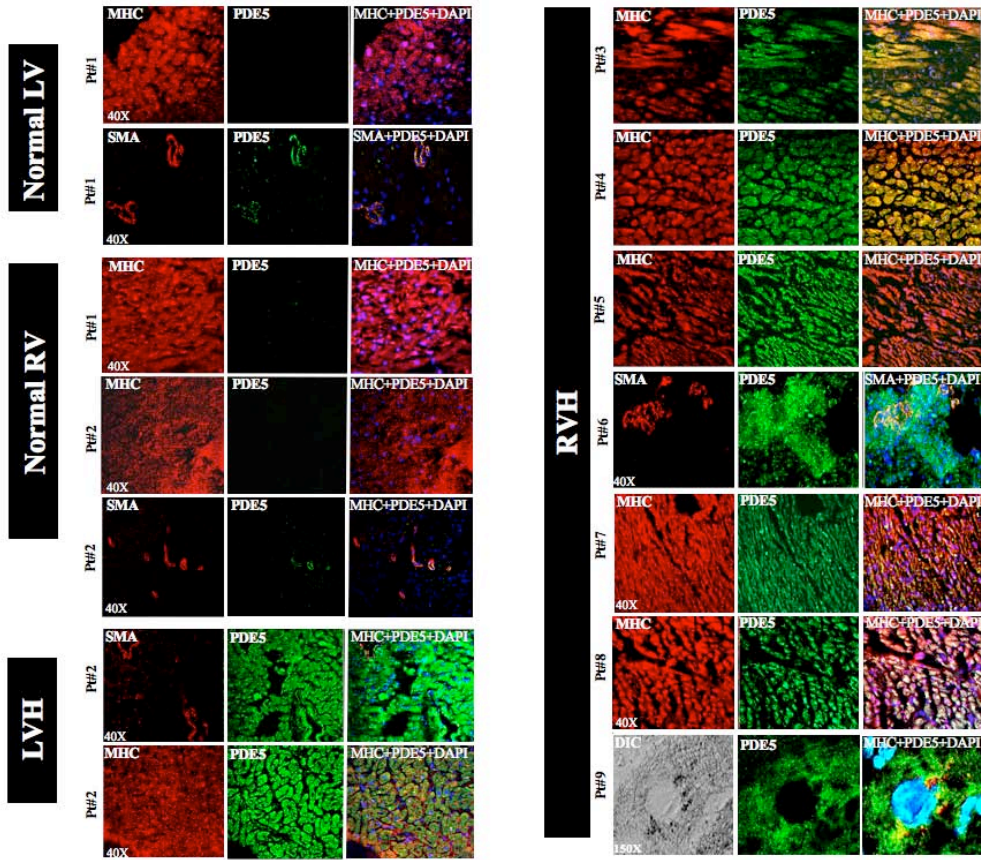


Figure 1: PDE5 expression is increased in the hypertrophied, but not the normal human RV.

Multiple staining immunohistochemistry technique and multi-photon confocal microscopy show that PDE5 protein expression is expressed only in the media of the coronary vessels (co-localization with smooth muscle actin, SMA) in the normal RV and LV and is markedly upregulated in the myocardium (co-localization with myosin heavy chain, MHC) of the hypertrophied ventricles. The left column (red) shows expression of either SMA or MHC. The middle column (green) shows PDE5 expression on the same slide. The third column is a merged picture of the red and green channels, plus a nuclear stain with DAPI (blue). Patient numbers correspond to Table 1. All magnifications are 40x except in patient #9 (right lower corner), where a 150x image shows a single cardiomyocyte.

Figure 2:

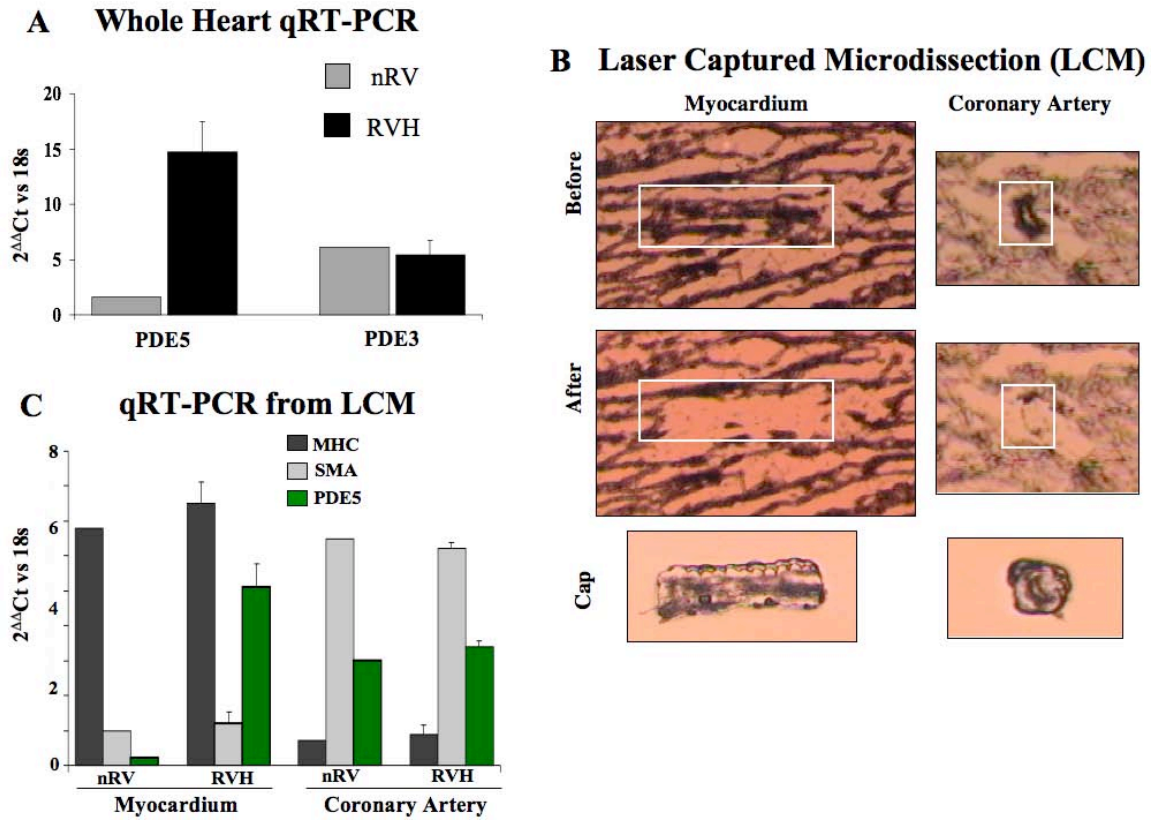


Figure 2: PDE5 mRNA in human normal and hypertrophied RV reveals regulation of expression in a tissue-specific manner.

A: Whole human heart qRT-PCR shows that PDE5 mRNA is increased in RVH hearts (n=7), in contrast to PDE3. For the normal RVs (nRV) the mean of n=2 is shown.

B-C: Laser-Captured Microdissection (LCM) and qRT-PCR was applied on human RV tissue. LCM was used to isolate myocardium versus coronary arteries in normal and hypertrophied human RV for qRT-PCR. A myocardium sample was characterized by high MHC and low SMA expression. In contrast, a coronary artery sample was characterized by high SMC and low MHC expression. PDE5 mRNA is markedly increased in RVH compared to normal RV myocardium, while is expressed in the coronary vessels in both hearts, in agreement with our immunohistochemistry data in Figure 1.

Figure 3:

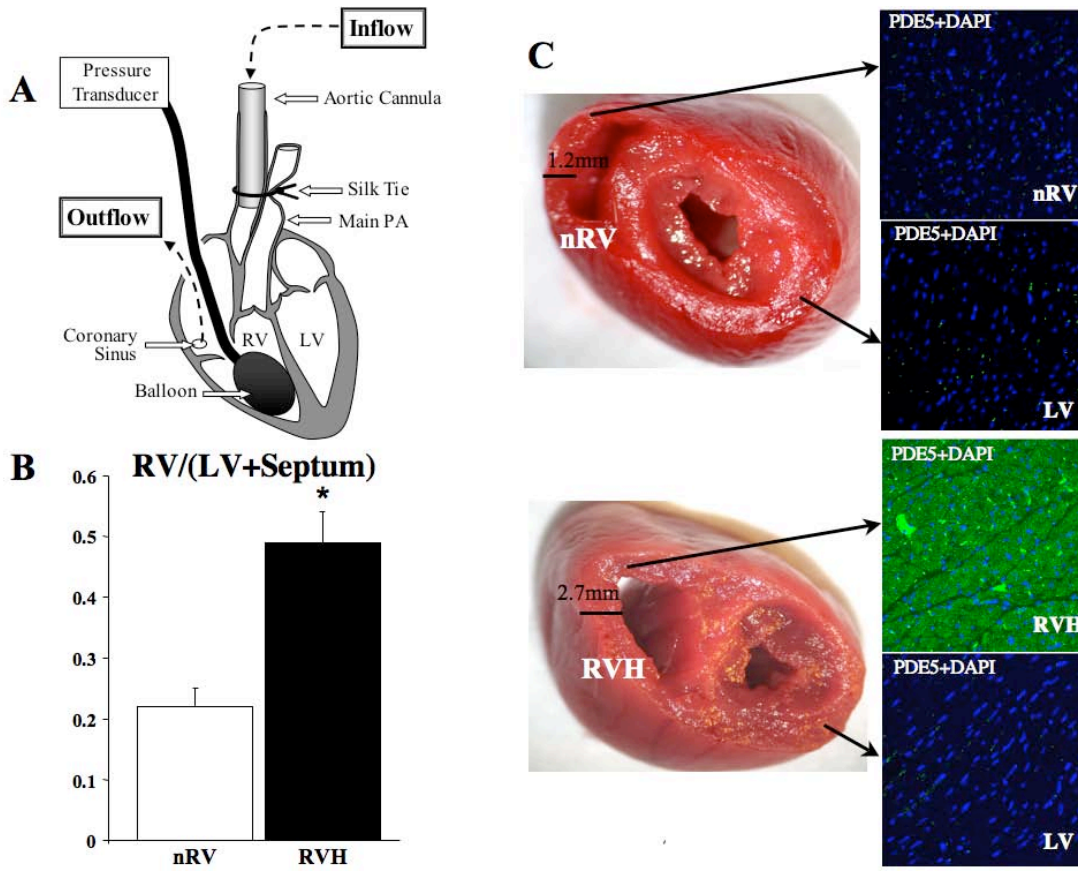


Figure 3: Rat model of RVH and modified Langendorff isolated perfused heart.

A: Schematic of our isolated perfused RV (modified Langendorff preparation)/

B: Rat model of RVH. The RV was significantly hypertrophied in the rats with experimental PAH, 3 weeks post monocrotaline injection (RVH, n=9) compared to control rats with normal RVs (nRV, n=7), as shown by the RV to LV plus septum weight ratio (*p<0.01).

C: RVH was the only heart chamber that showed significant PDE5 expression (green). DAPI (blue) was used to stain the nuclei (all images are controlled to background level set by secondary only slides).

Figure 4:

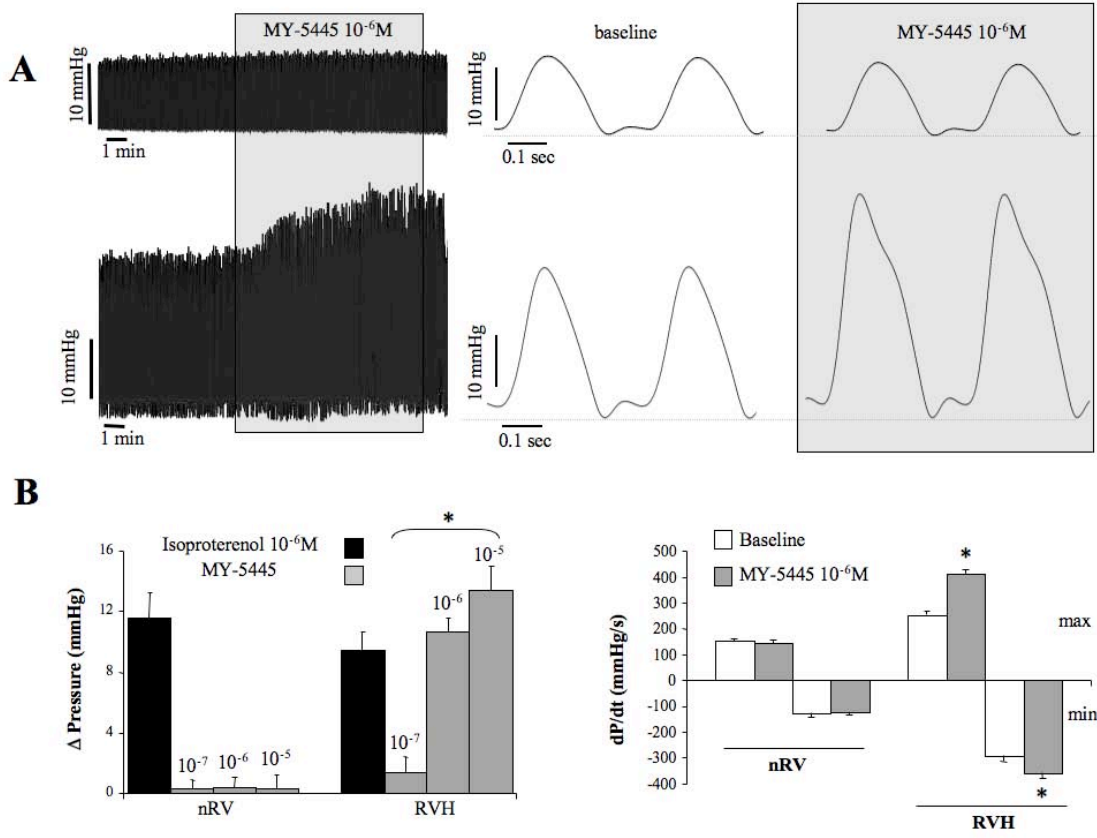


Figure 4: Representative and mean data of acute RV contractility with PDE5 inhibition.

A: Representative traces of the developed contractile pressure in the normal RV (top) or RVH (bottom) at different time scales, before and after the addition of the PDE5 inhibitor MY-5445 in the perfusate (shaded area). Note the differences in both the amplitude and rate of development of pressure in systole and diastole.

B: Mean data showing that the PDE5 inhibitor MY5445 increased contractile pressure and both max and min dP/dt in a dose-dependent manner in the RVH (n=9) but not the normal RV (nRV, n=7), whereas both normal and hypertrophied RV responded similarly to isoproterenol (*p<0.01).

Figure 5:

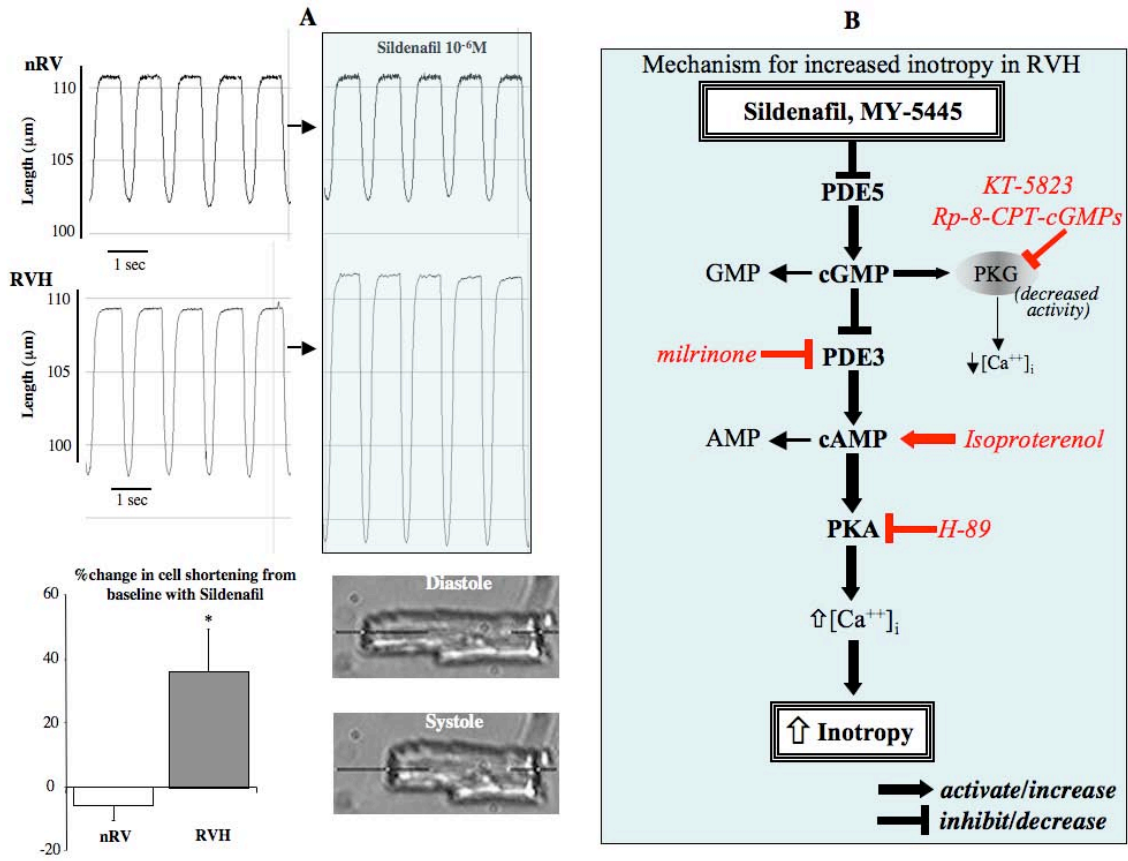


Figure 5: Isolated single RV cardiomyocyte cell shortening experiments and proposed mechanism for the inotropic effects of PDE5 inhibitors in RVH.

A: Representative and mean data of single RV cardiomyocyte cell shortening for normal (nRV) and hypertrophied (RVH) cardiomyocytes, before and after sildenafil treatment (n=5 rats/group, 16-18 cells/group, p<0.01).

B: Our proposed mechanism for acute PDE5 inhibition causing increased inotropy in RVH. The site of action of drugs used (see below) is shown in red.

Figure 6:

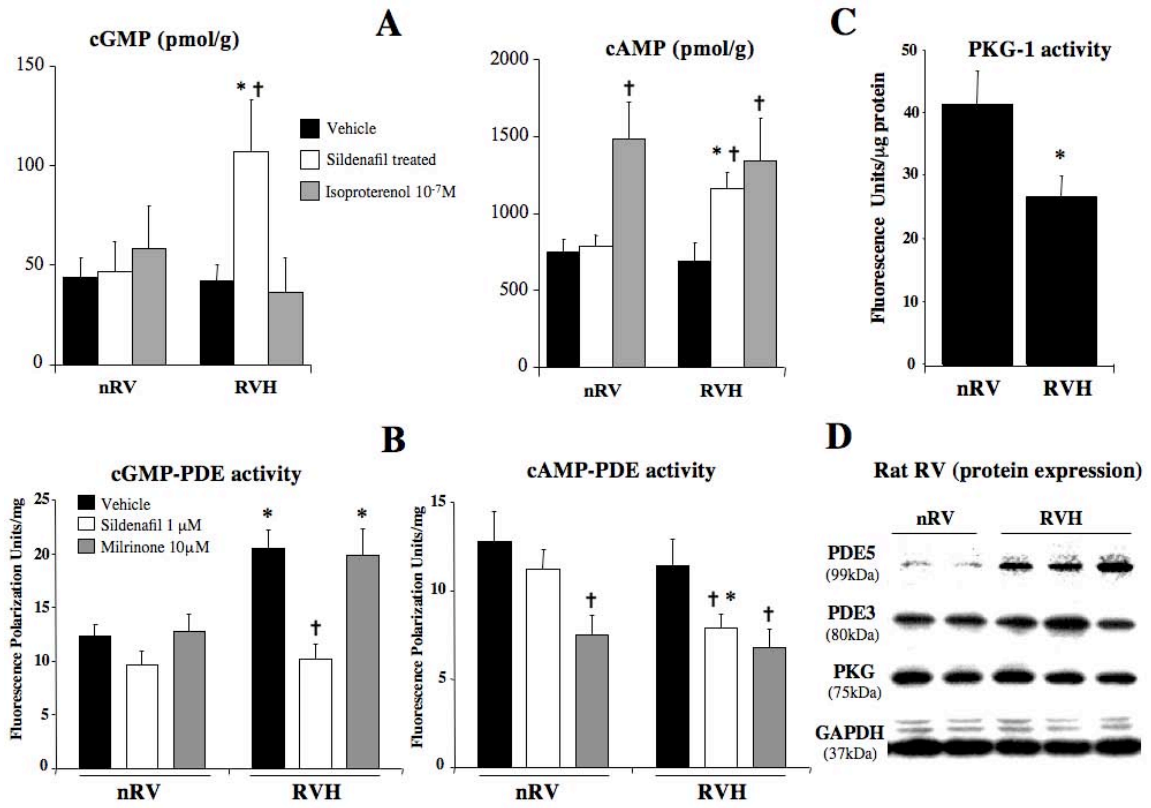


Figure 6: Enzymatic activity and expression of PDE3, PDE5 and PKG in normal RV and RVH.

A: cGMP and cAMP levels in the RV (normal versus RVH) from untreated rats, sildenafil-treated (50 mg gavage 60 minutes prior to sacrifice), and isoproterenol perfused hearts (n=5/group, * p<0.01 versus nRV, † p<0.01 versus untreated).

B: cGMP- and cAMP-phosphodiesterase activities in normal and hypertrophied RVs treated acutely with vehicle (perfusate), sildenafil, or milrinone (n=6/group, * p<0.01 versus nRV, † p<0.01 versus vehicle).

C: PKG-1 activity in RV homogenates from normal controls and rats with RVH (n=6/group, * p<0.01)

D: Immunoblots of rat normal and hypertrophied RVs. There is a marked up-regulation of PDE5 expression in the hypertrophied RV, while PDE3, and PKG-1 expression is not significantly different.

Figure 7:

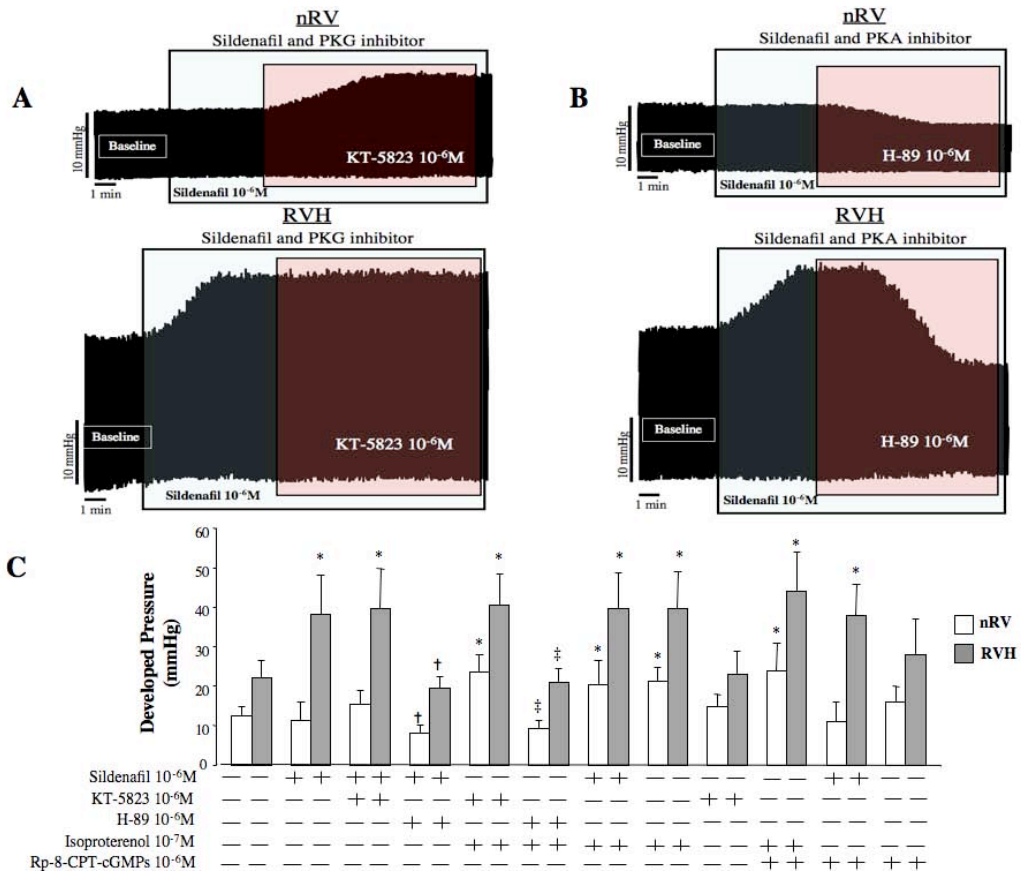


Figure 7: Effects of PKG and PKA inhibition on the PDE5 inhibitor- and isoproterenol-induced inotropy in normal and hypertrophied RVs.

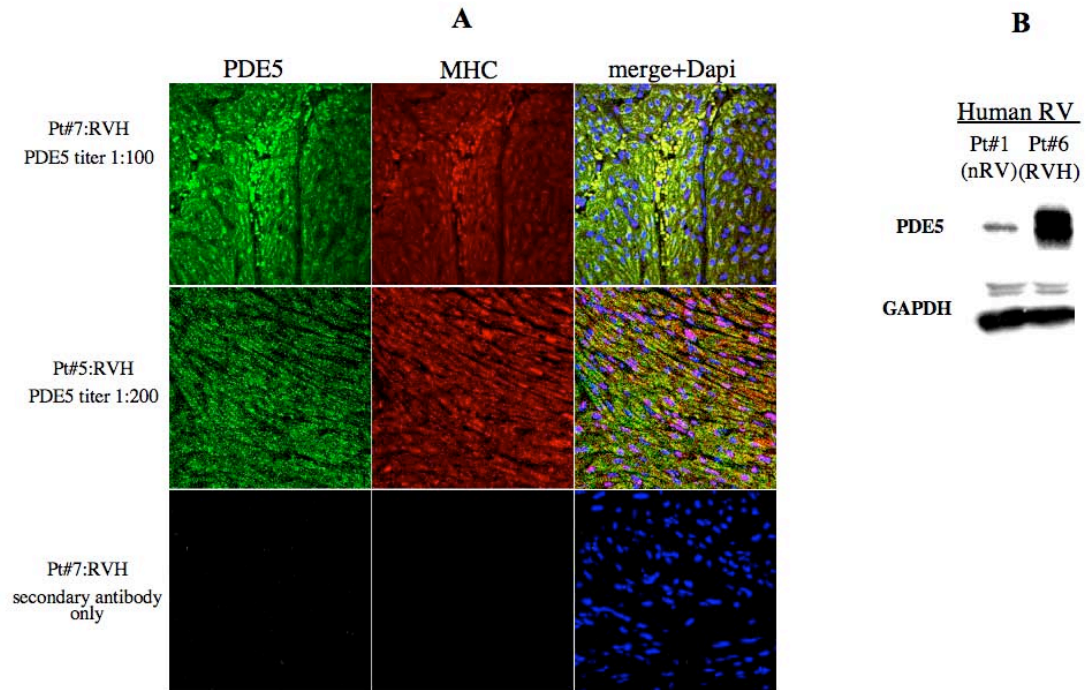
A: Representative trace of contractile pressure in a normal RV (upper panel) and RVH (lower panel) at baseline, with sildenafil, and concomitant PKG inhibitor (KT-5823).

B: Representative trace of contractile pressure in a normal RV (upper panel) and RVH(lower panel) at baseline, with sildenafil, and concomitant PKA inhibitor (H-89).

C: Mean data of developed RV pressures from modified Langendorff perfused hearts (n=6 per group, * p<0.01 versus baseline, † p<0.01 versus sildenafil, ‡ p<0.01 versus isoproterenol) in the presence of different drug combinations (see results).

Supplement Figure 1:

Supplement Figure 1



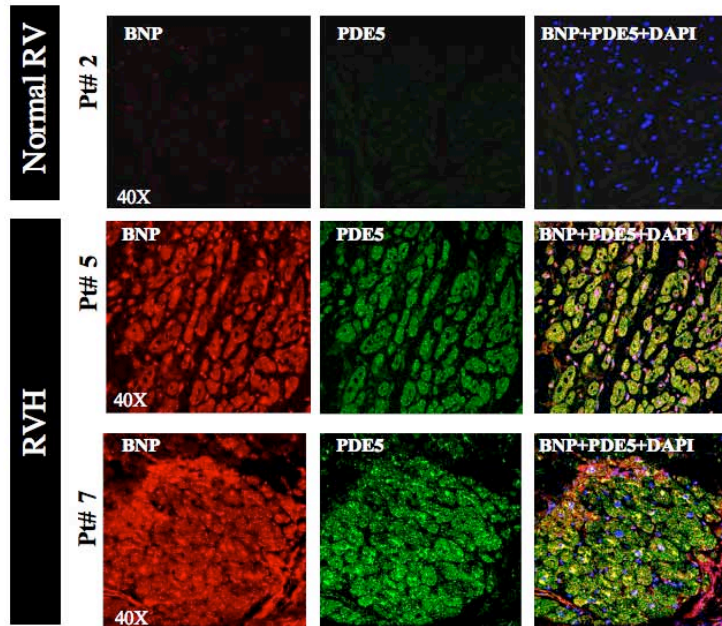
Supplement Figure 1: PDE5 expression in human RVH

A: Human hypertrophied RVs stained with PDE5 and MHC at PDE5 antibody titers of 1:100 and 1:200, showing strong expression of PDE5 at lower antibody titers, compared to the 1:50 titers shown in Figure 1.

B: Immunoblot of PDE5 expression in a normal human RV compared to a patient with RVH.

Supplement Figure 2:

Supplement Figure 2

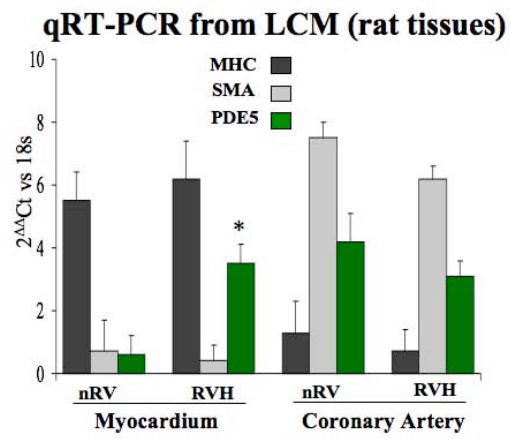


Supplement Figure 2: BNP expression is up-regulated in human RVH.

All hypertrophied human hearts were characterized by an up-regulation of brain natriuretic factor (BNP, a marker of hypertrophy) expression, compared to the normal hearts. Three representative examples are shown (Patients as in table 1).

Supplement Figure 3:

Supplement Figure 3

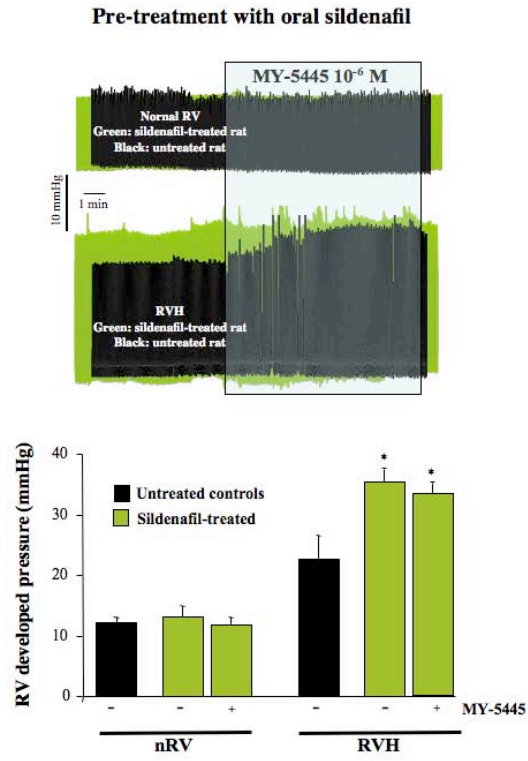


Supplement Figure 3: PDE5 is selectively upregulated in the rat RVH myocardium

Mean qRT-PCR data from laser captured microdissected tissues from rat right ventricles of control and RVH rats. (see also Figure 2 for a similar approach in human RVs)

Supplement 4:

Supplement Figure 4

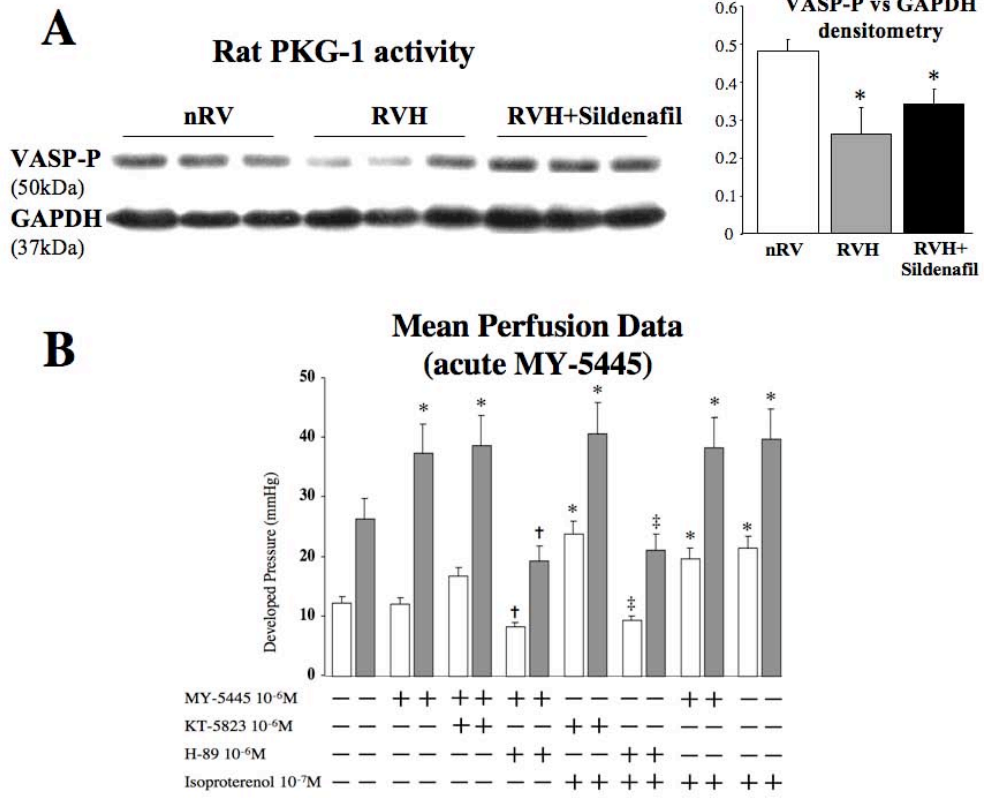


Supplement Figure 4: Oral sildenafil increases inotropy in the isolated hypertrophied, but not normal, rat RV.

Superimposed representative traces from normal (top) and hypertrophied (bottom) isolated RVs from rats treated with sildenafil (50 mg gavage, 60 minutes before the heart isolation) in green, versus untreated rats (in black). The effects of the addition of MY-5445 in the perfusate are shown in the shaded area. The mean effects on the contractile pressure are also shown (n=6 rats/group, *p<0.01 compared to untreated).

Supplement Figure 5:

Supplement Figure 5



Supplement Figure 5: PKG-1 activity with sildenafil treatment, cardiomyocyte upregulation of PDE5 expression from laser captured microdissection, and mean perfusion data using MY-5445.

The upper left shows the immunoblot of the PKG-1 activity with the corresponding densitometry graph to the right, showing a decrease in PKG-1 activity in RV hypertrophy compared the normal control, and a trend ($p=0.08$) for increase in PKG-1 activity in the RVH myocardium when treated with 50mg of gavage sildenafil 60 minutes prior to harvesting the heart (* $p<0.01$ versus nRV)

The lower left panel shows the mean qRT-PCR data from the laser captured microdissection data from rat right ventricles of control and RVH rats.

The lower right panel shows mean data of developed RV pressures form modified langendorff perfused hearts using MY-5445 as the PDE5 inhibitor ($n=4-6$ per group, * $p<0.01$ versus baseline, † $p<0.01$ versus MY-5445, ‡ $p<0.01$ versus isoproterenol).

Table 1

Patient	Age-Sex	Diagnosis	Tissue	RV thickness (cm)	Medications
1	19 y F	Left atrial sarcoma <i>Heart transplant</i>	Normal LV Normal RV	0.3	ASA
2	54 y M	Intractable angina Moderate LVH <i>Heart transplant</i>	LVH Normal RV	0.4	metoprolol, statin, ramipril, nitrates, ASA, ticlopidine
3	4 m F	Tetralogy of Fallot <i>Surgical specimen</i>	RVH	1	None
4	3 y M	RV outflow tract obstruction <i>Surgical specimen</i>	RVH	1.1	None
5	5 m M	Tetralogy of Fallot <i>Surgical specimen</i>	RVH	0.9	None
6	58 y F	Rheumatic valve disease <i>Heart transplant</i>	RVH	1.6	atenolol enalapril
7	11 d M	Hypoplastic Left Heart <i>Surgical specimen</i>	RVH	0.7	prostaglandin IV
8	4 m M	Tetralogy of Fallot <i>Surgical specimen</i>	RVH	0.9	None
9	62 y M	PAH <i>RV biopsy & transplant</i>	RVH	1.8	sildenafil flolan

References:

1. Chin KM, Kim NH, Rubin LJ. The right ventricle in pulmonary hypertension. *Coron Artery Dis.* 2005; 16:13-18.
2. Voelkel NF, Quaife RA, Leinwand LA, Barst RJ, McGoon MD, Meldrum DR, Dupuis J, Long CS, Rubin LJ, Smart FW, Suzuki YJ, Gladwin M, Denholm EM, Gail DB. Right ventricular function and failure: report of a National Heart, Lung, and Blood Institute working group on cellular and molecular mechanisms of right heart failure. *Circulation.* 2006; 114:1883-1891.
3. Galie N, Ghofrani HA, Torbicki A, Barst RJ, Rubin LJ, Badesch D, Fleming T, Parpia T, Burgess G, Branzi A, Grimminger F, Kurzyna M, Simonneau G. Sildenafil citrate therapy for pulmonary arterial hypertension. *N Engl J Med.* 2005; 353:2148-2157.
4. Cheitlin MD, Hutter AM, Jr., Brindis RG, Ganz P, Kaul S, Russell RO, Jr., Zusman RM. ACC/AHA expert consensus document. Use of sildenafil (Viagra) in patients with cardiovascular disease. American College of Cardiology/American Heart Association. *J Am Coll Cardiol.* 1999; 33:273-282.
5. Corbin J, Rannels S, Neal D, Chang P, Grimes K, Beasley A, Francis S. Sildenafil citrate does not affect cardiac contractility in human or dog heart. *Curr Med Res Opin.* 2003; 19:747-752.
6. Wallis RM, Corbin JD, Francis SH, Ellis P. Tissue distribution of phosphodiesterase families and the effects of sildenafil on tissue cyclic nucleotides, platelet function, and the contractile responses of trabeculae carneae and aortic rings in vitro. *Am J Cardiol.* 1999; 83:3C-12C.
7. Cremers B, Scheler M, Maack C, Wendler O, Schafers HJ, Sudkamp M, Bohm M. Effects of sildenafil (viagra) on human myocardial contractility, in vitro arrhythmias, and tension of internal mammaria arteries and saphenous veins. *J Cardiovasc Pharmacol.* 2003; 41:734-743.
8. Jackson G, Benjamin N, Jackson N, Allen MJ. Effects of sildenafil citrate on human hemodynamics. *Am J Cardiol.* 1999; 83:13C-20C.
9. Herrmann HC, Chang G, Klugherz BD, Mahoney PD. Hemodynamic effects of sildenafil in men with severe coronary artery disease. *N Engl J Med.* 2000; 342:1622-1626.
10. Michelakis E, Tymchak W, Lien D, Webster L, Hashimoto K, Archer S. Oral sildenafil is an effective and specific pulmonary vasodilator in patients with pulmonary arterial hypertension: comparison with inhaled nitric oxide. *Circulation.* 2002; 105:2398-2403.
11. Michelakis ED, Tymchak W, Noga M, Webster L, Wu XC, Lien D, Wang SH, Modry D, Archer SL. Long-term treatment with oral sildenafil is safe and improves functional capacity and hemodynamics in patients with pulmonary arterial hypertension. *Circulation.* 2003; 108:2066-2069.
12. Wharton J, Strange JW, Moller GM, Growcott EJ, Ren X, Franklyn AP, Phillips SC, Wilkins MR. Antiproliferative effects of phosphodiesterase type 5 inhibition in human pulmonary artery cells. *Am J Respir Crit Care Med.* 2005; 172:105-113.

13. Lepore JJ, Maroo A, Pereira NL, Ginns LC, Dec GW, Zapol WM, Bloch KD, Semigran MJ. Effect of sildenafil on the acute pulmonary vasodilator response to inhaled nitric oxide in adults with primary pulmonary hypertension. *Am J Cardiol.* 2002; 90:677-680.
14. Ghofrani HA, Voswinckel R, Reichenberger F, Olschewski H, Haredza P, Karadas B, Schermuly RT, Weissmann N, Seeger W, Grimminger F. Differences in hemodynamic and oxygenation responses to three different phosphodiesterase-5 inhibitors in patients with pulmonary arterial hypertension: a randomized prospective study. *J Am Coll Cardiol.* 2004; 44:1488-1496.
15. Cowan KN, Heilbut A, Humpl T, Lam C, Ito S, Rabinovitch M. Complete reversal of fatal pulmonary hypertension in rats by a serine elastase inhibitor. *Nat Med.* 2000; 6:698-702.
16. McMurtry MS, Archer SL, Altieri DC, Bonnet S, Haromy A, Harry G, Bonnet S, Puttagunta L, Michelakis ED. Gene therapy targeting survivin selectively induces pulmonary vascular apoptosis and reverses pulmonary arterial hypertension. *J Clin Invest.* 2005; 115:1479-1491.
17. McMurtry MS, Bonnet S, Wu X, Dyck JR, Haromy A, Hashimoto K, Michelakis ED. Dichloroacetate prevents and reverses pulmonary hypertension by inducing pulmonary artery smooth muscle cell apoptosis. *Circ Res.* 2004; 95:830-840.
18. Huang W, Zhang Y, Sportsman JR. A fluorescence polarization assay for cyclic nucleotide phosphodiesterases. *J Biomol Screen.* 2002; 7:215-222.
19. Li Z, Xi X, Gu M, Feil R, Ye RD, Eigenthaler M, Hofmann F, Du X. A stimulatory role for cGMP-dependent protein kinase in platelet activation. *Cell.* 2003; 112:77-86.
20. Pfeifer A, Aszodi A, Seidler U, Ruth P, Hofmann F, Fassler R. Intestinal secretory defects and dwarfism in mice lacking cGMP-dependent protein kinase II. *Science.* 1996; 274:2082-2086.
21. Bouchard RA, Clark RB, Giles WR. Role of sodium-calcium exchange in activation of contraction in rat ventricle. *J Physiol.* 1993; 472:391-413.
22. Light P, Shimoni Y, Harbison S, Giles W, French RJ. Hypothyroidism decreases the ATP sensitivity of KATP channels from rat heart. *J Membr Biol.* 1998; 162:217-223.
23. Schiller NB, Sahn DJ. Pulmonary pressure measurement by Doppler and two-dimensional echocardiography in adult and pediatric populations. In: Weir EK, Archer SL, Reeves JT, eds. *The diagnosis and treatment of pulmonary hypertension.* Mount Kisco, New York: Futura; 1992:41-59.
24. Magga J, Vuolteenaho O, Tokola H, Marttila M, Ruskoaho H. B-type natriuretic peptide: a myocyte-specific marker for characterizing load-induced alterations in cardiac gene expression. *Ann Med.* 1998; 30 Suppl 1:39-45.
25. Hasegawa K, Fujiwara H, Doyama K, Miyamae M, Fujiwara T, Suga S, Mukoyama M, Nakao K, Imura H, Sasayama S. Ventricular expression of brain natriuretic peptide in hypertrophic cardiomyopathy. *Circulation.* 1993; 88:372-380.
26. Degerman E, Belfrage P, Manganiello VC. Structure, localization, and regulation of cGMP-inhibited phosphodiesterase (PDE3). *J Biol Chem.* 1997; 272:6823-6826.

27. Phillips BG, Kato M, Pesek CA, Winnicki M, Narkiewicz K, Davison D, Somers VK. Sympathetic activation by sildenafil. *Circulation*. 2000; 102:3068-3073.
28. Hagiwara M, Endo T, Kanayama T, Hidaka H. Effect of 1-(3-chloroanilino)-4-phenylphthalazine (MY-5445), a specific inhibitor of cyclic GMP phosphodiesterase, on human platelet aggregation. *J Pharmacol Exp Ther*. 1984; 228:467-471.
29. Xu HL, Wolde HM, Gavriilyuk V, Baughman VL, Pelligrino DA. cAMP modulates cGMP-mediated cerebral arteriolar relaxation in vivo. *Am J Physiol Heart Circ Physiol*. 2004; 287:H2501-2509.
30. Takimoto E, Champion HC, Li M, Belardi D, Ren S, Rodriguez ER, Bedja D, Gabrielson KL, Wang Y, Kass DA. Chronic inhibition of cyclic GMP phosphodiesterase 5A prevents and reverses cardiac hypertrophy. *Nat Med*. 2005; 11:214-222.
31. Su J, Zhang Q, Moalem J, Tse J, Scholz PM, Weiss HR. Functional effects of C-type natriuretic peptide and nitric oxide are attenuated in hypertrophic myocytes from pressure-overloaded mouse hearts. *Am J Physiol Heart Circ Physiol*. 2005; 288:H1367-1373.
32. Zaffran S, Kelly RG, Meilhac SM, Buckingham ME, Brown NA. Right ventricular myocardium derives from the anterior heart field. *Circ Res*. 2004; 95:261-268.
33. Borlaug BA, Melenovsky V, Marhin T, Fitzgerald P, Kass DA. Sildenafil inhibits beta-adrenergic-stimulated cardiac contractility in humans. *Circulation*. 2005; 112:2642-2649.
34. Senzaki H, Smith CJ, Juang GJ, Isoda T, Mayer SP, Ohler A, Paolocci N, Tomaselli GF, Hare JM, Kass DA. Cardiac phosphodiesterase 5 (cGMP-specific) modulates beta-adrenergic signaling in vivo and is down-regulated in heart failure. *Faseb J*. 2001; 15:1718-1726.
35. Wilkins MR, Paul GA, Strange JW, Tunariu N, Gin-Sing W, Banya WA, Westwood MA, Stefanidis A, Ng LL, Pennell DJ, Mohiaddin RH, Nihoyannopoulos P, Gibbs JS. Sildenafil versus Endothelin Receptor Antagonist for Pulmonary Hypertension (SERAPH) study. *Am J Respir Crit Care Med*. 2005; 171:1292-1297.
36. Archer SL, Michelakis ED. An evidence-based approach to the management of pulmonary arterial hypertension. *Curr Opin Cardiol*. 2006; 21:385-392.
37. DiBianco R, Shabetai R, Kostuk W, Moran J, Schlant RC, Wright R. A comparison of oral milrinone, digoxin, and their combination in the treatment of patients with chronic heart failure. *N Engl J Med*. 1989; 320:677-683.
38. Webster LJ, Michelakis ED, Davis T, Archer SL. Use of sildenafil for safe improvement of erectile function and quality of life in men with New York Heart Association classes II and III congestive heart failure: a prospective, placebo-controlled, double-blind crossover trial. *Arch Intern Med*. 2004; 164:514-520.

Chapter 4:

A dynamic and chamber-specific mitochondrial remodeling in right ventricular hypertrophy can be therapeutically targeted

Abstract

Objectives: The right ventricle (RV) fails quickly after increases in its afterload (i.e. pulmonary hypertension) compared to the left ventricle (LV) (i.e. systemic hypertension), resulting in significant morbidity and mortality. We hypothesized that the poor performance of the hypertrophied RV (RVH) is caused, at least in part, by a suboptimal mitochondrial/metabolic remodeling.

Methods/Results: We studied mitochondrial membrane potential, a surrogate for mitochondrial function, in human (n=11) and rat hearts with physiologic (neonatal) and pathologic (pulmonary hypertension) RVH in vivo and in vitro. Mitochondrial membrane potential is higher in normal LV compared to RV, but is highest in RVH, both in myocardium and isolated cardiomyocytes ($p < 0.01$). Mitochondrial membrane potential correlated positively with the degree of RVH in vivo and was recapitulated in phenylephrine-treated neonatal cardiomyocytes, an in-vitro model of hypertrophy. The phenylephrine-induced mitochondrial hyperpolarization was reversed by VIVIT, an inhibitor of the Nuclear-Factor-of-Activated-T-lymphocytes (NFAT), a transcription factor regulating the expression of several mitochondrial enzymes during cardiac development and hypertrophy. The clinically used drug Dichloroacetate (DCA, known to increase the mitochondria-based glucose oxidation) reversed both the phenylephrine-induced mitochondrial hyperpolarization and NFAT activation. In Langendorff perfusions DCA increased rat RV inotropy in RVH ($p < 0.01$) but not normal RVs,

suggesting that mitochondrial hyperpolarization in RVH might be associated with its suboptimal performance.

Conclusions: The dynamic changes in mitochondrial membrane potential during RVH are chamber-specific, associated with NFAT activation, and can be pharmacologically reversed (leading to improved contractility). This mitochondrial remodeling might provide a framework for development of novel RV-specific therapies.

Word Count: 248

Background:

Although mechanisms of left ventricular (LV) heart failure are well documented, right ventricular (RV) failure remains understudied, despite its high clinical importance. RV dysfunction is a major cause of morbidity and mortality in many conditions, including pulmonary arterial hypertension (PAH), congenital heart disease or lung transplant surgery^{1,2}. In response to increased afterload (as seen in PAH), the thin RV of the normal adult heart hypertrophies, but eventually quickly dilates and fails. There are however situations in congenital heart disease where the RV remains hypertrophied and compensated for years despite the development of PAH. These cases are typically seen when there is no involution of the physiologic neonatal RV hypertrophy and the fetal morphology persists through adulthood. In contrast, the normal adult LV can develop hypertrophy and remain in a compensated state in response to an increase in its afterload (systemic hypertension) for decades. The relatively early failure of the RV in pulmonary hypertension explains largely the much worse survival of patients with PAH compared to patients with systemic hypertension; at the same time this raises the exciting possibility

that something in the neonatal hypertrophied RV (normal remodeling) offers superior function and protection compared to the acquired RV hypertrophy in adults with PAH (abnormal remodeling)³. The cause of this early failure remains unknown and understudied and explains the lack of RV-specific therapies^{1,2}.

We have recently described that phosphodiesterase 5 inhibitors, such as sildenafil, may be RV-specific inotropes⁴. This is based on the fact that phosphodiesterase type 5 is selectively expressed in the myocardium of the hypertrophied RV (RVH) but not in the LV of the same animal⁴. In the search for better RV-specific therapies, as opposed to the LV, identification of differences between the two ventricles is critical. There are several studies examining the metabolism of the LV^{5,6}, but there is an impressive lack of studies on the metabolism of the RV. There is some evidence for differences between the metabolism of the RV and LV, at least in hypoxic animals⁷. Potential differences in the metabolism or molecular biology between the two ventricles are not surprising given the recent discovery that the two ventricles have a different origin at early embryogenesis of the heart; while the RV develops from the anterior heart field, the LV develops from the early heart tube⁸. It is therefore not appropriate to extrapolate findings or conclusions from the LV to the RV. Also, the adaptation of the RV to increased afterload may be regulated by mechanisms different than in the LV⁹. The need to specifically study RV function and failure was recently recognized by the National Institutes of Health (NIH) as a priority¹.

In the neonatal heart, the RV is physiologically hypertrophied, in response to the high pulmonary vascular resistance *in utero*. However, after birth, the thickness of the RV eventually becomes only a third of that of the LV, as the pulmonary vascular

resistance gradually decreases¹⁰. The physiologic hypertrophy in the neonatal RV might be regulated by a “fetal gene program”¹¹, that might be reactivated (at whole or in part) in adult diseases states. Fetal and adult cardiac hypertrophy are also characterized by a predominantly glycolytic phenotype^{5, 6, 12}, which in the LV^{13, 14}, vascular biology¹⁵ or cancer¹⁶, is associated with a resistance to apoptosis. This has not been studied directly in the RV. The fact that metabolism and apoptosis are both directly regulated by mitochondria¹⁷ suggests that a potential mitochondrial and metabolic remodeling might be central to the regulation of RV hypertrophy.

We hypothesized that there is a chamber-specific and dynamic mitochondrial remodeling during RVH, which might be associated to its suboptimal performance; reversal of this mitochondrial remodeling might be beneficial, improving RV function. We studied mitochondrial membrane potential, a surrogate for overall mitochondrial function and metabolism¹⁵⁻¹⁹ in human and rat hearts. We used confocal microscopy and tetramethyl-rhodamine methyl ester (TMRM), a positively-charged dye that localizes at the most negative organelles in the cell, the mitochondria¹⁷. Mitochondrial hyperpolarization or depolarization is detected and quantified by an increase or decrease in TMRM fluorescence, respectively. We show that human and rat RVH is characterized by a dynamic increase in mitochondrial membrane potential (more hyperpolarized than that observed in the normal RV and LV) and that inhibition of this by the clinically-used metabolic modulator Dichloroacetate (DCA, an inhibitor of the mitochondrial pyruvate dehydrogenase kinase²⁰) increases inotropy in RVH, but not in the normal RV. Our work has significant translational potential since DCA is being used in humans with mitochondrial diseases²¹, and has recently been shown to reverse mitochondrial

hyperpolarization, increase glucose oxidation and reverse disease phenotype in both cancer¹⁶ and PAH¹⁵.

Methods: Complete details are available on-line in the **Methods Supplement** section.

Permission from the University of Alberta committees on human ethics and animal policy and welfare was attained for all experiments on human and rat tissues, respectively.

Human Heart Tissue Samples: Human samples were acquired from patients undergoing surgery for congenital heart disease or transplantation at the University of Alberta Hospital. Excised ventricular tissue samples (free wall) were immediately placed on ice and stained with TMRM and Hoechst (a nuclear stain) for 40 minutes and visualized under confocal microscopy^{15, 16, 19}. The presence of hypertrophy was documented by the use of echocardiography for every patient (Table 1) and confirmed macroscopically by the surgeon.

Animal model of RVH: We studied RVH using a model of experimental PAH by injecting monocrotaline, an alkaloid from *crotalaria spectabilis*, a well-established rat PAH model, as previously described^{15,19} (Supplement Methods).

Isolation of adult rat cardiomyocytes: Adult Sprague-Dawley rats (300-350 grams) were used and cardiomyocytes were isolated from the ventricles as previously described⁴ (Supplement Methods).

Isolation and culture of neonatal rat cardiomyocytes: Neonatal Sprague-Dawley rat pups 2-days old were used to isolate RV and LV cardiomyocytes, which were then separated from fibroblasts and placed in culture, as previously described²² (Supplement Methods). Immunocytochemistry for myosin heavy chain confirmed that the studied cultured cells were cardiomyocytes (Supplement Figure 1).

Staining and confocal microscopy of Cells and Tissues : TMRM was made up to a concentration of 20nM in plating media along with 0.5 μ M of Hoechst nuclear stain. Each 35mm X 10mm plate of cells received 2mL of the staining solution for a period of 30 minutes at 37°C. For ventricular rat tissue, the exposure was 40 minutes. The staining media was then removed, and each plate was rinsed and left at 37°C in another 2mL of plating media. Staining of plates was staggered in order to give each plate from each ventricle the same amount of exposure to TMRM, and same amount of time before imaging.

Immunohistochemistry and confocal microscopy were performed on a Zeiss LSM 510 multiphoton confocal microscope using antigen retrieval and Image enhancer IT (Invitrogen) for NFATc3 and DAPI (a nuclear stain) as previously described^{4, 15, 16, 19, 23} (also see Supplement Methods).

Isolated rat RV Langendorff perfusion: Adult rats with normal and hypertrophied RVs (due to monocrotaline-induced PAH) were used. The right ventricles were removed and perfused in a modified Langendorff preparation, designed to study RV contractility as we recently described⁴ (also see Supplement Methods).

Statistics: Comparison between LV and RV cardiomyocytes (from either neonatal or adult models) was done using a t-test. Analysis of ventricular tissue (from either adult rat or human) and neonatal cultured neonatal cardiomyocytes were completed via one-way ANOVA with post-hoc Bonferroni correction. Significance was defined at a p-value of less than 0.05.

Results:

Dynamic and chamber-specific increase in mitochondrial membrane potential in human and rat RVH.

We first examined fresh human myocardial samples that were excised during surgical procedures within 30 minutes from excision. We attained tissues from 11 patients with normal or hypertrophied RVs based on pre-operative echocardiography (RV free wall thickness, Table 1). We were able to secure tissues from only two normal RVs and LVs. All specimens were loaded with TMRM and handled and imaged under identical conditions. There was increased TMRM fluorescence in the normal LV samples

compared to the RV from the same patient (Figure 1A). There was also increased TMRM fluorescence in RVH samples compared to the normal RV (Figure 1B-C). Because we were only able to secure 2 normal hearts, direct comparisons among groups cannot be performed. However, results observed in the rat ventricular tissues were similar to the human RV and LV samples, where the normal adult rat LV had a higher mitochondrial membrane potential compared to the RV (Figure 2A, $p < 0.01$). To determine if this was due to differences in cardiomyocytes, rather than other cells (i.e. fibroblasts), we isolated rat adult RV and LV cardiomyocytes. Indeed, the differences in mitochondrial membrane potential from whole myocardial tissue persisted at the level of individual cardiomyocytes (Figure 2B). The mean TMRM fluorescence data showed a similar increase in myocardial and cardiomyocyte mitochondrial membrane potential in the LV versus the RV, respectively (Figure 2C). Though these results are interesting descriptive findings between the two ventricles, the possibility to exploit these differences in targeted therapeutic strategies required further assessment of the changes that occur in disease states.

To examine the effects of hypertrophy on mitochondrial membrane potential, we used the model of monocrotaline-induced PAH and subsequent RV hypertrophy in the rat. After injection with monocrotaline, the rat hearts were explanted day 14 (moderate PAH and RVH) and day 28 (severe PAH and RVH). RV myocardium was loaded with TMRM and compared with vehicle-injected control animals (Figure 3). The worsening RVH was measured by ECHO (free wall thickness) and later confirmed macroscopically at autopsy (RV/LV+Septum, data not shown). The increased PA pressure was shown by measurement of the pulmonary artery acceleration time (PAAT), which we have

previously shown to correlate negatively with mean PA pressure in simultaneous right heart catheterization in rats^{15, 19}. As hypertrophy progressed, there was a progressive increase in mitochondrial membrane potential in a “dose-dependent” manner (Figure 3).

Once again, in order to determine whether the cardiomyocytes develop mitochondrial hyperpolarization in hypertrophy and exclude possible effects of circulating factors in vivo, we used in vitro models. *Neonatal* cardiomyocytes (isolated from the neonatal RV which is physiologically hypertrophied) can be cultured for 48-72 hours without significant change in phenotype, whereas isolated *adult* cardiomyocytes cannot be reliably sustained in culture²². We looked to mimic pressure overload hypertrophy by exposing cultured neonatal cardiomyocytes to phenylephrine. In this classic model of hypertrophy in vitro cardiomyocytes have increased levels of intracellular calcium and develop hypertrophy within 48 hours²². Phenylephrine caused the predicted increase in cell size and a significant increase in mitochondrial membrane potential, compared to vehicle-treated cardiomyocytes (Figure 4A). The response to phenylephrine resulted in hyperpolarization of the mitochondria similar to that seen in physiological RVH (723±41 versus 587±10 FU/mm², respectively, p<0.01). Although it cannot definitely be excluded, it is unlikely that phenylephrine led to mitochondria biogenesis and an increased absolute number of mitochondria (which by itself would contribute to the increased TMRM signal), as the cells were only treated for 48 hours.

We then sought to determine a potential molecular mechanism for this mitochondrial remodeling and whether its normalization would lead to improved RV function.

Molecular and metabolic targeting of the remodeled mitochondria in hypertrophy: the role of NFAT.

The increase in mitochondrial membrane potential in hypertrophy is likely multifactorial in etiology. First, there is an increase in intracellular and intra-mitochondrial calcium. Increased calcium leads to activation of mitochondrial enzymes that in turn cause an increase in Krebs cycle production of reducing equivalents, reactive oxygen species, and ATP. All of which alter mitochondrial function and mitochondrial membrane potential. Second, the increase in cytoplasmic calcium results in activation of the critical transcription factor Nuclear-Factor-of-Activated-T-lymphocytes (NFAT)²⁴, which is activated and regulates anatomic and metabolic remodeling during heart development²⁵ and LV hypertrophy²⁶. NFAT regulates the expression of many mitochondrial and metabolic genes (including adenylosuccinate synthetase 1²⁷, pyruvate decarboxylase, heart-fatty acid binding protein, and the electron transport chain enzymes succinate dehydrogenase and cytochrome c oxidase²⁵). NFAT is critical for heart development, as knockout of NFAT is fatal by embryonic day 10.5²⁵. This transcription factor is highly conserved amongst species with the same isoforms found in humans and mice²⁴. Thus, we studied whether the increase in mitochondrial membrane potential was NFAT dependent by culturing neonatal cardiomyocytes with phenylephrine and VIVIT (a selective NFAT inhibitor²⁸). VIVIT abolished the increase in mitochondrial membrane potential caused by phenylephrine to a level similar to untreated control neonatal cardiomyocytes (Figure 4A). To confirm that VIVIT inhibited NFAT, we performed immunohistochemistry on fixed neonatal cardiomyocytes for NFATc3 (the isoform that

has been studied the most in the heart) and DAPI (nuclear stain). NFAT activation is associated with a translocation of NFAT into the nucleus, whereas inhibition of NFAT with VIVIT restricts NFAT to the cytoplasm^{23, 24}. As expected, phenylephrine caused translocation of NFAT into the nucleus, while treatment with VIVIT inhibited this translocation and kept NFAT in the cytoplasm (Figure 4B).

Dichloroacetate (DCA) inhibits the mitochondrial enzyme pyruvate dehydrogenase kinase, which in turn causes increased activity of pyruvate dehydrogenase, and thus DCA promotes the influx of pyruvate into the mitochondria, increasing glucose oxidation. Recently, DCA has been shown to reverse NFAT activation, mimicking the effects of VIVIT in cancer, increasing glucose oxidation, decreasing mitochondrial membrane potential in human cancer cell lines and regressing tumor growth in-vitro and in-vivo¹⁶. DCA mimicked VIVIT and caused a decrease in mitochondrial membrane potential and inhibited the nuclear translocation of NFAT in the cultured neonatal cardiomyocytes, despite continued exposure to phenylephrine (Figure 4A-B). Although we did not measure metabolism directly, DCA is known to increase the coupling of glycolysis to glucose oxidation in the post-ischemic heart, and although it does not have significant effects in the normal LV, it improves ischemia-reperfusion recovery in mild LV hypertrophy²⁹.

To determine whether DCA and VIVIT will depolarize mitochondria from physiologically hypertrophied hearts (as in the phenylephrine-induced hypertrophy) and whether this is ventricle-specific, we harvested neonatal rat hearts and isolated cardiomyocytes from separated RV (which is hypertrophied) versus LV (which is not hypertrophied) free walls. Similar to the adult RVH myocardium from monocrotaline

induced PAH, the isolated neonatal hypertrophied cardiomyocytes from the RV free wall had more hyperpolarized mitochondria compared to those isolated from the LV free wall (Figure 4C). Both DCA and VIVIT reversed this mitochondrial hyperpolarization and brought the mitochondrial membrane potential to the levels of the non-hypertrophied LV cardiomyocyte. Interestingly, DCA and VIVIT had no effect on the LV cardiomyocyte mitochondria (Figure 4C).

These data show that in both physiologic and pathologic RVH, cardiomyocyte mitochondria are hyperpolarized, that this is, at least in part, due to NFAT activation, and can be reversed by DCA. Does this translate into improved RV function?

Dichloroacetate improves RV inotropy in RVH

Since several patients with PAH or RVH secondary to congenital heart disease only have affected RVs (their LVs are normal), the mitochondria-targeting DCA may selectively augment RV function in the setting of RVH. We used the ex-vivo modified Langendorff perfused heart⁴ to measure RV contractility (Figure 5A). This modified model allows for real time measurement of ex-vivo developed pressures in the perfused RV, while its preload is constant (the balloon in the RV has a fixed volume) and is beating against no afterload (pulmonary artery transected). Interestingly, when perfusing hearts 28 days after monocrotaline injection (severe RVH) compared to control animals, there was a significant and dose-dependent increase in developed pressure in the hypertrophied but not the normal RVs, while both had a similar increase in contractility by isoproterenol (Figure 5B,C). Compatible with the expected DCA-induced increased

glycolysis to glucose oxidation coupling, there was also an accompanied decrease in coronary effluent lactate only in the hearts with RVH (Figure 5D).

Discussion

We describe dynamic and chamber-specific changes in mitochondrial function during the development of human and rat RVH, both at the level of the myocardium and the isolated cardiomyocyte (Figures 1 and 2). RVH is characterized in human and rat hearts by increased mitochondrial membrane potential compared to the normal RV, and this hyperpolarization appears to progress in parallel with the development of hypertrophy (Figure 3). We used monocrotaline induced RV hypertrophy over PA-banding to better mimic acquired pulmonary hypertension in humans, where the RV is exposed to a gradual (not acute) rise in afterload. Even in the setting of physiologic RVH that occurs in the neonatal heart, RV cardiomyocytes have more hyperpolarized mitochondria compared to LV myocytes (Figure 4C). Cardiomyocyte hypertrophy can be induced *in vitro* by phenylephrine, which also leads to significant increases in mitochondrial membrane potential within 48 hours (Figure 4A). Interestingly, this hyperpolarization is reversed by inhibition of a crucial transcription factor, NFAT, which has been shown to play a significant role in heart development¹⁸ and LV hypertrophy²⁶ but has not been previously studied in the RV (Figure 4A-B). Furthermore, directly targeting mitochondria with DCA, reversed the mitochondrial hyperpolarization in hypertrophy (Figure 4) and led to improved RV function (Figure 5). DCA did not affect the mitochondria and did not increase the contractile pressure of the normal RV. It is

possible that the mitochondrial effects that we describe in RVH both in-vivo and in-vitro reflect a suboptimal mitochondrial remodeling, which may be responsible for suboptimal RV energy production and the relatively weak response of the RV to increased afterload. To the best of our knowledge, this is the first time in which the degree of hypertrophy is correlated to mitochondrial membrane potential and that inotropic effects of a drug are related to the level of mitochondrial membrane potential, at least in the RV.

Although the RV and LV are currently approached and treated the same from a clinical perspective, the diversity of mitochondria between the RV and LV is not surprising given their different embryologic origin⁸ and the increasing evidence for significant diversity of mitochondria among different organs, such as the liver and kidney^{30, 31}. The diversity of mitochondria extend beyond that of different organs to find diversity even within individual myocytes^{32, 33}. We have previously shown that differences in mitochondrial function between the pulmonary and systemic arterial smooth muscle cells (SMC), where systemic SMC mitochondria are more hyperpolarized than pulmonary artery SMC mitochondria and account, at least in part, for the different response of the 2 vasculatures to hypoxia (the pulmonary arteries constrict while the renal arteries dilate)³⁴. We subsequently demonstrated that in PAH, the mitochondrial membrane potential in the pulmonary artery SMC is hyperpolarized compared to the SMC mitochondria from normal pulmonary artery SMC, and that treatment with DCA both normalized mitochondrial membrane potential and reversed PAH^{15, 35}. It is also intriguing that the proliferative pulmonary artery SMC from PAH patients also have activated (i.e. nuclear) NFAT (like the RVH cardiomyocytes), while the normal pulmonary artery smooth muscle cells do not (like the normal RV cardiomyocytes)²³.

The molecular basis for mitochondrial remodeling in hypertrophy is unknown, although mitochondrial diversity among other organs is associated with varying degrees of electron transport chain complexes expression, which needs to be explored between the RV and LV, as well as possible changes during hypertrophy from the normal ventricles. We provide preliminary evidence that NFAT might play an important role in this mitochondrial remodeling in RVH, similar to its recently described role in PAH²³ and cancer¹⁶. Our work cannot exclude the possibility that the increase in mitochondrial membrane potential is not secondary to an increase in mitochondrial number. However, the fact that a short-term exposure to DCA and VIVIT normalize the mitochondrial membrane potential and the fact that DCA acutely improves RVH function suggests that the increased mitochondrial membrane potential has a functional basis.

The profile of DCA's effects in cancer and PAH (where it selectively increases apoptosis by depolarizing mitochondria) might raise concerns, since it might increase RV apoptosis after chronic use. However, it is remarkable that chronic use of DCA has been shown to reverse PAH and RVH, and improve functional capacity and mortality in several animal PAH models^{15, 16, 36}. It is possible that the DCA-induced mitochondrial depolarization in RVH cardiomyocytes is enough to lead to improved contractile function but not enough to induce apoptosis by itself.

Furthermore, another medication that causes regression of PAH by inducing apoptosis in pulmonary artery SMC is sildenafil, which we recently showed it also increases contractility in RVH, much like DCA⁴. However, long-term use of sildenafil (>2 years) in patients with PAH has not resulted in any cardiovascular related deaths and

has led to improvement of RV function³⁷. Nonetheless, this theoretical concern would need to be studied properly in the setting of a clinical trial.

The improved contractility of the hypertrophied RV with DCA is a novel finding. Based on the differences of the mitochondrial function between the 2 ventricles we predicted that the effects of DCA would be restricted to the hypertrophied RV (and spare the normal RV and the LV). Indeed, DCA has failed to improve contractility from baseline in the LV, though there was a better recovery after ischemia²⁹. The lack of improvement in LV contractility with DCA has also been shown in human studies where patients with coronary artery disease or congestive heart failure did not show improved LV contractility or cardiac output with acute administration of intravenous DCA^{38,39}.

Our findings that DCA improved RV contractility acutely might also be relevant to the many clinical conditions where RV-specific inotropy is needed including patients with post-cardiotomy shock that have pre-operative RV dysfunction, or in the surgery of pediatric patients with congenital heart disease and RVH.

Limiations:

The study of mitochondrial membrane potential as a surrogate for mitochondrial metabolism is a validated and accepted in the literature³⁵; however, there are assumptions made using an in-vitro model to represent in-vivo findings. Most importantly, the in-vitro environment of isolated cardiomyocytes does not mimic in-vivo conditions, and though this is a confounding factor, it is common to all isolated cells and we base our deductions from the delta membrane potential between the RV, LV, and treatment arms. Another

limitation of the study is the small number of human samples attained. However, we feel that these unselected human data are worthy of presentation because they are in agreement with our data from several *in vivo* and *in vitro* animal models, generally supporting the relevance of our hypothesis.

Conclusions:

Selective agents targeting the diseased RV are highly desirable, given the poor performance of the RV in states of pressure overload (congenital heart disease, PAH, and post transplant surgery). We provide evidence that therapeutically targeting mitochondria may allow for potential ventricular-specific treatments. This concept may help build the framework for a new class of drugs designed to only affect the diseased ventricle (i.e. hyperpolarized mitochondria in RVH), while having little or no impact on the other more normal ventricle in the same patient. DCA is one such candidate therapy which has minimal effects on normal cells throughout the body and does not significantly change the hemodynamics of normal animals¹⁵; this was also supported by our finding in the *ex-vivo* perfused hearts, where treatment with DCA did not have significant effects on the developed pressures generated by the normal RV (Figure 5). The documented effects of DCA in PAH, and now on RVH, raise the possibility to study this drug in humans with PAH. The ability for a combined, “double-hit” mechanism where pulmonary vascular remodeling and PAH is reversed, and at the same time RV function is directly enhanced, will be very desirable clinically. We recently described a similar mechanism in which sildenafil dilates the pulmonary circulation in PAH and at the same time directly

increases RVH inotropy⁴. The fact that DCA has been used in humans with mitochondrial diseases for more than 30 years²¹ supports the need for such phase-II studies.

Table 1

Patient	Age-Sex	Diagnosis	Tissue	RV thickness (cm)
1	19 y F	Left atrial sarcoma <i>Heart transplant</i>	Normal LV Normal RV	0.3
2	46 y M	RV failure post-heart transplant <i>Re-Heart transplant</i>	Normal LV	-
3	54 y M	Intractable angina no PAH Moderate LVH <i>Heart transplant</i>	Normal RV	0.4
4	4 m F	Tetralogy of Fallot <i>Surgical specimen</i>	RVH	1.0
5	3 y M	RV outflow tract obstruction <i>Surgical specimen</i>	RVH	1.1
6	5 m M	Tetralogy of Fallot <i>Surgical specimen</i>	RVH	0.9
7	58 y F	Rheumatic valve disease <i>Heart transplant</i>	RVH	1.6
8	11 d M	Hypoplastic Left Heart <i>Surgical specimen</i>	RVH	0.7
9	2 y F	Coarctation of Aorta and Ventricular Septal Defect	RVH	1.0

10	6 m M	<i>Surgical specimen</i> Pulmonary Stenosis and Ventricular Septal Defect	RVH	0.8
11	4 m M	<i>Surgical specimen</i> Tetralogy of Fallot <i>Surgical specimen</i>	RVH	0.9

Figure 1:

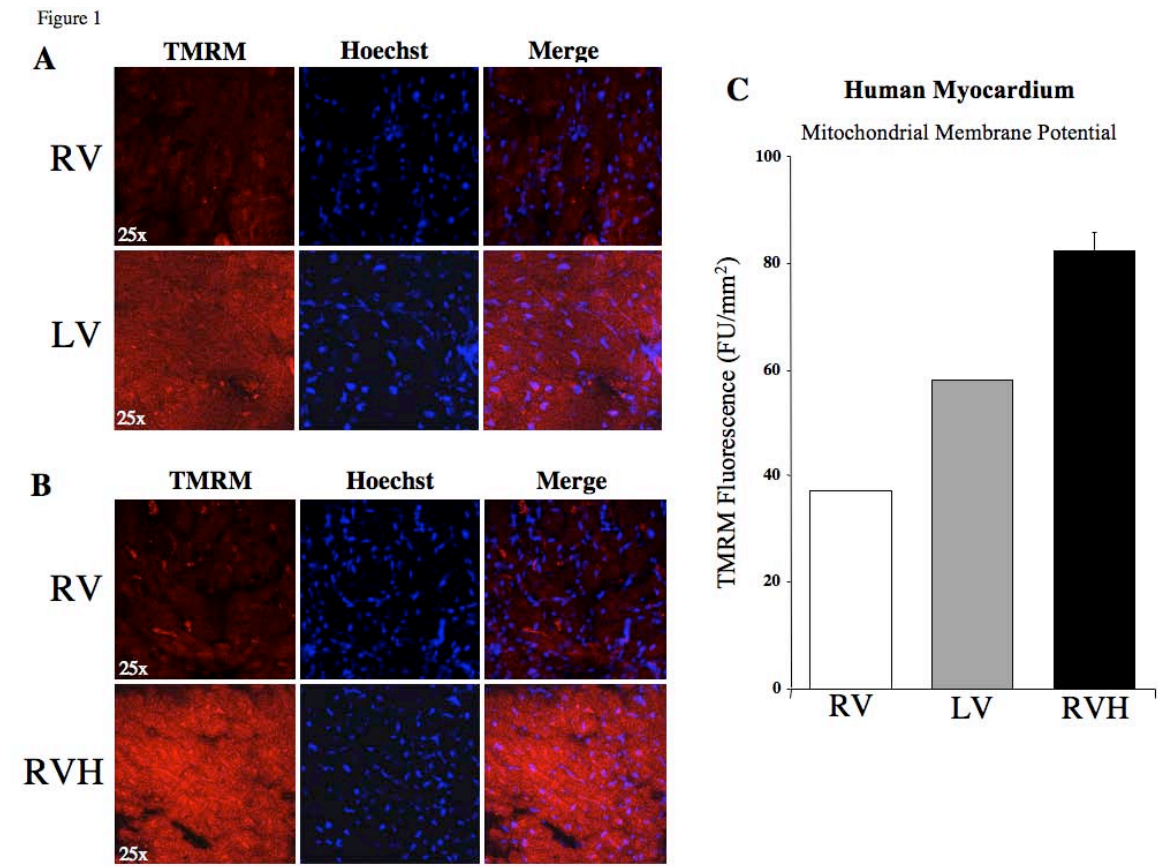


Figure 1: Differences in mitochondrial membrane potential between human RV and LV myocardium.

A-B: Confocal microscopy images of acutely TMRM and Hoechst loaded normal RV and LV myocardium from Patient#1 (A) and normal RV and RVH from Patient#3 and #6, respectively (B).

C: Mean TMRM fluorescence from all patients expressed in fluorescence units per area (n=2 RV, n=2 LV, n=8 RVH).

Figure 2:

Figure 2

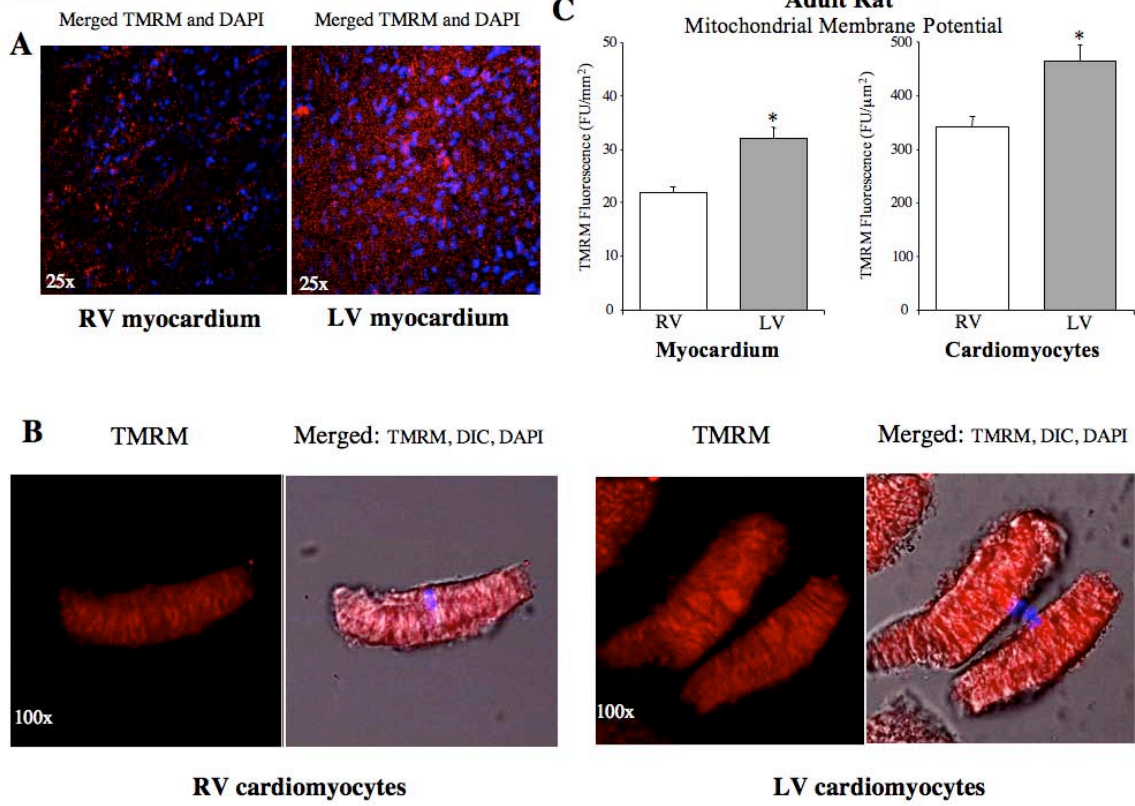


Figure 2: Similar Mitochondrial membrane potential differences in adult rat RV and LV myocardium, which also exist in isolated adult rat RV and LV cardiomyocytes.

A: Confocal microscopy images of adult rat RV and LV myocardium loaded with TMRM and Hoechst.

B: Isolated adult rat RV and LV cardiomyocytes loaded with TMRM and Hoechst. Merge panels also show Differential Interference Contrast (DIC) channel for cell surface details.

C: Mean TMRM fluorescence from all rat myocardial samples (n=17 RV, n=17 LV, *p<0.01 versus RV myocardium). Mean TMRM fluorescence for individual cardiomyocytes (n=58 RV, n=83 LV, *p<0.01 versus RV cardiomyocytes).

Figure 3:

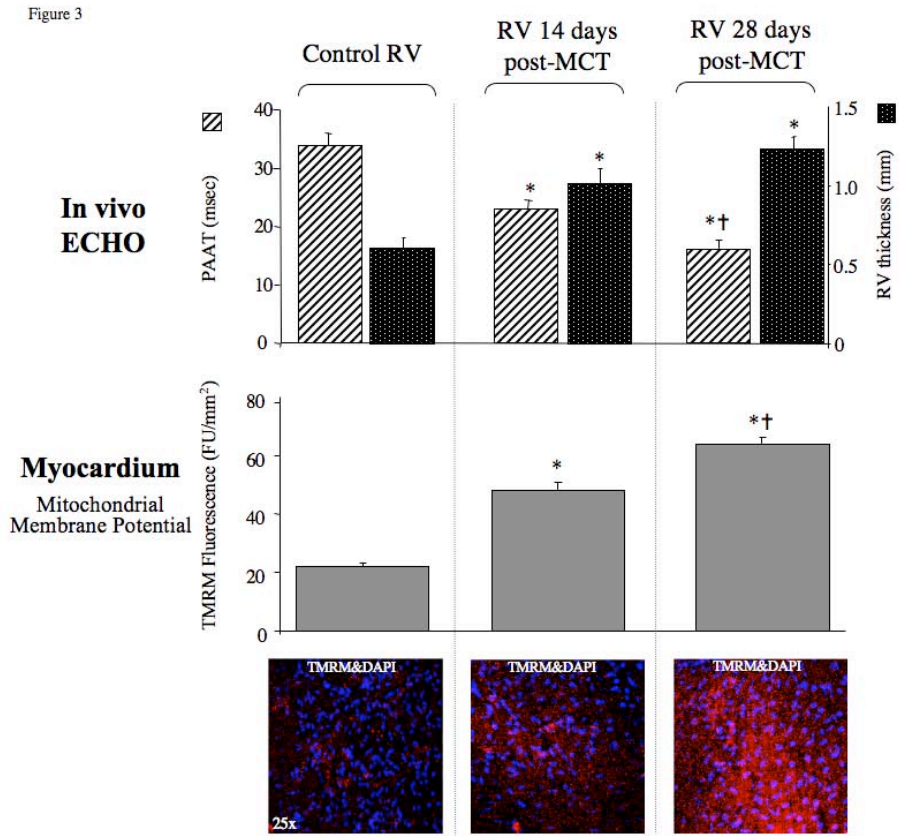


Figure 3: Mitochondrial membrane potential progressively increases with the development of pathologic RVH.

Upper third: Pulmonary artery acceleration time (hatched bars) progressively decreased from control to 14 days to 28 days post-MCT injection, while this was mirrored by a subsequent increase in RV free wall thickness (solid bars); * $p < 0.01$ versus control, † $p < 0.01$ versus RV 14 days post-MCT.

Middle third: Mean TMRM fluorescence from all rat RV myocardial samples with progression of RVH after monocrotaline (MCT) injection (n=17 control RV, n=5 RV 14 days post-MCT, n=11 RV 28 days post-MCT; * $p < 0.01$ versus control, † $p < 0.01$ versus RV 14 days post-MCT).

Bottom third: Representative confocal images of RV myocardium loaded with TMRM and Hoechst.

Figure 4:

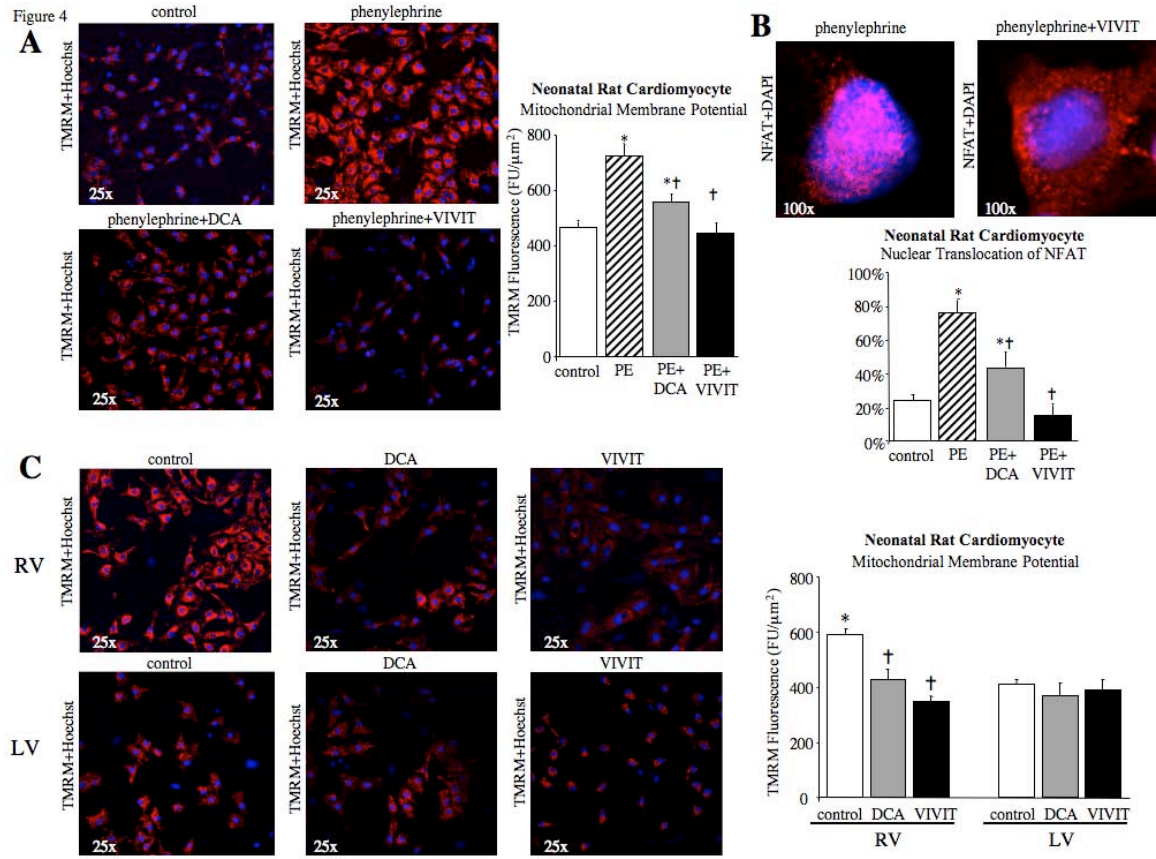


Figure 4: DCA and NFAT inhibition reverse the mitochondrial hyperpolarization seen in RV cardiomyocytes from physiologic (neonatal RV) and pathologic (phenylephrine-induced) hypertrophy in vitro.

A: Representative confocal images of neonatal rat cardiomyocytes treated with vehicle, phenylephrine (PE), PE+DCA, or PE+VIVIT and cultured for 48 hours prior to loading with TMRM and Hoechst. Mean TMRM fluorescence for individual cardiomyocytes (n>140 cardiomyocytes per treatment, *p<0.01 versus control, †p<0.01 versus phenylephrine).

B: Immunocytochemistry performed in fixed neonatal cardiomyocytes after phenylephrine or phenylephrine+VIVIT treatment show the prevention of NFAT (red) translocation into the nucleus (blue) by VIVIT. (n=6 plates per group [>150 cells/plate], *p<0.01 versus control, †p<0.01 versus phenylephrine).

C: Isolated neonatal rat RV and LV cardiomyocytes treated with vehicle, DCA, or VIVIT and cultured for 48 hours prior to loading with TMRM and Hoechst. Mean TMRM fluorescence for individual cardiomyocytes (n=473 LV, n=449 RVH, *p<0.01 versus LV cardiomyocytes, †p<0.01 versus control).

Figure 5:

Figure 5

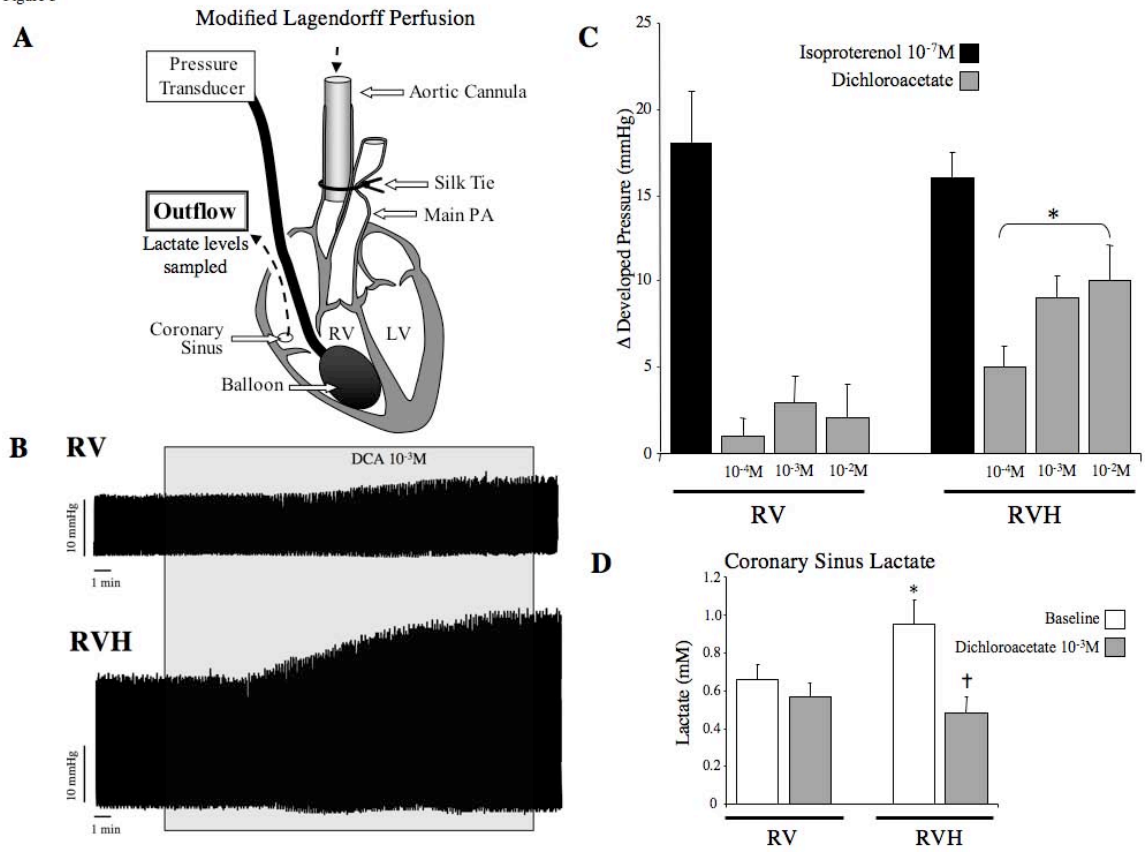


Figure 5: Targeted metabolic modulation by DCA acutely improves RV inotropy in the ex-vivo modified Langendorff perfused heart.

A: Schematic of the isolated perfused RV (Langendorff preparation) to measure developed pressure.

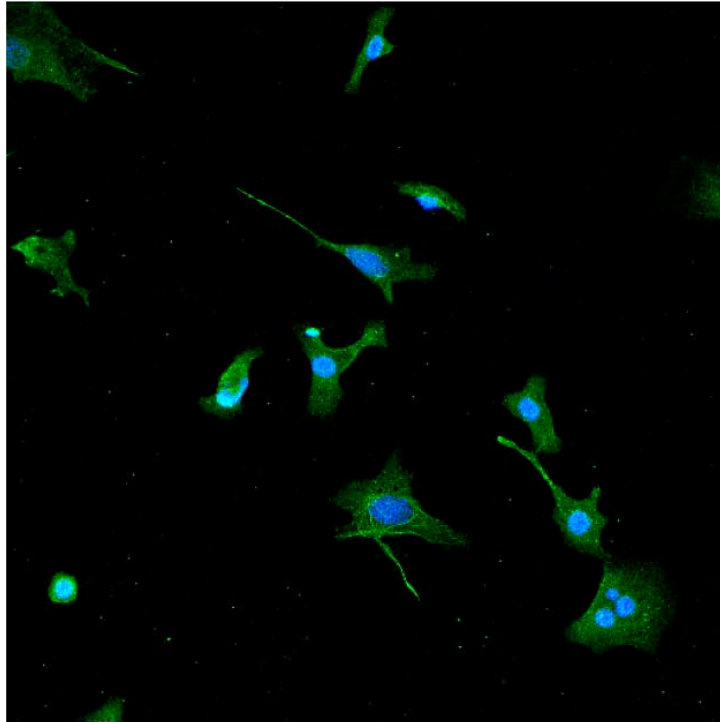
B: Representative real-time traces of the developed pressures from the normal RV (upper) and 28 days post-MCT injection RVH (lower), before and after the addition of DCA into the perfusate (shaded area). Note the significant increase in developed pressure only in the RVH hearts with acute DCA treatment.

C: Mean data showing that DCA increased developed pressure (delta pressure from baseline developed pressure) in a dose-dependent manner in the RVH (n=5) but not the normal RV (nRV, n=6), whereas both normal and hypertrophied RV responded similarly to isoproterenol (*p<0.01 versus normal RV).

D: Coronary sinus effluent was collected on ice from the modified Langendorff perfusions 5 minutes after a steady baseline was established and 10 minutes after initiating perfusion with DCA, and analyzed for lactate concentration (n=6 RV, n=5 RVH, *p<0.01 versus normal RV, †p<0.01 versus baseline).

Supplement Figure 1:

Supplement Figure 1



Supplement Figure 1: Verification of Cardiomyocyte cell type

Representative confocal microscopy image of isolated neonatal rat cardiomyocytes stained for myosin heavy chain (green) and Dapi (blue) to confirm the cell isolation methods were specific for attaining cardiomyocytes over fibroblasts and/or vascular cells, with >97% of cells staining positive for myosin heavy chain.

References:

1. Voelkel NF, Quaipe RA, Leinwand LA, Barst RJ, McGoon MD, Meldrum DR, Dupuis J, Long CS, Rubin LJ, Smart FW, Suzuki YJ, Gladwin M, Denholm EM, Gail DB. Right ventricular function and failure: report of a National Heart, Lung, and Blood Institute working group on cellular and molecular mechanisms of right heart failure. *Circulation*. 2006; 114:1883-1891.
2. Chin KM, Kim NH, Rubin LJ. The right ventricle in pulmonary hypertension. *Coron Artery Dis*. 2005; 16:13-18.
3. Archer SL, Michelakis ED. An evidence-based approach to the management of pulmonary arterial hypertension. *Curr Opin Cardiol*. 2006; 21:385-392.
4. Nagendran J, Archer S, Soliman D, Gurtu V, Moudgil R, Haromy A, St Aubin C, Webster L, Rebeyka I, Ross D, Light P, Dyck J, Michelakis ED. Phosphodiesterase type 5 (PDE5) is highly expressed in the hypertrophied human right ventricle and acute inhibition of PDE5 improves contractility. *Circulation*. 2007; 116:238-248.
5. Lopaschuk GD. Optimizing cardiac energy metabolism: how can fatty acid and carbohydrate metabolism be manipulated? *Coron Artery Dis*. 2001; 12 Suppl 1:S8-11.
6. Stanley WC, Recchia FA, Lopaschuk GD. Myocardial substrate metabolism in the normal and failing heart. *Physiol Rev*. 2005; 85:1093-1129.
7. Adroque JV, Sharma S, Ngumbela K, Essop MF, Taegtmeyer H. Acclimatization to chronic hypobaric hypoxia is associated with a differential transcriptional profile between the right and left ventricle. *Mol Cell Biochem*. 2005; 278:71-78.
8. Zaffran S, Kelly RG, Meilhac SM, Buckingham ME, Brown NA. Right ventricular myocardium derives from the anterior heart field. *Circ Res*. 2004; 95:261-268.
9. Baudet S, Kuznetsov A, Merciai N, Gorza L, Ventura-Clapier R. Biochemical, mechanical and energetic characterization of right ventricular hypertrophy in the ferret heart. *J Mol Cell Cardiol*. 1994; 26:1573-1586.
10. Joyce JJ, Dickson PI, Qi N, Noble JE, Raj JU, Baylen BG. Normal right and left ventricular mass development during early infancy. *Am J Cardiol*. 2004; 93:797-801.
11. Colucci WS. Molecular and cellular mechanisms of myocardial failure. *Am J Cardiol*. 1997; 80:15L-25L.
12. Nascimben L, Ingwall JS, Lorell BH, Pinz I, Schultz V, Tornheim K, Tian R. Mechanisms for increased glycolysis in the hypertrophied rat heart. *Hypertension*. 2004; 44:662-667.
13. Bueno OF, De Windt LJ, Tymitz KM, Witt SA, Kimball TR, Klevitsky R, Hewett TE, Jones SP, Lefer DJ, Peng CF, Kitsis RN, Molkentin JD. The MEK1-ERK1/2 signaling pathway promotes compensated cardiac hypertrophy in transgenic mice. *Embo J*. 2000; 19:6341-6350.
14. De Windt LJ, Lim HW, Taigen T, Wencker D, Condorelli G, Dorn GW, 2nd, Kitsis RN, Molkentin JD. Calcineurin-mediated hypertrophy protects cardiomyocytes from apoptosis in vitro and in vivo: An apoptosis-independent model of dilated heart failure. *Circ Res*. 2000; 86:255-263.

15. McMurtry MS, Bonnet S, Wu X, Dyck JR, Haromy A, Hashimoto K, Michelakis ED. Dichloroacetate prevents and reverses pulmonary hypertension by inducing pulmonary artery smooth muscle cell apoptosis. *Circ Res.* 2004; 95:830-840.
16. Bonnet S, Archer SL, Allalunis-Turner J, Haromy A, Beaulieu C, Thompson R, Lee CT, Lopaschuk GD, Puttagunta L, Bonnet S, Harry G, Hashimoto K, Porter CJ, Andrade MA, Thebaud B, Michelakis ED. A mitochondria-K⁺ channel axis is suppressed in cancer and its normalization promotes apoptosis and inhibits cancer growth. *Cancer Cell.* 2007; 11:37-51.
17. Duchen MR. Contributions of mitochondria to animal physiology: from homeostatic sensor to calcium signalling and cell death. *J Physiol.* 1999; 516 (Pt 1):1-17.
18. Akao M, O'Rourke B, Teshima Y, Seharaseyon J, Marban E. Mechanistically distinct steps in the mitochondrial death pathway triggered by oxidative stress in cardiac myocytes. *Circ Res.* 2003; 92:186-194.
19. McMurtry MS, Archer SL, Altieri DC, Bonnet S, Haromy A, Harry G, Bonnet S, Puttagunta L, Michelakis ED. Gene therapy targeting survivin selectively induces pulmonary vascular apoptosis and reverses pulmonary arterial hypertension. *J Clin Invest.* 2005; 115:1479-1491.
20. Stacpoole PW, Henderson GN, Yan Z, James MO. Clinical pharmacology and toxicology of dichloroacetate. *Environ Health Perspect.* 1998; 106 Suppl 4:989-994.
21. Berendzen K, Theriaque DW, Shuster J, Stacpoole PW. Therapeutic potential of dichloroacetate for pyruvate dehydrogenase complex deficiency. *Mitochondrion.* 2006; 6:126-135.
22. Chan AY, Soltys CL, Young ME, Proud CG, Dyck JR. Activation of AMP-activated protein kinase inhibits protein synthesis associated with hypertrophy in the cardiac myocyte. *J Biol Chem.* 2004; 279:32771-32779.
23. Bonnet S, Rochefort G, Sutendra G, Archer SL, Haromy A, Webster L, Hashimoto K, Bonnet S, Michelakis ED. The Nuclear Factor of Activated T cells in Pulmonary Arterial Hypertension can be therapeutically targeted. *PNAS.* 2007; 104:11418-11423.
24. Macian F. NFAT proteins: key regulators of T-cell development and function. *Nat Rev Immunol.* 2005; 5:472-484.
25. Bushdid PB, Osinska H, Waclaw RR, Molkentin JD, Yutzey KE. NFATc3 and NFATc4 are required for cardiac development and mitochondrial function. *Circ Res.* 2003; 92:1305-1313.
26. McKinsey TA, Olson EN. Toward transcriptional therapies for the failing heart: chemical screens to modulate genes. *J Clin Invest.* 2005; 115:538-546.
27. Xia Y, McMillin JB, Lewis A, Moore M, Zhu WG, Williams RS, Kellems RE. Electrical stimulation of neonatal cardiac myocytes activates the NFAT3 and GATA4 pathways and up-regulates the adenylosuccinate synthetase 1 gene. *J Biol Chem.* 2000; 275:1855-1863.
28. Aramburu J, Yaffe MB, Lopez-Rodriguez C, Cantley LC, Hogan PG, Rao A. Affinity-driven peptide selection of an NFAT inhibitor more selective than cyclosporin A. *Science.* 1999; 285:2129-2133.

29. Wambolt RB, Lopaschuk GD, Brownsey RW, Allard MF. Dichloroacetate improves postischemic function of hypertrophied rat hearts. *J Am Coll Cardiol.* 2000; 36:1378-1385.
30. Kovacevic Z, McGivan JD, Chappell JB. Conditions for activity of glutaminase in kidney mitochondria. *Biochem J.* 1970; 118:265-274.
31. Kunz WS. Different metabolic properties of mitochondrial oxidative phosphorylation in different cell types - important implications for mitochondrial cytopathies. *Exp Physiol.* 2003; 88:149-154.
32. Palmer JW, Tandler B, Hoppel CL. Biochemical properties of subsarcolemmal and interfibrillar mitochondria isolated from rat cardiac muscle. *J Biol Chem.* 1977; 252:8731-8739.
33. Weinstein ES, Benson DW, Fry DE. Subpopulations of human heart mitochondria. *J Surg Res.* 1986; 40:495-498.
34. Michelakis ED, Hampl V, Nsair A, Wu X, Harry G, Haromy A, Gurtu R, Archer SL. Diversity in mitochondrial function explains differences in vascular oxygen sensing. *Circ Res.* 2002; 90:1307-1315.
35. Bonnet S, Michelakis ED, Porter CJ, Andrade-Navarro MA, Thebaud B, Bonnet S, Haromy A, Harry G, Moudgil R, McMurtry MS, Weir EK, Archer SL. An abnormal mitochondrial-hypoxia inducible factor-1alpha-Kv channel pathway disrupts oxygen sensing and triggers pulmonary arterial hypertension in fawn hooded rats: similarities to human pulmonary arterial hypertension. *Circulation.* 2006; 113:2630-2641.
36. Michelakis ED, McMurtry MS, Wu XC, Dyck JR, Moudgil R, Hopkins TA, Lopaschuk GD, Puttagunta L, Waite R, Archer SL. Dichloroacetate, a metabolic modulator, prevents and reverses chronic hypoxic pulmonary hypertension in rats: role of increased expression and activity of voltage-gated potassium channels. *Circulation.* 2002; 105:244-250.
37. Galie N, Ghofrani HA, Torbicki A, Barst RJ, Rubin LJ, Badesch D, Fleming T, Parpia T, Burgess G, Branzi A, Grimminger F, Kurzyna M, Simonneau G. Sildenafil citrate therapy for pulmonary arterial hypertension. *N Engl J Med.* 2005; 353:2148-2157.
38. Lewis JF, DaCosta M, Wargowich T, Stacpoole P. Effects of dichloroacetate in patients with congestive heart failure. *Clin Cardiol.* 1998; 21:888-892.
39. Wargovich TJ, MacDonald RG, Hill JA, Feldman RL, Stacpoole PW, Pepine CJ. Myocardial metabolic and hemodynamic effects of dichloroacetate in coronary artery disease. *Am J Cardiol.* 1988; 61:65-70.

Chapter 5:

Endothelin receptor antagonists decrease contractility in the hypertrophied right ventricle: Direct clinical implications for patients with PAH.

Abstract:

Background: Patients with pulmonary arterial hypertension (PAH) often have significant right ventricular hypertrophy (RVH). PAH therapies include Endothelin-1 (ET-1) receptor inhibitors (ETRIs), which modestly improve functional capacity. The effects of ETRIs on the RV are unknown despite the fact that ETRIs were associated with increased mortality in early left ventricular failure trials. We hypothesized that the modest effects of ETRIs in PAH might be in part due to a negative inotropic effect in the RV, antagonizing their beneficial vasodilating and anti-proliferative effects in pulmonary vessels.

Methods and Results: We examined 28 surgical biopsies of patients with RVH (confirmed macroscopically at surgery and by pre-op ECHO) compared to 13 normal RV samples; and 23 rats with PAH (monocrotaline) and RVH (RV/LV+septum increase by $56.2\pm 7.4\%$) vs 28 normal controls. In humans, confocal immunohistochemistry showed that in RVH, expression increased ($p<0.01$) for ET-Receptor-A (ETR-A) by 2.14X (in rats by 3.61X) and for ET-1 by 3.58X (in rats by 4.66X) over normal myocardium while ET Receptor-B levels were not different. This was confirmed with immunoblots. qRT-PCR in laser-capture microdissected RV myocardium showed increased ETR-A mRNA in RVH versus normal RVs in patients ($164.1\pm 23.6\%$) and rats ($202.4\pm 16.5\%$), $p<0.01$ for both. In modified Langendorff perfusions ETRIs (BQ-123 and Bosentan 10^{-7} - 10^{-5} M) decreased contractility in RVH (but not normal RV) by $32.2\pm 8.3\%$ ($p<0.01$) in a dose-dependent manner ($p<0.01$).

Conclusions: Patients and rats with PAH have an increase in ETA receptors in RVH myocardium. This might be a compensatory mechanism to preserve RV contractility

when the afterload increases and ETRIs might be inhibiting it, limiting their efficacy. Further studies are needed in patients with RVH (ex. congenital heart disease) and caution is needed interpreting data from clinical trials using ETRIs. Our results might not be applicable to patients with non-hypertrophied, dilated RVs.

The number one predictor of mortality in patients with pulmonary arterial hypertension (PAH) is right ventricular (RV) failure. Though there have been advances in the treatment of PAH, there has been a paucity in the effect of PAH therapies on the RV. The specific focus on the right ventricle is gaining recognition as an area of interest and opportunity as mandated by both North American¹ and European (Haworth EurHJ 2007) granting bodies. The awareness that the right ventricle may be directly affected by therapies targeting PAH has been recently described with the expression of phosphodiesterase-5 (PDE5) in the hypertrophied RV and the increase in inotropy caused by PDE5 inhibitors².

Another such approved class of drugs for the treatment of PAH is endothelin receptor antagonists (ETRA). Endothelin-1 (ET-1) is a 21 amino acid peptide discovered in 1988³. Endothelin-1 is predominantly secreted by vascular endothelium, which leads to paracrine potent vasoconstrictive effects in the surrounding vascular bed⁴. In the processing of Endothelin-1, it is translated from mRNA to a large 205 amino acid peptide prepro-endothelin, which is then modified to become big-endothelin (a 38 amino acid peptide), which in turn is cleaved by Endothelin converting enzyme-1 to ET-1. Though the pulmonary vascular endothelium produces the majority of circulating endothelin-1, the G-protein Endothelin Receptor A and B is found on pulmonary smooth muscle cells⁵, while mainly ET_A-R is found in the heart myocardium⁶. This family of drugs is currently approved for the treatment of PAH in North America and Europe and vary in affinity for

Endothelin Receptor A and B. Where Bosentan (Tracleer; Actelion Pharmaceuticals) is a mixed ET_A-R and ET_B-R antagonist which was the first ETRA approved in 2001 for the treatment of PAH with ET_A-R: ET_B-R affinity ratio of 40:1⁴. A more recently developed pharmaceutical agent that was approved in Europe in 2006 was Sitaxsentan (Thelin; Encysive Pharmaceuticals) with an ET_A-R: ET_B-R affinity ratio of 6000:1. The varying affinity of ETRA to ET_A-R versus ET_B-R will likely have significance on clinical efficacy as both receptors are expressed in the pulmonary and coronary vasculature, though this has yet to be elucidated, and likely to be examined in ongoing and future clinical trials.

The ET_A-R binding of ET-1 leads to a significant vasoconstriction by G-protein coupled activation of phospholipase C, which leads to potentiating of vasoconstriction by 3 pathways. Firstly, there is a hydrolysis of phosphatidylinositol-4,5 biphosphate into inositol triphosphate and diacylglycerol, where inositol triphosphate leads to increased calcium release from the sarcoplasmic reticulum. Secondly, the metabolite of inositol triphosphate (inositol tetraphosphate) combined with increased intracellular calcium released by calcium stores causes voltage-gated L-type Ca⁺⁺ channels to activate and opening further influx of calcium into the cell. Thirdly, diacylglycerol activates protein kinase C, which also has downstream effects of increased contraction⁷.

The genesis of ETRAs was originally targeted for the treatment of congestive heart failure (CHF). Pre-clinical studies demonstrated that patients with CHF had increased serum levels of endothelin and it was hypothesized that blocking this vasoconstrictive peptide may lead to coronary, systemic, and pulmonary vasodilation causing

improvement in symptoms⁴. The theoretical benefits of ETRAs in CHF did not correlate with the results of clinical trials in both the management of acute and chronic CHF⁸. In spite of the lack of efficacy observed in CHF trials, the predominance of endothelin production and ET_A-R in the pulmonary vasculature in both control and PAH provided optimism for investigators who considered the use of this orphan family of therapeutics for the treatment of PAH⁹. In the landmark randomized controlled clinical trial in 2001 there was a mild, yet significant improvement in six-minute walk test in patients with PAH treated with Bosentan at a dose of 125mg¹⁰. This clinical trial led to the FDA approval of bosentan for the treatment of PAH.

The widespread use of ETRAs in the treatment of PAH has been very successful, yet the specific effects of ETRAs on the RV remain unknown. It is well described that PAH leads to the compensatory pressure overload hypertrophy of the RV resulting in RVH and eventual RV failure. Interestingly, endothelin is a known cardiac inotrope, leading to increased contractility¹¹, though the ET_A-R is only expressed in low concentrations in the RV compared to the normal LV, and thus ETRAs are unlikely to have significant decreases in normal RV contractility. However, in PAH and subsequent RVH, there is a significant increase in both endothelin-1 and ET_A-R expression¹². This at least suggests that ETRAs may have a negative affect on RVH contractility in patients with PAH and RVH utilizing these agents. Indeed, the clinical efficacy of ETRAs is less than expected by the significant decrease in pulmonary vascular resistance without improvement in cardiac output¹³. This would imply that a decrease in pulmonary vascular resistance that is not accompanied by an increase in cardiac output is secondary to a decrease in cardiac inotropy. It is based on this clinical outcome of only minor improvements in patient

functionality on treatment with ETRAs that we hypothesize that ETRAs decrease contractility in patients with RVH.

In part, lessons learned from CHF trials may lead to the better understanding of the effects of ETRAs on the hypertrophied RV. This is very clinical relevant in the design and interpretation of clinical trials evaluating ETRAs as therapies for PAH. We hypothesized that the modest benefit of ETRAs compared to the expected improved outcomes may be caused by a negative inotropic effect on the RV in patients with PAH and RVH.

Methods:

The authors had full access to and take full responsibility for the integrity of the data. All authors have read and agree to the manuscript as written. All experiments on human tissues and rats were obtained with permission from the University of Alberta committees on human ethics and animal policy and welfare respectively.

Human tissue biopsies: Intra-operative excised ventricular tissue were placed immediately on ice on the back operative table and then snap frozen in liquid nitrogen in the operating theater. Samples were stored in an -80°C freezer. Samples were transferred into OCT (water soluble compound containing glycol's and resins that does not leave a residue during staining).

Immunohistochemistry and confocal microscopy: Were performed on paraffin sections after heat mediated antigen retrieval with citrate/citric acid buffer pH 6. Image enhancer IT (Invitrogen Canada Inc., Burlington, ON, Canada) was used for blocking, followed by Super Block Buffer #37535 + 0.05% Tween20 (Pierce, Rockford Il. U.S.A). Primary antibodies used included: goat anti-human Myosin Heavy Chain (Y-20) #sc-12117 (dilution 1:50), Santa Cruz Biotechnology Inc., Santa Cruz, CA); goat anti-human Endothelin-1 #sc-21625 (dilution 1:100), Santa Cruz Biotechnology Inc., Santa Cruz, CA); rabbit anti-rat Endothelin Receptor-A #AB3260-50uL (dilution 1:50);(Chemicon International). Secondary antibodies included: donkey anti goat tritc 1:100 for MHC (Molecular Probes, Invitrogen); goat anti-rabbit fitc 1:100 for ERA (Molecular Probes, Invitrogen); donkey anti goat fitc 1:100 for ET1 (Molecular Probes, Invitrogen); goat anti rabbit tritc 1:100 for ERA (Molecular Probes, Invitrogen). Antibodies were applied for 1

hr at 37 C. Lack of nonspecific staining for the antibodies used was confirmed by application of secondary antibody only. All slides were also stained with a nuclear stain, DAPI #D21490 (Invitrogen) 1 μ M for 10 minutes at room temperature. Slides were imaged on a Zeiss LSM 510 confocal microscope (FITC: 488nm excitation, 505-530 nm emission; TRITC: 543nm excitation, 565-615nm emission; DAPI: 740 nm two photon excitation, 390-465nm emission).

Imaging and Analysis of Data: All imaging was performed using a Zeiss LSM 510 confocal microscope. Densitometry analysis was done by the use of Zeiss Image Browser software. Fluorescence intensity of Endothelin-1 or Endothelin Receptor A was performed by measuring circular regions of interest (0.126mm² in area). A region of interest was drawn into each field of view where the circle encompassed myocardial tissue only and not coronary vessels.

Laser captured microdissection: Was performed on human and rat RV tissues for ET_R-A and ET as described in Chapter 2.

Animal model of RVH: We studied RVH using a model of experimental PAH by injecting monocrotaline, an alkaloid from *crotalaria spectabilis*, a well rat PAH established model. Monocrotaline is selectively toxic to the pulmonary arterial endothelium and causes significant RV hypertrophy in 3-4 weeks post-intraperitoneal injection. We further quantified RVH macroscopically at autopsy, using the dry weight ratio of the RV/LV+Septum, as described in Chapter 2.

Isolated RV Langendorff perfusion: Rats were anesthetized with intra-peritoneal injection of 60 mg/kg pentobarbital. A midline sternotomy was performed and within 1 minute the heart was isolated and the aorta was cannulated and perfused with Krebs buffer at 12-13 cc/min. The hearts had a mean intrinsic rate of ~180-190bpm (hearts with a native rate <160 bpm were not used). A 0.03 cc latex balloon (Harvard Apparatus, Saint-Laurent, Quebec, Canada) filled with water and attached to a pressure transducer (Cobe, Richmond Hill, Ontario, Canada) was placed in the RV via the right atrium and pressure traces were sampled at a rate of 1000 Hz by PowerLab. Pressure readings were converted into first derivative traces to give dP/dt and analyzed with Chart 5.4 software (ADInstruments Inc, Colorado Springs, CO).

Endothelin immunoassay for coronary effluent and blood samples (Cayman Chemicals, Ann Arbor, MI, USA): a double-antibody sandwich technique is used. The wells of the plates are coated with a monoclonal antibody specific for endothelin. An acetylcholinesterase:Fab' conjugate, which binds the opposite side of the endothelin molecule that the monoclonal antibody binds. The excess reagent is washed off and the sandwiched endothelin molecules are quantified by measuring the enzymatic activity of the acetylcholinesterase by adding Ellman's reagent to the wells. The product of the acetylcholinesterase-catalyzed reaction is yellow and absorbs at 412nm. The intensity of yellow attained by spectrophotometry is compared to the standards to calculate concentration of endothelin.

Data Analysis: Data were expressed as mean \pm SEM, and significant differences were evaluated using the Student *t* test for unpaired data or 1-way ANOVA followed by post-

hoc Bonferroni correction. Significance was defined at a p-value of less than 0.05.

Results

We studied RV specimens from 41 patients (hypertrophied RV= 28, normal RV= 13). The diagnosis of RVH was made by echocardiography pre-operatively and by macroscopic inspection at the time of surgery. Confocal microscopy and multiple-staining technique and time-coursed images were used to quantify the expression of ET-1 and ET_R-A in RV myocardium. There was a significant increase in expression of both ET-1 and ET_R-A in the patients with RVH compared to those with normal RVs (Figure 1). Increased RVH ET-1 and ET_R-A were also seen on immunoblots (Figure 1). The technique of multiple-staining confocal microscopy was used to show expression of ET-1 and ET_R-A in the myocardium by co-localization with myosin heavy chain (Figure 2). Interestingly, the other subtype of endothelin receptor seen in the pulmonary vasculature, ET_R-B, was only observed in the coronary vasculature of both RVH and normal RV hearts, and not present in the myocardium (Figure 2).

To determine whether ET and ET_R-A mRNA were also increased in RVH and that it indeed was in the myocardium, we used laser-captured microdissection. The technique allowed for cuts of tissue that were specifically muscle or vessel based on the amount of MHC and SMA that amplified with the cut. Laser captured cuts that appeared to be myocardium on microscopy were verified by having a high ratio of MHC:SMA, whereas the opposite findings were demonstrated in coronary cuts (Figure 3). The results confirm the immunohistochemistry data, that there is an increased expression of ET and ET_R-A in the myocardium of patients with RVH (Figure 3). While there was a significant expression of both ET and ET_R-A in the vasculature of both normal and hypertrophied RV, there was only a significant up-regulation of expression in the myocardium of

patients with RVH.

The human data of immunohistochemistry and laser captured microdissection were reproduced in our rat model of RVH secondary to monocrotaline induced PAH (Figure 4). Rats injected with monocrotaline compared to vehicle developed significant RVH secondary to PAH as we have previously described². In the rat model, the RV/LV+Septum weight ratio for RVH versus normal RV was 0.41 ± 0.03 versus 0.26 ± 0.02 ($p<0.01$), respectively. The immunofluorescence data confirmed that as in patients with RVH, rats with RVH also had increased expression of ET_R-A and ET-1 compared to vehicle treated rats. The results on laser-captured microdissection were found to be similar in rats as in humans with RVH (Figure 4).

Is the increased expression of ET and ET_R-A of physiological relevance in patients with RVH? It is challenging to isolate the direct effects on the RV without the confounding effects on the pulmonary vasculature, where ET_RA would cause vasodilation and decreased afterload, thus augmenting cardiac output in-vivo. Therefore use of these drugs in an ex-vivo setting where the pulmonary vasculature can be removed and only developed pressure in the RV can be evaluated would help identify the direct effects on the RV. To isolate the effects on the RV, we used a modified Langendorff preparation to study RV inotropy in the presence of ET_RA in the buffer delivered to the coronary arteries by perfusion into the ascending aorta. The afterload is irrelevant in this non-working model of heart perfusion and the preload is kept constant by fixing the balloon volume inside the RV, which is attached to a pressure transducer to measure real time developed RV pressure.

The modified Langendorff perfusion showed an increase in ET-1 concentration in

the coronary effluent collected from the coronary sinus in hearts with RVH at baseline (Figure 5A). Both RVH and normal RV hearts had a significant increase in ET-1 secretion into the coronary sinus effluent after stimulation with the β -agonist isoproterenol (Figure 5A), suggesting a potential paracrine effect of ET-1 on contractility of the hypertrophied RV when responding to adrenergic stimuli. The venous blood from rats with RVH also had increased concentrations of ET-1 (Figure 5B). Developed pressures measured in the RV data were acquired as previously described². Real time developed pressure tracings (Figure 6) were analyzed for both mean developed pressure from baseline and contractility by taking the derivative of pressure over time. Both RVH and normal RV hearts showed a similar increase in developed pressure from baseline when treated with isoproterenol between the two groups, this was also found to be similar when treated with ET-1 (Figure 7A); however, ETAs (BQ-123 and Bosentan) caused a significant decrease in RV developed pressure in rats with RVH compared to control rats without RVH (Figure 7A). There was also a smaller, though significant decrease in normal RV developed pressure when treated with Bosentan (Figure 7A). The decrease in developed pressure dropped below baseline values, demonstrating a negative inotropic effect on the hearts with RVH, which was also seen on the mean contractility data (Figure 7B).

Discussion:

We report that Endothelin-1 and the Endothelin Receptor-A are up-regulated in human right ventricular hypertrophy (Figure 1). There is a similar increase in both ET-1 and ET_R-A in rats with RVH secondary to PAH. The up-regulation of the endothelin system is at the level of the myocardium as seen by both confocal microscopy multi-staining immunohistochemistry showing co-localization with myosin heavy chain (Figure 2), as well as laser capture microdissection where mRNA of ET-1 and ET_R-A are elevated in myocardial cuts in RVH (Figure 3). These observations were also consistent in the rat model of RVH (Figure 4). In *ex-vivo* perfusions of the rat hearts with RVH, there was an increased concentration of ET-1 in the effluent from the coronary sinus (Figure 5), which was further augmented by stimulation with isoproterenol. Most clinically relevant, there were significant decreases in contractility observed when ETRAs were used in RVH hearts (Figure 6 and 7), where there was a blunting of developed RV pressures below baseline values when hearts were perfused with ETRAs, suggesting a primary negative inotropic effect on the RVH myocardium. Our findings have immediate clinical implications for patients with RVH being treated with ETRAs. Also, study designs and interpretation of results where ETRAs are utilized will need to be cognizant of potential deleterious effects on RVH contractility.

The secretion of ET-1 into the coronary sinus effluent of rat hearts undergoing modified Langendorff perfusion, along with increased secretion when stimulated by a β -agonist suggest a possible paracrine effect of ET-1 in the RV myocardium. Though the role of ET-1 secreted from the myocardium is a small contribution compared to the

circulating venous blood levels of ET-1 at a magnitude of 100X greater than the concentration in the coronary sinus (Figure 5).

The applied physiology experiments using the ex-vivo apparatus show an interesting difference in magnitude of decrease in developed pressure in the RVH hearts when perfused with BQ-123 compared to Bosentan (Figure 7A). A possible explanation for Bosentan having a stronger negative inotropic effect results from Bosentan being a mixed ETRA that antagonizes both ET_R-A and ET_R-B; whereas BQ-123 is a more selective ET_R-A blocker. Immunohistochemistry data did reveal that ET_R-B was expressed in the vasculature of both RVH and normal RV coronary arteries (Figure 2). Since ET_R-B stimulation leads to the secretion of nitric oxide and subsequent vasodilation of the coronary vasculature¹⁴, a mixed ETRA may lead to further negative contractility by increasing coronary vascular resistance and worsen ischemia. These results are in contrast to our previous study that showed an increase in contractility of RVH hearts with acute PDE5 inhibition (Figure 6)², which may support a strategy of combination therapy in patients with PAH to maximize pulmonary vasodilation and minimize negative inotropy on the RVH myocardium.

The use of ETAs in the treatment of PAH has risen exponentially since the approval by the FDA, based on randomized clinical trials demonstrating the efficacy of ETAs to improve 6-minute walk results and decrease the progression of symptoms in patients with PAH^{10, 15}. Unfortunately, the prognosis for patients with PAH continues to be very limited, in spite of being on therapies like ETAs. The importance of the RV when interpreting results from PAH trials has been overlooked thus far. Our results suggest that previously unappreciated negative inotropic effects on the RV may minimize

the benefits derived from ETRAs. Recently, efforts to improve the understanding of the RV in health and disease have been mandated by North American¹ and European¹⁶ scientific bodies. Specifically, in the management of PAH, translational researchers have placed right ventricular function in response to therapies as a priority for future research¹⁷. Given the overall paucity in the literature of the endothelin system on the RV in PAH, there are few studies that have looked only at animal models that are relevant to the results we present in this paper. Ueno et al assessed the myocardial expression of the ET-1 system in the RV of rats with monocrotaline induced PAH¹², and protein quantification showed an increase in ET_R-A in rats with RVH, consistent with our results. The results of Jasmin et al, where the animal model of MCT induced PAH in rats, also revealed an increase in ET-1 in hearts with RVH; however, there was no increase in ET_R-A expression observed¹⁸. The authors measured ET_R-A densities by radioligand binding of radiolabeled iodinated ET in the presence of BQ-123, and though BQ-123 is relatively specific for ET_R-A, there is a small amount of binding to the ET_R-B receptor¹⁹. This may partially explain the differences in our results that looked specifically at ET_R-A antibody binding in immunofluorescence and immunoblotting, as well as specific ET_R-A primers for RT-PCR. Further controversy exists in the literature as another group also studying the MCT-induced model of RVH in rats do not even show an increase in ET-1 in the myocardium of rats with RVH, indeed they show the opposite, a decrease in ET-1 expression in rats with RVH^{20, 21}. The experimental design in these publications by Brunner's group study a different subset of rats exposed to MCT, they study rats 9 weeks after MCT injection, while over 50% of their injected cohort have died from end-stage PAH and RV failure. This selected group is considered to be in compensated hypertrophy

by the authors, though the clinical correlation of such a group is difficult, as patients with PAH progress quickly to RV failure and death without treatment. Our experimental design is more consistent with the literature, where animals are used 3-4 weeks post-injection, with a <5% rate of mortality of the cohort at this time frame, representing the clinical scenario of patients with progressive symptoms requiring therapeutic intervention.

The importance of the endothelin system in maintaining contractility is also observed in a physiologic animal model of RVH, which is neonatal RVH. Nagasaka et al report the positive inotropic effect of ET-1 on neonatal mouse RV strips by measuring increased contractile force when exposed to rising concentrations of ET-1, and a blunting of contractile force when exposed to BQ-123 (ETRA)²². Their publication further dissects the effects to the myocardium by examining muscle strips that are not influenced by coronary flow as in our ex-vivo model. Yet, the results complement our data of ex-vivo perfused hearts with RVH also experiencing decreases in developed pressure with BQ-123. As BQ-123 is a relatively specific ET_R-A inhibitor, previous work at the level of rabbit LV isolated cardiomyocytes use another selective ET_R-A inhibitor (ABT-627) to show that it is through this receptor that endothelin causes increased contractility at the level of the cardiomyocyte¹¹. Though our work is specifically on the RV and data collected on the LV and LV derived cardiomyocytes cannot be directly extrapolated to the RV, or RVH.

Stimulation of the LV myocardium by endothelin results in increased contractility²³. The receptor for myocardial effects of endothelin is primarily through ET_R-A¹¹. The physiological effects of endothelin receptor antagonism on contractility

have been evaluated, where ET_R -A antagonists cause decreased contractility²⁴. In conditions of LV hypertrophy, endothelin stimulation has been shown to contribute to systolic performance²⁵. It is possible that the decrease in contractility caused by ETAs may contribute to the lack of benefit this class of drugs have in patients with CHF²⁶, where even marginal decrease in inotropy may worsen symptoms and increase cardiac event rates. Yet, human clinical trials on patients with PAH showed modest improvement in 6-minute walk test¹⁰. The direct consequences of ETAs on the RV have not been evaluated in the normal or hypertrophied RV. Our results show that there are potential primary negative inotropic effects on the RV by ETAs. The decrease in RV contractility is worse in the setting of RVH, which exists in many patients with PAH being treated with ETAs. Though the overall in-vivo effect of ETAs combined with the beneficial reduction in pulmonary vascular resistance may indeed result in a net improvement of symptoms. Yet, clinicians should be aware of potential unwanted decrease in RV function. The results presented in this paper may better explain human trial data, including one of the earlier trials on patients with CHF where patient hemodynamic were recorded after treatment with ETAs, where mean pulmonary arterial pressures were reduced and left atrial pressures were unchanged, yet there was no increase in cardiac output²⁷. A lack of increase in cardiac output, when there is decrease in pulmonary arterial pressures suggests a negative inotropic effect, as there should be an increase in cardiac output when transpulmonary gradients are reduced.

The up-regulation of ET-1 and ET_R -A in the RVH myocardium suggests a possible compensatory mechanism to maintain RV contractility in PAH. This feedback mechanism may also seem superficially similar to the use of β -blockers in CHF patients

with LV failure; however, the difference of function between the LV and RV make the role of decreased RV function with ETRAs more challenging. In LV failure, β -blockers help decrease the LV afterload by decreasing systemic vascular resistance, as do ETRAs on the RV afterload. The difference in LV failure is that oxygenated blood from the LV is required to flow forward to nourish the tissue beds of the body, which is improved by β -blockers. The role of the RV is not to provide oxygen to lung tissue, merely to actively pass blood through the lung vasculature for the purpose of oxygenating the pumped blood. Hence the negative inotropic effects on the LV from β -blockers may be better tolerated because total body oxygenation and symptoms may improve. In the case of RV failure in PAH, decreased contractility may be less tolerated, as decreased PVR may not improve the nutritive function of the ventricle. The negative inotropic effects of ETRAs on the myocardium may also provide a mechanism for increased edema and ascites seen in clinical trails where higher doses of ETRAs were initially utilized.

Endothelin-1 is formed after cleavage of big-Endothelin by endothelin converting enzyme (ECE), another potential target of the Endothelin system for therapeutics. The limited data on ECEs in the heart makes the use of ECE inhibitors less likely to be beneficial for the treatment of PAH with RVH for two reasons. Firstly, the use of ECE inhibitors compared to ETRAs appear to have less of a systemic and renal vasodilator effect in CHF²⁸. Secondly, the compensatory role of endothelin production in cardiomyocytes is also likely to be blunted significantly by ECE inhibitors, as there is a five-fold increase in ECE mRNA in CHF cardiomyocytes²⁹. Also, ECE inhibitors are not approved clinical therapies for PAH, while ETRAs are in current clinical practice.

The use of ETRAs without evaluation of RV contractility warrants further

concern in popularization of their approval for mildly symptomatic patients with PAH in World Health Organization Functional Class II³⁰. These studies do not show a statistically significant improvement in 6-minute walk test over 6 months, yet there is a growing enthusiasm for their prescription. The potential negative inotropy on the RV is evident in recent studies, where RV function by MRI on patients with PAH being treated with bosentan were examined 12 months after therapy, which showed no improvement in RVEF³¹. It is possible that the positive effects on PVR may outweigh the negative effects on the RVH myocardium, however clinical awareness of this possibility should be considered when treating these patients.

Limitations:

We are limited in our human samples of RVH to come predominantly from patients with congenital heart disease and subsequent RVH that leads to operative indications where tissue can be procured from surgical specimens. A more specific patient population to our adult patients are those with acquired RVH from PAH that is often idiopathic in etiology. If we are to verify our implications of ETRAs on the RVs of patients with PAH and RVH, we would need to place conductance catheters into our patients with RVH and treat them acutely with ETRAs to actually measure changes in RV contractility in-vivo.

Conclusions:

We show that the Endothelin system is up-regulated in human RVH myocardium and that in an animal model, the use of ETRAs decrease contractility in animals with RVH greater than in hearts without RV. The receptor that is up-regulated in RVH myocardium

is ET_R -A. The use of ETAs in patients with PAH and RVH need to be followed for potential negative effects on the RV, which may lead to failed efficacy of this class of drugs in patients.

Figure 1A

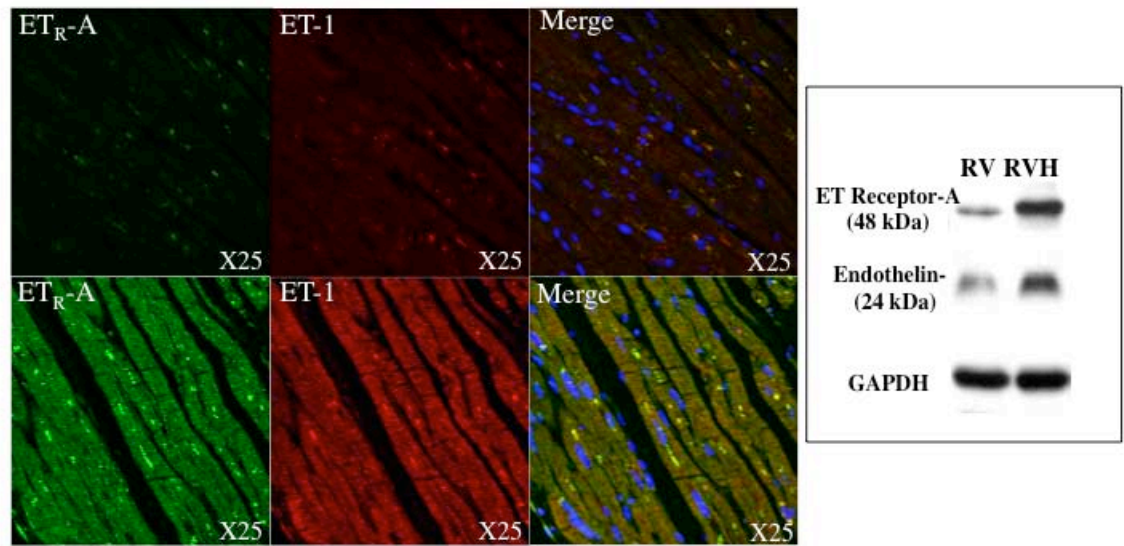


Figure 1B

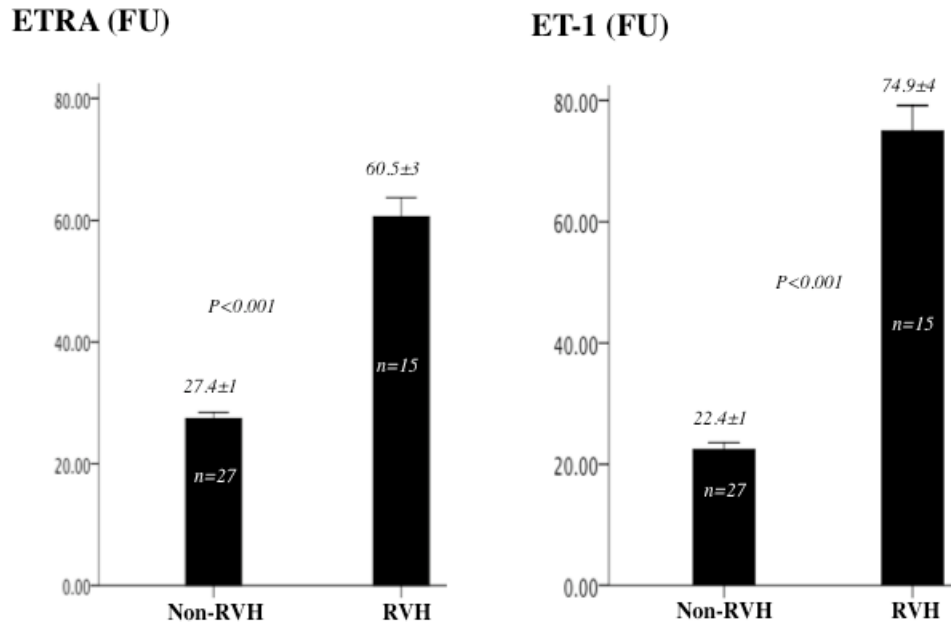


Figure 1: The Endothelin axis is up-regulated in human RVH.

A: Multiple staining immunohistochemistry technique and multi-photon confocal microscopy show that both ET-1 and ET_R-A protein expression is increased in RVH (top). Immunoblots also show increased expression of ET-1 and ET_R-A in RVH (bottom).

B: Mean fluorescence of human RVs for ET_R-A and ET-1, where both show a significant increase in expression in RVH compared to the normal RV (*p<0.01).

Figure 2

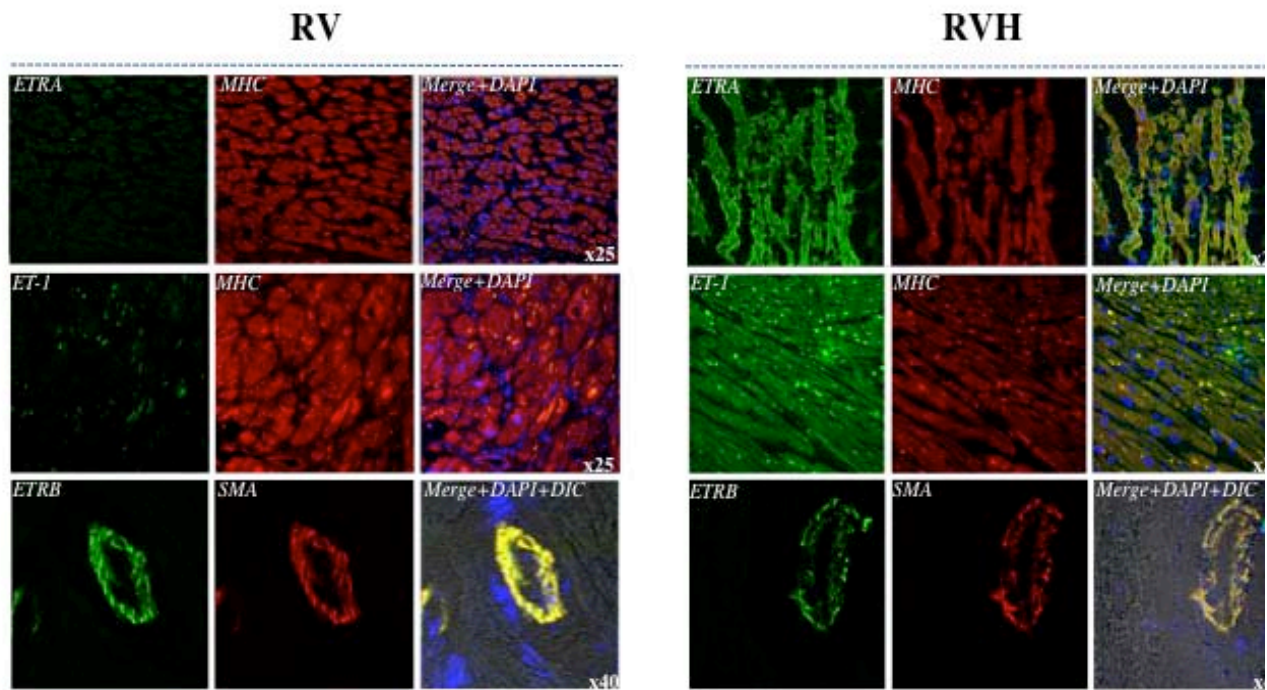


Figure 2: ET_R-A and ET-1 expression is increased in the myocardium of RVH.

Multiple staining immunohistochemistry technique and multi-photon confocal microscopy show that ET_R-A (green in upper third) protein expression and ET-1 (green in middle third) expression is in the myocardium of RVH (co-localization with MHC (red)), seen on the merge panel on the right (magnification of 25X). While the only significant expression of ET_R-B (green in bottom third) was found in the vasculature of both the normal and hypertrophied RV (co-localization with SMA (red)), seen on the merge + DIC panel (magnification of 40X).

Figure 3

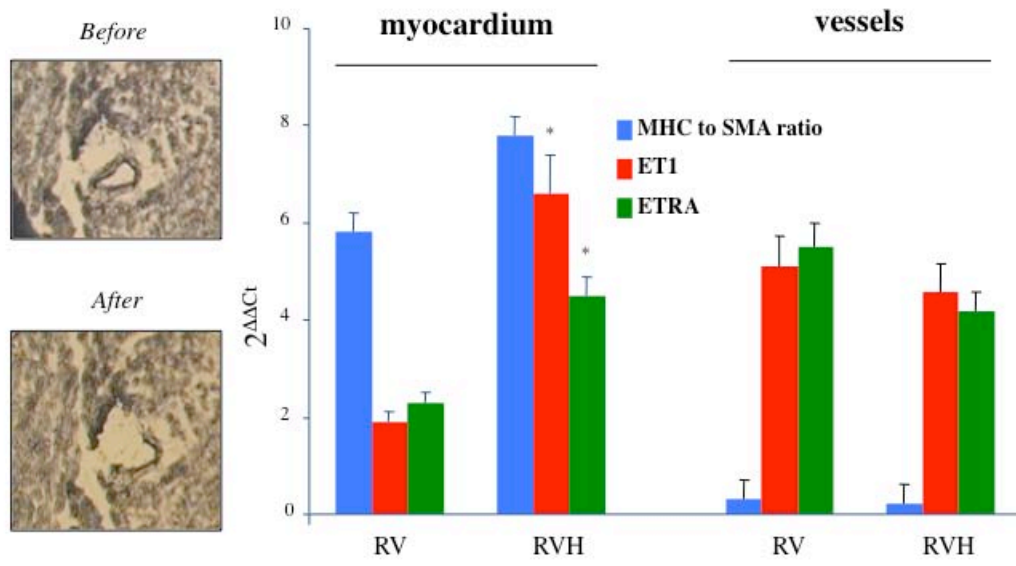


Figure 3: ET_R-A and ET-1 mRNA in human normal and hypertrophied RV reveals regulation of expression in a tissue-specific manner.

Laser-Captured Microdissection (LCM) and qRT-PCR was applied on human RV tissue. LCM was used to isolate myocardium versus coronary arteries in normal and hypertrophied human RV for qRT-PCR. A high MHC to SMA ratio characterized a myocardium sample. In contrast, low MHC to SMA ratio characterized a coronary artery sample. ET_R-A and ET-1 mRNA is increased in RVH compared to normal RV myocardium, in agreement with our immunohistochemistry data in Figure 2 (*p<0.01).

Figure 4A

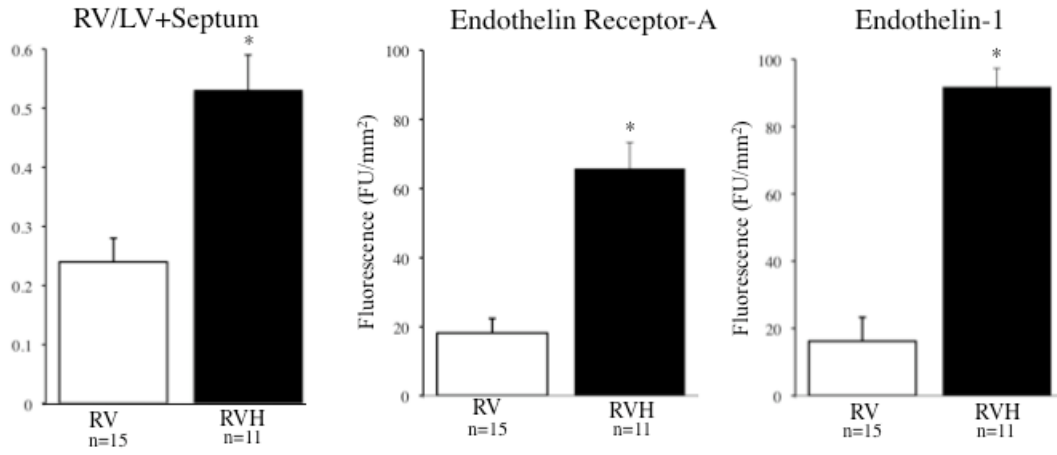


Figure 4B

qRT-PCR from Laser Captured Microdissection in Rats

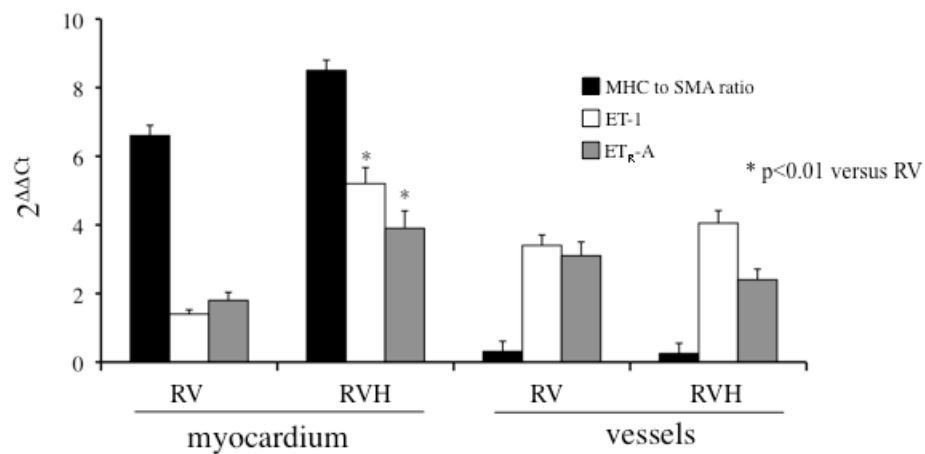


Figure 4: Rat model of RVH show similar increases in protein and mRNA expression of ET_R-A and ET-1 as observed in human samples.

A: Mean fluorescence of rat RVs for ET_R-A and ET-1 from immunohistochemistry staining, where both show a significant increase in expression in RVH compared to the normal RV (*p<0.01).

B: Laser-Captured Microdissection (LCM) and qRT-PCR was applied on rat RV tissue. LCM was used to isolate myocardium versus coronary arteries in normal and hypertrophied rat RV for qRT-PCR. ET_R-A and ET-1 mRNA is increased in RVH compared to normal RV myocardium (*p<0.01).

Figure 5

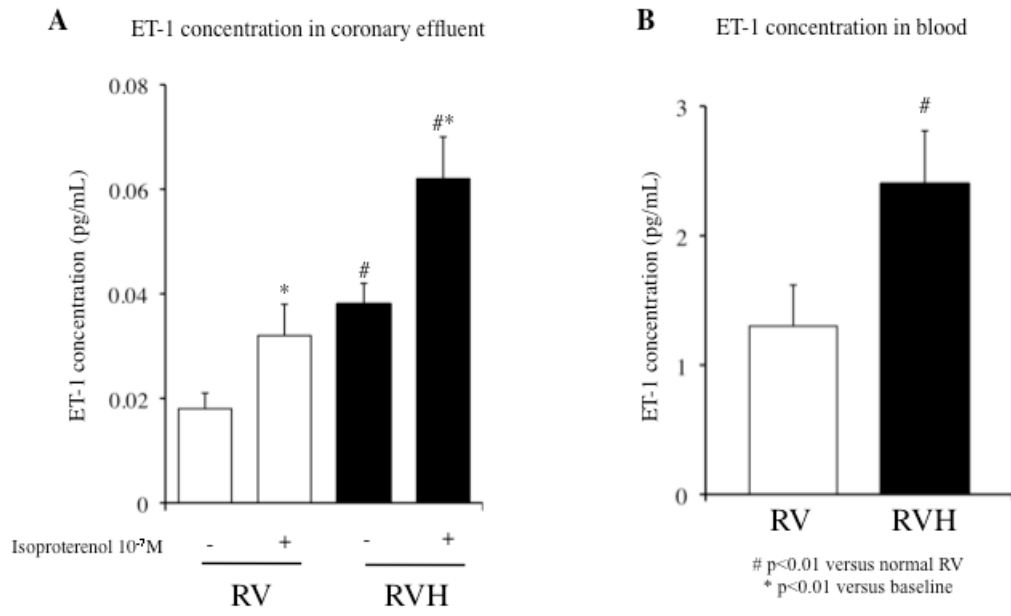


Figure 5: ET-1 concentrations from coronary sinus effluent from modified Langendorff perfusions and ET-1 concentrations in the venous blood of rats with RVH and normal RV.

A: ET-1 concentrations from coronary sinus effluent during modified Langendorff perfusions show a significant increase in ET-1 secretion in hearts with RVH compared to the normal RV. Both RVH and normal RV hearts secreted increased concentrations of ET-1 into coronary sinus effluent when stimulated with isoproterenol.

B: ET-1 concentrations in the venous blood of rats with RVH were significantly higher than control animal blood (* $p < 0.01$).

Figure 6

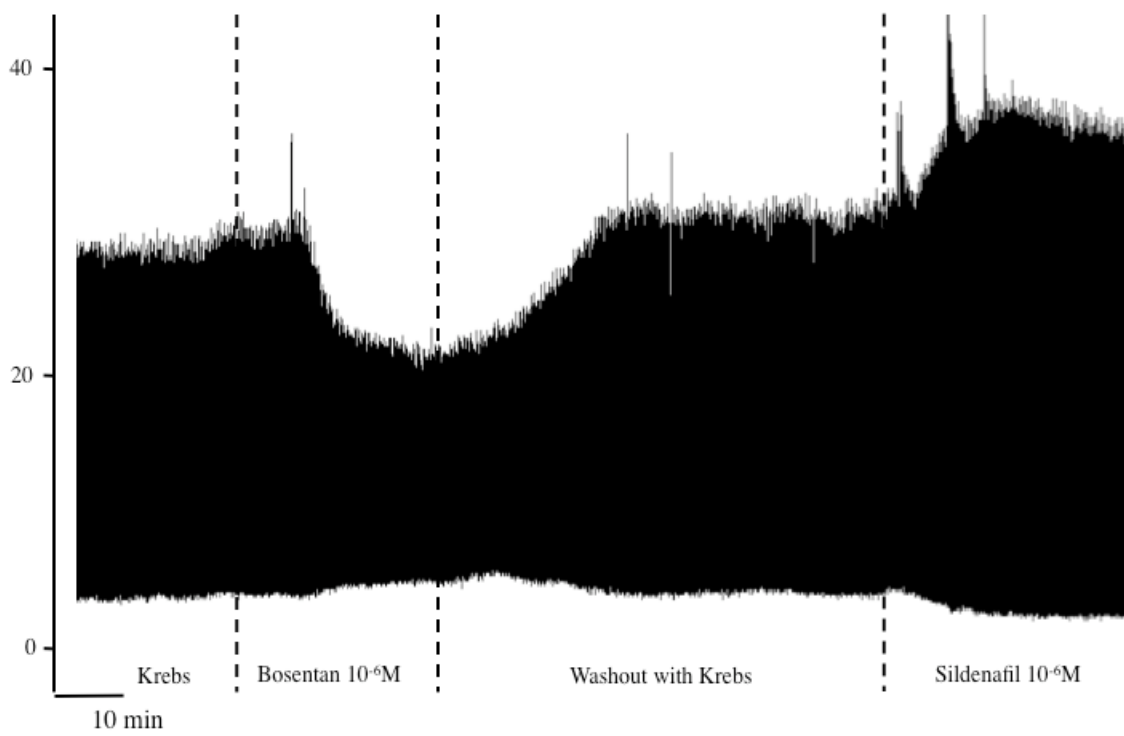


Figure 6: Representative developed pressure tracing of acute RVH contractility with ETRA followed by PDE5 inhibition.

Representative trace of the developed contractile pressure in the RVH rat heart before the addition of bosentan followed a wash out phase and then addition of sildenafil in the perfusate. Time in minutes is on the x-axis and developed pressure in mmHg is on the y-axis. The hashed red lines represent changes in perfusate.

Figure 7A

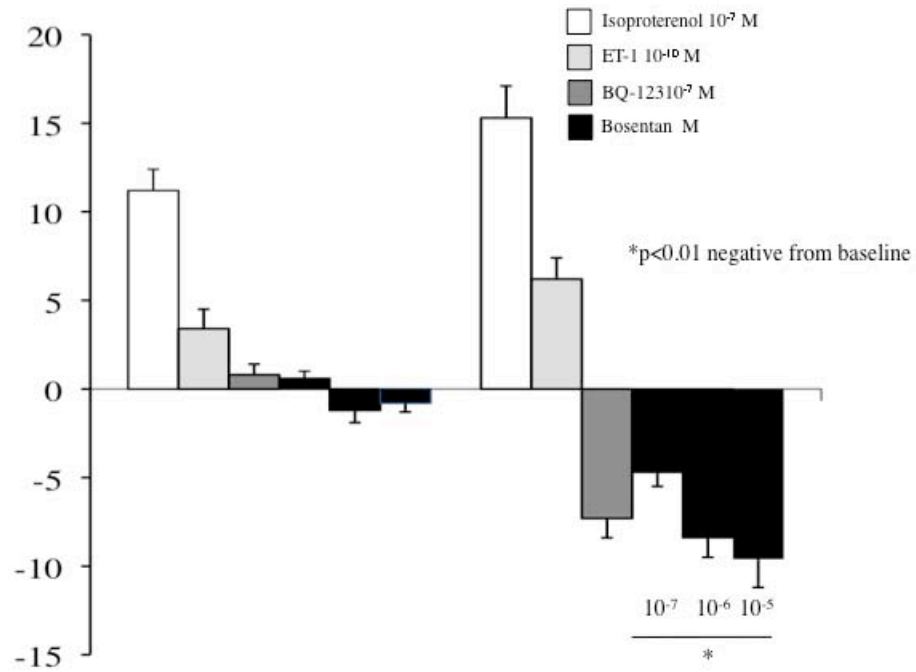


Figure 7B

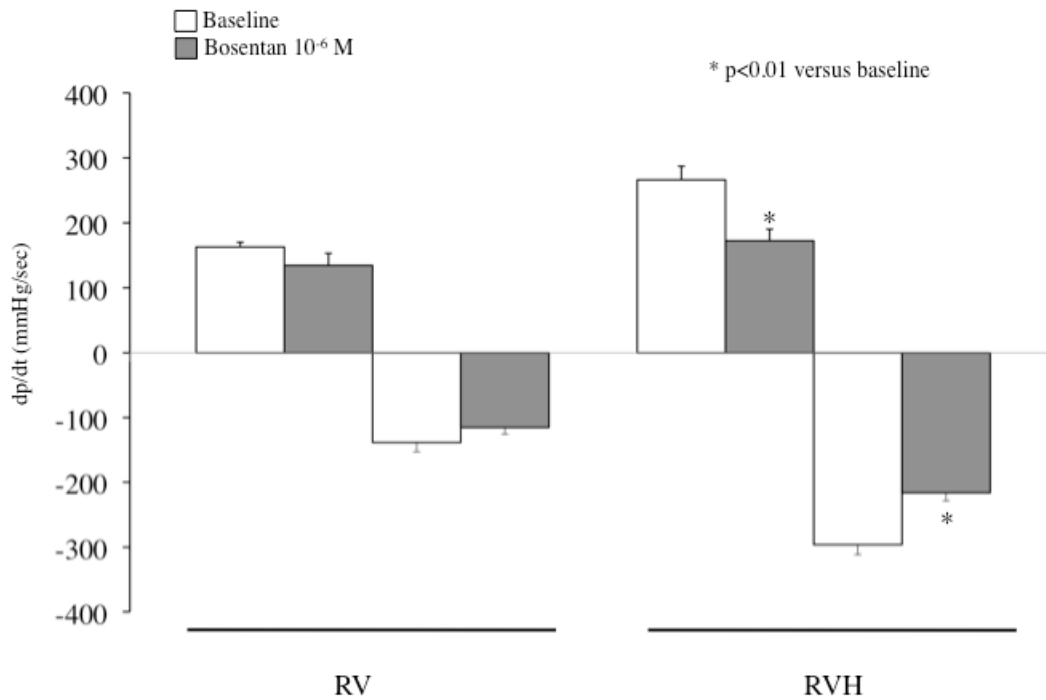


Figure 7: Mean data of acute RV and RVH contractility with ETAs.

A-B: Mean data showing that the ETAs (BQ-123 (blue) and bosentan (green)) decreased contractile pressure from baseline and both max and min dP/dt in the RVH hearts. ETAs did also decrease developed pressure in the normal RV to a lesser magnitude, whereas both normal and hypertrophied RV responded similarly to isoproterenol and ET-1.

Table 1

Patient	Age-Sex	Diagnosis	Tissue
1	19y F	Left atrial sarcoma	Normal RV
2	54y M	Intractable angina, no PAH	Normal RV
3	4y F	Ross procedure	Normal RV
4	56y F	Dilated cardiomyopathy	Normal RV
5	15y F	Dilated cardiomyopathy	Normal RV
6	42y M	Dilated cardiomyopathy	Normal RV
7	30y M	Dilated cardiomyopathy	Normal RV
8	37y M	Dilated cardiomyopathy	Normal RV
9	19y F	Dilated cardiomyopathy	Normal RV
10	22y F	Post-partum cardiomyopathy	Normal RV
11	27y M	Dilated cardiomyopathy	Normal RV
12	36y F	Dilated cardiomyopathy	Normal RV
13	14y M	Dilated cardiomyopathy	Normal RV
14	23y M	Tetralogy of Fallot	RVH
15	1.3y M	Tetralogy of Fallot	RVH
16	6 d M	Hypoplastic Left Heart Syndrome	RVH
17	13 d M	Truncus Arteriosus	RVH
18	3y M	Double Outlet Right Ventricle	RVH
19	8mo M	Ventricular Septal Defect	RVH

20	16d M	Hypoplastic Left Heart Syndrome	RVH
21	1y M	Double Outlet Right Ventricle	RVH
22	7mo M	Tetralogy of Fallot	RVH
23	6mo M	Tetralogy of Fallot	RVH
24	2mo M	Tetralogy of Fallot	RVH
25	50y F	End-stage rheumatic heart disease	RVH
26	3mo M	Tetralogy of Fallot	RVH
27	1y M	Pulmonary Atresia	RVH
28	3y M	RV outflow tract obstruction	RVH
29	2mo M	Ventricular Septal Defect	RVH
30	5mo M	Tetralogy of Fallot	RVH
31	3y M	Double Outlet Right Ventricle	RVH
32	6mo F	Ventricular Septal Defect	RVH
33	11y M	Tetralogy of Fallot	RVH
34	4mo M	Tetralogy of Fallot	RVH
35	8mo M	Ventricular Septal Defect	RVH
36	13y F	RV outflow tract obstruction	RVH
37	6mo M	Tetralogy of Fallot	RVH
38	11d M	Hypoplastic Left Heart Syndrome	RVH
39	1mo F	Tetralogy of Fallot	RVH
40	4mo F	Tetralogy of Fallot	RVH
41	3mo F	Tetralogy of Fallot	RVH

1. Voelkel NF, Quaife RA, Leinwand LA, Barst RJ, McGoon MD, Meldrum DR, Dupuis J, Long CS, Rubin LJ, Smart FW, Suzuki YJ, Gladwin M, Denholm EM, Gail DB. Right ventricular function and failure: report of a National Heart, Lung, and Blood Institute working group on cellular and molecular mechanisms of right heart failure. *Circulation*. 2006; 114:1883-1891.
2. Nagendran J, Archer SL, Soliman D, Gurtu V, Moudgil R, Haromy A, St Aubin C, Webster L, Rebeyka IM, Ross DB, Light PE, Dyck JR, Michelakis ED. Phosphodiesterase type 5 is highly expressed in the hypertrophied human right ventricle, and acute inhibition of phosphodiesterase type 5 improves contractility. *Circulation*. 2007; 116:238-248.
3. Yanagisawa M, Kurihara H, Kimura S, Tomobe Y, Kobayashi M, Mitsui Y, Yazaki Y, Goto K, Masaki T. A novel potent vasoconstrictor peptide produced by vascular endothelial cells. *Nature*. 1988; 332:411-415.
4. Dupuis J, Hoeper MM. Endothelin receptor antagonists in pulmonary arterial hypertension. *Eur Respir J*. 2008; 31:407-415.
5. Masuda Y, Miyazaki H, Kondoh M, Watanabe H, Yanagisawa M, Masaki T, Murakami K. Two different forms of endothelin receptors in rat lung. *FEBS Lett*. 1989; 257:208-210.
6. Modesti PA, Vanni S, Paniccia R, Bandinelli B, Bertolozzi I, Polidori G, Sani G, Neri Serneri GG. Characterization of endothelin-1 receptor subtypes in isolated human cardiomyocytes. *J Cardiovasc Pharmacol*. 1999; 34:333-339.
7. Ortega Mateo A, de Artinano AA. Highlights on endothelins: a review. *Pharmacol Res*. 1997; 36:339-351.
8. McMurray JJ, Teerlink JR, Cotter G, Bourge RC, Cleland JG, Jondeau G, Krum H, Metra M, O'Connor CM, Parker JD, Torre-Amione G, van Veldhuisen DJ, Lewsey J, Frey A, Rainisio M, Kobrin I. Effects of tezosentan on symptoms and clinical outcomes in patients with acute heart failure: the VERITAS randomized controlled trials. *Jama*. 2007; 298:2009-2019.
9. Williamson DJ, Wallman LL, Jones R, Keogh AM, Scroope F, Penny R, Weber C, Macdonald PS. Hemodynamic effects of Bosentan, an endothelin receptor antagonist, in patients with pulmonary hypertension. *Circulation*. 2000; 102:411-418.
10. Channick RN, Simonneau G, Sitbon O, Robbins IM, Frost A, Tapson VF, Badesch DB, Roux S, Rainisio M, Bodin F, Rubin LJ. Effects of the dual endothelin-receptor antagonist bosentan in patients with pulmonary hypertension: a randomised placebo-controlled study. *Lancet*. 2001; 358:1119-1123.

11. Kelso EJ, McDermott BJ, Silke B, Spiers JP. Endothelin(A) receptor subtype mediates endothelin-induced contractility in left ventricular cardiomyocytes isolated from rabbit myocardium. *J Pharmacol Exp Ther.* 2000; 294:1047-1052.
12. Ueno M, Miyauchi T, Sakai S, Kobayashi T, Goto K, Yamaguchi I. Effects of physiological or pathological pressure load in vivo on myocardial expression of ET-1 and receptors. *Am J Physiol.* 1999; 277:R1321-1330.
13. Naeije R, Huez S. Expert opinion on available options treating pulmonary arterial hypertension. *Expert Opin Pharmacother.* 2007; 8:2247-2265.
14. Cannan CR, Burnett JC, Jr., Brandt RR, Lerman A. Endothelin at pathophysiological concentrations mediates coronary vasoconstriction via the endothelin-A receptor. *Circulation.* 1995; 92:3312-3317.
15. Rubin LJ, Badesch DB, Barst RJ, Galie N, Black CM, Keogh A, Pulido T, Frost A, Roux S, Leconte I, Landzberg M, Simonneau G. Bosentan therapy for pulmonary arterial hypertension. *N Engl J Med.* 2002; 346:896-903.
16. Sanchez MA, Torbicki A. Foreword: right ventricular function and pulmonary hypertension. *European Heart Journal Supplements.* 2007; 9:H3-H4.
17. Michelakis ED, Wilkins MR, Rabinovitch M. Emerging concepts and translational priorities in pulmonary arterial hypertension. *Circulation.* 2008; 118:1486-1495.
18. Jasmin JF, Cernacek P, Dupuis J. Activation of the right ventricular endothelin (ET) system in the monocrotaline model of pulmonary hypertension: response to chronic ETA receptor blockade. *Clin Sci (Lond).* 2003; 105:647-653.
19. Ihara M, Ishikawa K, Fukuroda T, Saeki T, Funabashi K, Fukami T, Suda H, Yano M. In vitro biological profile of a highly potent novel endothelin (ET) antagonist BQ-123 selective for the ETA receptor. *J Cardiovasc Pharmacol.* 1992; 20 Suppl 12:S11-14.
20. Brunner F. Cardiac endothelin and big endothelin in right-heart hypertrophy due to monocrotaline-induced pulmonary hypertension in rat. *Cardiovasc Res.* 1999; 44:197-206.
21. Wolkart G, Stromer H, Brunner F. Calcium handling and role of endothelin-1 in monocrotaline right ventricular hypertrophy of the rat. *J Mol Cell Cardiol.* 2000; 32:1995-2005.
22. Nagasaka T, Izumi M, Hori M, Ozaki H, Karaki H. Positive inotropic effect of endothelin-1 in the neonatal mouse right ventricle. *Eur J Pharmacol.* 2003; 472:197-204.
23. Takanashi M, Endoh M. Characterization of positive inotropic effect of endothelin on mammalian ventricular myocardium. *Am J Physiol.* 1991; 261:H611-619.
24. Leite-Moreira AF, Bras-Silva C, Pedrosa CA, Rocha-Sousa AA. ET-1 increases distensibility of acutely loaded myocardium: a novel ETA and Na⁺/H⁺ exchanger-mediated effect. *Am J Physiol Heart Circ Physiol.* 2003; 284:H1332-1339.
25. Piuhola J, Szokodi I, Kinnunen P, Ilves M, deChatel R, Vuolteenaho O, Ruskoaho H. Endothelin-1 contributes to the Frank-Starling response in hypertrophic rat hearts. *Hypertension.* 2003; 41:93-98.

26. Kalra PR, Moon JC, Coats AJ. Do results of the ENABLE (Endothelin Antagonist Bosentan for Lowering Cardiac Events in Heart Failure) study spell the end for non-selective endothelin antagonism in heart failure? *Int J Cardiol.* 2002; 85:195-197.
27. Givertz MM, Colucci WS, LeJemtel TH, Gottlieb SS, Hare JM, Slawsky MT, Leier CV, Loh E, Nicklas JM, Lewis BE. Acute endothelin A receptor blockade causes selective pulmonary vasodilation in patients with chronic heart failure. *Circulation.* 2000; 101:2922-2927.
28. Wada A, Tsutamoto T, Ohnishi M, Sawaki M, Fukai D, Maeda Y, Kinoshita M. Effects of a specific endothelin-converting enzyme inhibitor on cardiac, renal, and neurohumoral functions in congestive heart failure: comparison of effects with those of endothelin A receptor antagonism. *Circulation.* 1999; 99:570-577.
29. Ergul A, Walker CA, Goldberg A, Baicu SC, Hendrick JW, King MK, Spinale FG. ET-1 in the myocardial interstitium: relation to myocyte ECE activity and expression. *Am J Physiol Heart Circ Physiol.* 2000; 278:H2050-2056.
30. Galie N, Rubin L, Hoeper M, Jansa P, Al-Hiti H, Meyer G, Chiossi E, Kusic-Pajic A, Simonneau G. Treatment of patients with mildly symptomatic pulmonary arterial hypertension with bosentan (EARLY study): a double-blind, randomised controlled trial. *Lancet.* 2008; 371:2093-2100.
31. Chin KM, Kingman M, de Lemos JA, Warner JJ, Reimold S, Peshock R, Torres F. Changes in right ventricular structure and function assessed using cardiac magnetic resonance imaging in bosentan-treated patients with pulmonary arterial hypertension. *Am J Cardiol.* 2008; 101:1669-1672.

Discussion:

General:

The body of work presented in this thesis represents an understudied and growing area of interest, the right ventricle (RV) in normal and hypertrophied states. There is clearly a developing interest in the RV as it can highly influence the outcomes of patients by evidence of RV failure being the number one predictor of morbidity and mortality in patients with pulmonary arterial hypertension (PAH). Though there have been significant advances in the treatment of PAH, the potential effects on the RV have not been specifically examined. The nature of these investigations was predominantly to examine the role of known therapies both FDA approved and experimental therapies on the function of the RV in normal and hypertrophied states. Several studies have examined both the in-vitro and in-vivo effects of therapies for PAH and their subsequent effects on the RV secondary to pulmonary arterial vasodilation. We set out to examine the specific effects on the RV, which were primary, that occurred directly based on therapeutic targets of PAH drugs being present in the RV myocardium. A novel concept that alters the interpretation of data already attained from clinical trials and gives clinicians further perspective on mechanisms for how therapies are changing the hemodynamics of patients with PAH. The first step in these investigations was to determine if there would be a clinical impact by in-vitro studies of human myocardial tissue on the RV. We started by attaining surgical specimens of RV myocardium from patients undergoing open-heart

surgery with either normal RVs or patients with RV hypertrophy, based on macroscopic examination and echocardiographic measurements of RV free wall thickness. These tissue samples were analyzed for targets of therapies used in the treatment of PAH, including phosphodiesterase-5 and endothelin receptors for molecular markers. We also examined the metabolic state of the cardiomyocytes based on mitochondrial function using mitochondrial membrane potential as a surrogate. From the analysis of human tissue, we were able to confirm that targets of therapies used in PAH are indeed present in RV myocardium (phosphodiesterase-5 and Endothelin Receptor-A) and there were significant differences in expression between the normal and hypertrophied RV, including altered states of mitochondrial hyperpolarization in RV hypertrophy. Once the establishment of potential clinical relevance in human tissue, we went on to recapitulate conditions of comparing the normal RV to RVH in the animal model. We used the well-established model of intraperitoneal injection of monocrotaline to induce PAH in rats, which leads to subsequent RVH. This model was chosen as monocrotaline causes RVH in a progressive fashion over the course of 14-28 days, which is similar to a progressive insult sustained by the RVH in humans with PAH. In the model of monocrotaline induced PAH, we were able to serially document RV hypertrophy by non-invasive echocardiography, where RV free wall thickness as well as pulmonary artery acceleration time could be monitored. Similar analyzes of human tissues were conducted on rat RV tissues and confirmation of our human observations were seen in the rat model of RVH. Pivotal to studying the RV in isolation is the creation of an ex-vivo model to determine RV contractility outside of the in-vivo environment, where the pulmonary vasculature can be separated from the RV. To do this, we modified the well-established model of the

Langendorff perfused heart preparation, where a balloon tipped catheter of fixed volume was attached to a pressure transducer and inserted into the RV via a right atriotomy and through the tricuspid valve. The ascending aorta is cannulated and perfusate is run into the coronary arteries with pharmacological agents to test their effects on contractility of the RV. As such, we are able to study the direct effects of therapeutics on the RV.

Chapter 2: Phosphodiesterase-5 expression in RVH

These studies were spurred by a clinical enigma found in patients with PAH being treated with sildenafil. In one of the first clinical settings where sildenafil was used compared to inhaled nitric oxide, Michelakis et al found that there was a significant increase in cardiac output in patients receiving sildenafil compared to patients receiving inhaled nitric oxide¹. This could not be explained at the time this study was published in 2002, as sildenafil was thought not to have any specific effects on the myocardium, since it was thought that the target of sildenafil, phosphodiesterase-5 (PDE5), was not present in the myocardium of the heart. The presence of phosphodiesterase-5 was performed on humans and animals with normal hearts, as such they may not have truly represented the myocardium of the RV in patients with PAH, where the RV myocardium is often hypertrophied secondary to the increased pulmonary vascular resistance.

Indeed, we were able to show that there was a significant increase in PDE5 expression in the myocardium of the hypertrophied human and rat heart. We were able to specify the increase in PDE5 to the myocardium over the vasculature by showing multi-staining confocal microscopy showing co-localization of PDE5 with myosin heavy chain, as well

as using laser capture microdissection, where we were able to show an increase in PDE5 in cuts of RVH myocardium (high expression of myosin heavy chain) compared to the normal RV; whereas, vascular cuts (high expression of smooth muscle actin) showed similar expression of PDE5 in normal and hypertrophied RVs. With these data, we went on to perform ex-vivo modified langendorff perfusions to determine the effects on RV contractility and we were able to show that sildenafil significantly increased the isolated contractility of the RVH rat hearts, while having minimal effects on the normal RV. This was an important observation, as it is the first time a PDE5 inhibitor was found to have direct inotropic effects on the myocardium. These findings were further dissected to the level of isolated cardiomyocytes as change in length of contraction from baseline of cardiomyocytes from an RVH heart was significantly increased when treated with sildenafil, while there was no significant change from baseline length of contraction when normal RV cardiomyocytes were treated with sildenafil.

The summary of these findings led to the conclusion that PDE5 is up-regulated in the hypertrophied human and rat RV myocardium and that acute PDE5 inhibition leads to an increase in RV contractility. These findings have been further verified recently in human trials of patients with improved RV contractility after use of sildenafil in patients with left ventricular assist device insertion and fixed pulmonary vascular resistance².

The mechanism for PDE5 inhibition leading to increased contractility in RVH required significant further investigation. The inhibition of PDE5 leads to an increase in cGMP, a second messenger, which primarily activates Protein Kinase-G (PKG) leading to increased phosphorylation of the down-stream targets. Activation of PKG leads to decrease flux of intracellular calcium, both from membrane voltage-gated calcium

channels and release from the sarcoplasmic reticulum; leading to a decrease in cardiac contractility. Increased PKG activity and decreased contractility directly opposes all data gathered in these studies. Thus we hypothesized that the PKG-axis is down-regulated in RVH, which was proven to be correct based on PKG activity by two assays showing decreased PKG activity in RVH compared to the normal RV. Interestingly, cGMP is the most potent endogenous inhibitor of cAMP-PDE3 and inhibition of PDE3 leads to an increase in cAMP, a second messenger, leading to activation of Protein Kinase-A (PKA) and down-stream phosphorylation causing an increase in intracellular calcium and contractility. Indeed, we were able to show that in RVH myocardium, PDE5 inhibition led to inhibition of cAMP-PDE3 and caused an increase in cAMP, we were also able to abolish the increase in RVH contractility by PDE5 inhibition by adding a PKA blocker.

These results reveal another very important conclusion of the study, that PKG activity is down regulated in RVH, and increased cGMP in RVH leads to inhibition of cAMP-PDE3.

Chapter 3- Dysfunctional mitochondrial remodeling in RVH can be therapeutically targeted

In chapter 2, the findings of molecular differences in expression of PDE5 in the normal and hypertrophied RV furthered in the consolidation of hypertrophy being associated with a reactivation of a fetal-gene program, where genes transcribed in the fetal heart are re-expressed in the hypertrophied heart. This notion of fetal genes being expressed in adult cardiac hypertrophy was established mainly in LV hypertrophy through work done

by Eric Olson³. Along with transcriptional changes seen in the hypertrophied RV, we hypothesized that there may also be mitochondrial differences seen between the two ventricles, and in RV hypertrophy there may be dysfunctional mitochondrial remodeling that may be therapeutically targeted to improve RV contractility.

The first step along these lines of investigation was to show a metabolic difference in human ventricular specimens between the normal and hypertrophied RV. We used mitochondrial membrane potential based on intensity of tetramethylrhodamine methylester (TMRM), which is a positively stained dye that specifically targets the mitochondria as the most negatively charged organelle in the cell. We observed that mitochondrial membrane potential was different between the normal RV and normal LV, where the normal RV was more depolarized than the LV, and interestingly the hypertrophied RV was most hyperpolarized compared to the normal RV and normal LV. We then used the rat model to observe similar significant differences in mitochondrial membrane polarity between the normal RV and LV. We first described this in ventricular tissue and then went on to isolate adult cardiomyocytes to also show these differences persisted at the level of the cardiomyocyte and was not attributed to other cell types in ventricular tissue. Then the previously described model of monocrotaline induced PAH and RV hypertrophy was used to show that the hypertrophied RV had the most hyperpolarized mitochondrial membrane potential based on TMRM fluorescence intensity. This increase in mitochondrial membrane potential was proportional to the amount of RV hypertrophy based on echocardiographic RV free wall thickness as well as inversely related to the pulmonary artery acceleration time. As such, the amount of TMRM fluorescence intensity was increased progressively as the RV

became more hypertrophied. If the concept of the fetal gene program was to be correlated to mitochondrial membrane potential and metabolic state, then similar finding of adult RV hypertrophy were required at the level of the neonatal heart. In the neonatal period, the RV starts in a hypertrophied state, based in increased pulmonary vascular resistance prior to ventilation. We used neonatal rat pups and performed similar TMRM staining on ventricular and isolated cardiomyocytes and observed that neonatal RV cardiomyocytes were significantly hyperpolarized compared to neonatal LV cardiomyocytes. These experiments were important to not only show the differences neonatal RV versus neonatal LV, but there was also a similar finding of mitochondrial hyperpolarization in both physiological and pathological RV hypertrophy. We wanted to also show that this phenomenon could be recapitulated through pharmacological induction of hypertrophy. We used neonatal culture for 48 hours with phenylephrine to induce neonatal normal cardiomyocytes to become hypertrophied. The neonatal cardiomyocytes exposed to phenylephrine also developed hyperpolarized mitochondrial membrane potential. Now that we had established an in-vitro model to induce cardiomyocyte hypertrophy and subsequent mitochondrial hyperpolarization, we attempted to target a transcription pathway in hypertrophy that may be inhibited to blunt the dysfunctional mitochondrial remodeling. Our lab's previous work have examined both pulmonary artery smooth muscle cell in PAH and cancer cell mitochondrial phenotypes based on mitochondrial membrane potential, and in both PAH and cancer there was a hyperpolarization of the mitochondrial membrane potential as observed in the RV hypertrophy cardiomyocytes^{4,5}. Also common to PAH and cancer is that levels of intracellular calcium are increased, as well established in ventricular hypertrophied cardiomyocytes. Increased intracellular

calcium leads to activation of the transcription factor NFAT (nuclear factor of activated T-cells) as confirmed in PAH⁶ and cancer⁵. Thus we targeted NFAT by blocking the binding of calcineurin to NFAT with a membrane permeable NFAT-specific inhibitor (VIVIT). We were able to incubate isolated neonatal cardiomyocytes with phenylephrine and VIVIT to show that there was an abolishment of mitochondrial membrane hyperpolarization when treated with VIVIT. These findings were further investigated by immunohistochemistry to determine if NFAT was truly being inhibited, by showing that in phenylephrine+VIVIT treated cardiomyocytes NFAT remained cytosolic and was not able to translocate to the nucleus, where it acts as a transcription factor. In cardiomyocytes only treated with phenylephrine, NFAT staining was found mainly co-localizing in the nucleus, where NFAT would be active. Beyond blocking the transcriptional pathway of hypertrophy and subsequent mitochondrial remodeling, we also looked to metabolically target mitochondrial function to see if that could revert the hyperpolarized phenotype back toward baseline. As previously described by our lab in the setting of PAH and cancer, dichloroacetate (DCA), a metabolic modulator was shown to depolarize hyperpolarized mitochondria back to levels similar to control. Indeed, treatment of neonatal cardiomyocytes with phenylephrine and DCA blunted the hyperpolarization of mitochondria. This was a critical experiment to show that a clinically used pharmacological metabolic modulator, DCA, was able to alter the phenotype of the mitochondrial metabolic state in-vitro. We then sought to determine if DCA could alter RV myocardial contractility ex-vivo by altering metabolism. The modified langendorff perfused heart was again used to show that DCA caused an increase in cardiac contractility in RVH rat hearts compared to normal RVs. This increase in

contractility was accompanied by a decrease in lactate measured in the coronary sinus, an indirect measure that DCA was improving glycolysis to glucose oxidation coupling to allow for more efficient energy production. These results suggest that DCA may be useful in the treatment of acute RV failure in patients with RV hypertrophy, as seen in patients with acutely decompensated PAH. In summary, there is a dysfunctional mitochondrial metabolic remodeling that occurs in RVH that can be targeted therapeutically to improve RVH contractility by depolarizing hyperpolarized mitochondria in cardiomyocytes, which is associated with a decrease in lactate production.

Chapter 4- Endothelin Receptor Antagonists Decrease Contractility in RVH

Another clinical discrepancy in the literature on therapies used on patients with RVH was the low efficacy of endothelin receptor antagonists (ETRAs) used on patients with PAH. Endothelin is a potent vasoconstrictor and there is a significant bed of endothelin receptors in the pulmonary vasculature. The use of ETRAs was thought to selectively vasodilate the pulmonary vasculature in PAH, which was shown to occur in-vitro. There have been several clinical trials leading to the approval of ETRAs for the treatment of PAH, yet a meta-analysis of several PAH trials showed that ETRAs did not significantly decrease death in patients with PAH and were only shown to improve surrogate outcomes, such as 6-minute walk test⁷. The ETRAs were first used in clinical trials for the treatment of CHF from LV failure, which did not show benefit, and trended toward harm including worsening edema and increased cardiac event rates⁸. Yet, these

medications have shown marginal clinical improvement in patients with PAH, which is counterintuitive as PAH eventual leads to RV failure, similar to CHF.

It is well described that Endothelin-1 (ET-1) is produced in cardiomyocytes, and that cardiomyocytes express Endothelin Receptor-A (ET_A-R) on their cell surface. Endothelin-1 is not only a vasoconstrictor in the vasculature, but it also causes increased contractility in cardiomyocytes⁹. In PAH, the RV is often hypertrophied to pump against the increased PVR, potentially expressing more ET_A-R to help increase contractility. Thus we hypothesized that ET_A-R would lead to a decrease in RVH contractility in patients with PAH, counterbalancing the decrease caused in the PVR.

As in the previous chapters, both human and animal tissues of RVH hearts were compared to normal RVs. Firstly, we examined the protein expression of both ET-1 and ET_A-R, where both showed increased expression in human and rat RVH. To further demonstrate that the increase in ET_A-R occurred at the level of the cardiomyocyte, we co-stained immunohistochemistry heart tissue slides with myosin heavy chain, which showed co-localization confirming that the increased receptor expression was in cardiomyocytes, and not vascular or interstitial tissue. When staining for Endothelin Receptor B, we only showed a co-localization with smooth muscle actin in vasculature and no significant expression in normal or hypertrophied myocardium. These results were also shown to be evident at the level of mRNA transcription as confirmed by qRT-PCR from laser-captured microdissection cut slides as described in chapter 2. The data significantly showed an up-regulation of the Endothelin axis in RVH myocardium for both ET-1 and ET_A-R, we then sought to determine if these results had any physiological consequences on the performance of the RVH myocardium.

The applied physiology experiments involved use of the modified langendorff perfused heart preparations as previously described in chapters 2 and 3. We examined secretion of ET-1 concentration found in the coronary sinus effluent of normal and RVH hearts, where there was an increased concentration of ET-1 in RVH effluent compared to the normal RV. The concentration of ET-1 was further increased by b-adrenergic stimulation with isoproterenol, suggesting that b-adrenergic stress may also increase cardiomyocyte secretion of ET-1 to allow for paracrine effects. However, the concentration of ET-1 released in the coronary effluent is significantly less than the circulating concentrations in the venous blood of the animals, making the role of cardiomyocyte secreted ET-1 less important. Nonetheless, the most important set of results were obtained by perfusing hearts with ETRAs and showing a very significant decrease in contractility in hearts with RVH. There was a lesser decrease in contractility by ETRAs in the normal RV as well. The summary of these data do verify that the Endothelin axis is up-regulated in RVH cardiomyocytes and ETRAs lead to a decrease in RVH inotropy, which may partially explain the modest efficacy of ETRAs in patients that would otherwise likely have much improved results with mere pulmonary vasodilation without negative effects on the RVH myocardium.

Future Directions:

Chronic effects on RVH by therapy:

In all of our applied physiology models of pharmacologic manipulation involved the use of ex-vivo modified langendroff perfusion model to isolate the effects on the RV from the rest of the heart. This model was ideal for isolating inotropic effects on the RV, by isolating the RV from effects on the pulmonary vasculature. The limitation of this technique was that only acute pharmacologic manipulation could be evaluated.

There are models that could isolate the RV from the pulmonary vasculature in a chronic nature, which would allow for inotropic assessment of the RV with prolonged drug therapy. This would involve the technique of pulmonary artery banding, where anesthetized and mechanically ventilated rats would undergo a left thoracotomy and a fixed caliber band is placed on the pulmonary artery to cause a fixed increase in RV afterload before the pulmonary vasculature. In PA banding, chronic effects of PDE5 inhibitors, ETRAs, and DCA could be studied. Experiments could examine multiple points along the RVH disease path from prevention to retardation of progression to reversal of established disease. Since primary prevention of RVH is not a significantly relevant clinical goal for society, these experiments would take less priority over the later. The most important experiments would examine the role of chronic PDE5 inhibition, ETRAs, and DCA on established RVH in PA banded animals that develop RVH. The experimental design would have PA banded animals with echocardiographic evidence of RVH placed on daily pharmacologic manipulation with the class of drugs in

each of the three chapters compared to vehicle fed animals. A model of severe increase in RV afterload could also be used with likely different results. The RV would not tolerate a severe acute PA banding with a fixed caliber band, as the RV would immediately fail and the animal would die prior to developing RVH. Rather an inflatable band that was increased in constriction over time to let the RV compensate would be used to apply severe increased RV afterload.

Potential Results and Interpretation: In the case of PDE5 inhibitors, we would hypothesize that there would be a decrease in the progression of RVH, as improved contractility in muscle strained by increased afterload will blunt pro-hypertrophy signaling as the myocardium will perform better with PDE5 inhibition. Since the downstream pathway of PDE5 inhibition leads to increased Protein Kinase-G activity, there may be exploration into the use of PA banded transgenic mice with PKG overexpression, or see the opposite in knockout mice of PKG^{-/-}. The above results would be expected if PA banding moderately increased RV afterload to a point where PDE5 inhibition would be able to improve contractility enough to overcome the burden of the fixed increase in afterload. In this case, there should be a blunted progression of disease, with the possibility of reversal and improved survival is expected. In a model of a severe increase in RV afterload, where even PDE5 inhibition was not enough to improve contractility to overcome the fixed increased afterload, then it is possible that increasing contractility in this setting may worsen the progression of disease, as pro-hypertrophic signals will still be released by the RV and there is a positive feedback exacerbation of this by increasing contractility with PDE5 inhibition.

In the case of metabolic modulators to improve mitochondrial dysfunction, chronic therapy with DCA in PA banded animals with RVH will lead to improved contractility and be beneficial in animals with a moderate PA band that can be compensated for by the improved contractility by increasing the coupling of glycolysis to glucose oxidation. This should decrease the progression of RVH and possibly lead to a reversal of established RVH, and lead to improved survival. In the setting of severe PA banding, then in the environment of ongoing RV decompensation, even though the contractility is improved, the reversion of hyperpolarized mitochondria to the normal state may remove the anti-apoptotic effects on the hypertrophied cardiomyocyte and ongoing acidosis and oxidative stress may cause increased apoptosis of hypertrophied cardiomyocytes and ultimately negatively influence survival and outcomes, as hypertrophied myocardium may be replaced by scar tissue with chronic therapy.

The ETRAs may show divergent results with hypertrophy and outcomes. The use of a negative inotrope in moderate disease will decrease RV contractility and may not allow for progression of RVH; however, the decreased contractility may lead to the earlier progression of RV failure than control animals, as the RV will be blunted from responding to the increased afterload, and there may be a negative influence on survival, even though RVH did not progress. This is likely to be more evident in severe PA banding.

Pathologic versus physiologic RVH:

The models used in our studies predominantly observed the effects on pathologic RVH, while mitochondrial membrane potential was studied in physiologic neonatal RVH as well. One model for physiologic RVH is the neonatal heart, and the neonatal rat heart is much smaller than a mouse heart, so *ex-vivo* contractility studies with the modified Langendorff perfusion apparatus is not likely to be utilized. Another model of physiologic right ventricular hypertrophy is the exercise-induced physiologic hypertrophy model. Exercise is a well-described method of causing physiologic LV hypertrophy, but is not described in animal studies for RVH. It is known that in athletes with physiologic hypertrophy that there is an associated 37% increase in RV mass analyzed by MRI¹⁰. It is likely that in established swim or treadmill models of animal physiologic hypertrophy that there will be RVH seen in humans, which could be studied by our current modified Langendorff perfused heart model. The *in-vitro* analysis of protein and mRNA expression could also be studied with this physiologic model of RVH.

Potential Results and Interpretation: In the case of PDE5 inhibitors, since the expression of PDE5 in cardiomyocytes is negligible in the normal RV myocardium, and physiologic hypertrophy is not associated with expression of other markers of pathologic hypertrophy (i.e. b-MHC, ANP, and BNP). As such, we would hypothesize that there would be very low expression of PDE5 in cardiomyocytes, and that there is unlikely to be a significant effect on RVH contractility beyond the effects on normal hearts.

In our studies on physiologic neonatal RVH, we did see that the mitochondrial membrane potential was hyperpolarized when comparing the RV to the LV; however,

induced neonatal cardiomyocyte hypertrophy by incubation with phenylephrine caused a more severe phenotype of hyperpolarization. Since there appears to be a gradient of progressive mitochondrial membrane hyperpolarization from physiologic to pathologic hypertrophy, we would hypothesize that DCA would improve contractility in physiologic RVH, though the increase in contractility may be less than observed in RVH hearts with pathologic RVH. These results would be very interesting, as they may have relevance to improve the performance of athletes by potentially improving cardiac output and decreasing the build up of lactic acidosis in muscles used in the body, by improving the coupling of glycolysis to glucose oxidation.

The ETRAs are likely to have similar effects to physiologic RVH as they do on normal RV muscle, which is a decrease in contractility. In pathologic RVH there is a significant up-regulation of ET_R-A , which leads to the more negative effect seen in pathologic RVH contractility than in the normal RV. It would be important to show the expression of ET_R-A , which would likely correlate to the contractility effects of ETRAs in physiologic RVH.

RVH versus LVH:

Clearly, the larger clinical entity in society is congestive heart failure from LVH and failure. Direct comparisons of RVH and LVH could be made in animals that were PA banded versus animals that undergo transverse aortic constriction to induce LVH. The most interesting and potentially clinically exploitable results would show differences between the two ventricles. There is a significant volume of literature on the use of PDE5

inhibitors in LVH models, which indeed show diverging results from our data on RVH as recently described by the group at Johns Hopkins, who discuss our paper in their discussion and state that differences between the RVH and LVH may explain these apparently conflicting results¹¹. In the case of mitochondrial membrane potential, use of DCA has only been used in animals with LVH to study ischemia reperfusion injury, and DCA did show a modest improvement in ischemic recovery in animals with LVH¹². We hypothesize that in pathologic LVH there may also exist a dysfunctional mitochondrial remodeling as increased glycolysis is observed in both RVH and LVH, though this may be less in LVH and the effects of DCA on LVH contractility will likely be less significant. The use of ETRAs in LVH has been seen in failed clinical trials on patients with CHF and LV failure, which led to the premature ending of the use of ETRAs in congestive heart failure, for either acute or chronic presentations⁸. These clinical results limit the enthusiasm to study ETRAs in LVH.

Clinical Applications:

As the goal of all translational research, our studies aim to be directly relevant and have the potential to directly translate to clinical trials and even offer further insight into current clinical practice. All classes of pharmacologic therapeutics used in our experiments represent medications used in current clinical practice, in the setting of RVH. The PDE5 inhibitors and the ETRAs are Class I therapies for the treatment of PAH, where RVH is often present. Dichloroacetate is used in clinical trials for PAH and now in cancer as well. As such, the novel clinical applications of patients with isolated

RVH would occur in patients with right ventricular outflow tract obstruction and subsequent RVH. These patients may not have PAH, though isolated right ventricular outflow tract obstruction is rare, and is often associated with ventricular septal defects. Therefore, the more clinically applicable cases would come in the acute treatment of PAH with these drugs where conductance catheters were used to isolate the effects of on the pulmonary vasculature versus RV contractility. These clinical data would confirm all applied physiology animal experiments done in this thesis. We are also confident that the clinical data will correlate to our animal experiments as all protein expression and mRNA expression was seen in human RVH as well as rat RVH. There have already been clinical data to confirm the findings in RVH coming from data of patients with left ventricular assist devices and RVH receiving sildenafil showing an increase in RVH contractility². Most importantly, these clinical applications may lead to the first truly accepted ventricle specific therapies for RVH, which specifically target the diseased ventricle while sparing effects on the normal ventricle, a true paradigm shift in the treatment of heart disease.

Summary:

- 1) Phosphodiesterase-5 is significantly expressed in hypertrophied human right ventricular cardiomyocytes, though not significantly expressed in normal RV cardiomyocytes.
- 2) Acute inhibition of PED5 increases contractility in the RVH myocardium, though has no significant effect on the normal RV contractility.

- 3) The increase in RVH contractility by PDE5 inhibition is by cGMP-mediated inhibition of cAMP-PDE3.
- 4) cGMP inhibition of cAMP-PDE3 is only occurs in RVH myocardium compared to normal RV myocardium.
- 5) cGMP inhibition of cAMP-PDE3 in RVH myocardium results from a down-regulation of Protein Kinase-G activity in RVH myocardium compared to normal RV myocardium.
- 6) There is a significant hyperpolarization of mitochondrial membrane potential in RVH cardiomyocytes.
- 7) The dysfunctional mitochondrial remodeling of RVH cardiomyocytes can be suppressed by inhibition of NFAT.
- 8) The dysfunctional mitochondrial remodeling of RVH cardiomyocytes can be suppressed by the metabolic modulator dichloroacetate (DCA).
- 9) RVH contractility is increased by acute treatment with DCA, which is associated with a decrease in lactate produced by RVH myocardium.
- 10) The Endothelin axis is up-regulated in RVH, including cardiomyocyte expression of Endothelin-1 and Endothelin Receptor-A.
- 11) Endothelin is secreted from RVH myocardium during ex-vivo perfusions and secretion is increased by b-adrenergic stimulation more than in the normal RV.
- 12) Endothelin receptor antagonists cause an acute decrease in RVH contractility, which is significantly greater than the decrease in contractility seen in the normal RV.

References:

1. Michelakis E, Tymchak W, Lien D, Webster L, Hashimoto K, Archer S. Oral sildenafil is an effective and specific pulmonary vasodilator in patients with pulmonary arterial hypertension: comparison with inhaled nitric oxide. *Circulation*. 2002;105(20):2398-2403.
2. Tedford RJ, Hemnes AR, Russell SD, Wittstein IS, Mahmud M, Zaiman AL, Mathai SC, Thiemann DR, Hassoun PM, Girgis RE, Orens JB, Shah AS, Yuh D, Conte JV, Champion HC. PDE5A Inhibitor Treatment of Persistent Pulmonary Hypertension After Mechanical Circulatory Support. *Circ Heart Fail*. 2008;1:21-219.
3. McKinsey TA, Olson EN. Toward transcriptional therapies for the failing heart: chemical screens to modulate genes. *J Clin Invest*. 2005;115(3):538-546.
4. McMurtry MS, Bonnet S, Wu X, Dyck JR, Haromy A, Hashimoto K, Michelakis ED. Dichloroacetate prevents and reverses pulmonary hypertension by inducing pulmonary artery smooth muscle cell apoptosis. *Circ Res*. 2004;95(8):830-840.
5. Bonnet S, Archer SL, Allalunis-Turner J, Haromy A, Beaulieu C, Thompson R, Lee CT, Lopaschuk GD, Puttagunta L, Bonnet S, Harry G, Hashimoto K, Porter CJ, Andrade MA, Thebaud B, Michelakis ED. A mitochondria-K⁺ channel axis is suppressed in cancer and its normalization promotes apoptosis and inhibits cancer growth. *Cancer Cell*. 2007;11(1):37-51.
6. Bonnet S, Rochefort G, Sutendra G, Archer SL, Haromy A, Webster L, Hashimoto K, Bonnet SN, Michelakis ED. The nuclear factor of activated T cells in pulmonary arterial hypertension can be therapeutically targeted. *Proc Natl Acad Sci U S A*. 2007;104(27):11418-11423.
7. Macchia A, Marchioli R, Marfisi R, Scarano M, Levantesi G, Tavazzi L, Tognoni G. A meta-analysis of trials of pulmonary hypertension: a clinical condition looking for drugs and research methodology. *Am Heart J*. 2007;153(6):1037-1047.
8. McMurray JJ, Teerlink JR, Cotter G, Bourge RC, Cleland JG, Jondeau G, Krum H, Metra M, O'Connor CM, Parker JD, Torre-Amione G, van Veldhuisen DJ, Lewsey J, Frey A, Rainisio M, Kobrin I. Effects of tezosentan on symptoms and clinical outcomes in patients with acute heart failure: the VERITAS randomized controlled trials. *Jama*. 2007;298(17):2009-2019.

9. Meyer M, Lehnart S, Pieske B, Schlottauer K, Munk S, Holubarsch C, Just H, Hasenfuss G. Influence of endothelin 1 on human atrial myocardium--myocardial function and subcellular pathways. *Basic Res Cardiol*. 1996;91(1):86-93.
10. Scharhag J, Schneider G, Urhausen A, Rochette V, Kramann B, Kindermann W. Athlete's heart: right and left ventricular mass and function in male endurance athletes and untrained individuals determined by magnetic resonance imaging. *J Am Coll Cardiol*. 2002;40(10):1856-1863.
11. Nagayama T, Hsu S, Zhang M, Koitabashi N, Bedja D, Gabrielson KL, Takimoto E, Kass DA. Sildenafil stops progressive chamber, cellular, and molecular remodeling and improves calcium handling and function in hearts with pre-existing advanced hypertrophy caused by pressure overload. *J Am Coll Cardiol*. 2009;53(2):207-215.
12. Wambolt RB, Lopaschuk GD, Brownsey RW, Allard MF. Dichloroacetate improves postischemic function of hypertrophied rat hearts. *J Am Coll Cardiol*. 2000;36(4):1378-1385.